Biomolecules, Combinatorics, and Statistical Physics

Citation
Williams, Mobolaji. 2019. Biomolecules, Combinatorics, and Statistical Physics. Doctoral dissertation, Harvard University, Graduate School of Arts & Sciences.

Permanent link
http://nrs.harvard.edu/urn-3:HUL.InstRepos:42029643

Terms of Use

Share Your Story

The Harvard community has made this article openly available.
Please share how this access benefits you. Submit a story .

Accessibility

Biomolecules, Combinatorics, and Statistical Physics

A thesis presented

by

Mobolaji Olukayode Williams

to

The Department of Physics

in partial fulfillment of the requirements

for the degree of

Doctor of Philosophy

in the subject of

Physics

Harvard University

Cambridge, Massachusetts

April 2019

Advisor: *Author:*

Eugene Shakhnovich   Mobolaji Olukayode Williams

Biomolecules, Combinatorics, and Statistical Physics

Abstract

Motivated by the combinatorial properties of the protein-design problem and the specific and non-specific interactions in biomolecular systems, we build exactly-solved models for the statistical physics of the symmetric group, permutation glasses, and the self-assembly of dimer systems. The first two models are studied for their statistical physics properties apart from the motivating system, and the third model is used to better understand the constraints of correct dimerization in biomolecular systems.

These models are exactly-solved in the sense that the sum-over-states defining their partition functions can be reduced to analytically more tractable expressions, and unlike most exactly-solved models in statistical physics whose motivations lie in condensed matter scenarios, these models are found by abstractly considering the combinatorial properties of biomolecular systems. This work suggests that there is a class of interesting but unexplored models in the statistical physics of biomolecules. We conclude by suggesting extensions to our presented models and starting points for new ones.

Contents

Contents

Contents

List of Previous Published Work

The content in the main chapters of this thesis has been published over the past three years in the *Physical Review E*. The publications associated with each chapter are as follows:

- **Chapter 2:** M. Williams, "Statistical physics of the symmetric group," *Physical Review E*, vol. 95, no. 4, p. 042126, 2017.

- **Chapter 3:** M. Williams, "Permutation glass," *Physical Review E*, vol. 97, no. 1, p. 012139, 2018.

- **Chapter 4:** M. Williams, "Self-assembly of a dimer system," *Physical Review E*, vol. 99, no. 4, p. 042133, 2019.

Acknowledgements

Each of the main chapters in this thesis is drawn from a specific paper, and in each paper I have thanked those who contributed to the content of that work. So in this acknowledgments, I thank those who provided auxiliary support for that work and who contributed to unpublished parts of the thesis.

In my thesis committee, I thank my advisor Eugene Shakhnovich for bringing me into his group in the summer of 2016, Michael Brenner for his helpful suggestions on career directions, and Vinothan Manoharan for his advice on the experimental and phenomenological aspects of all presented models. I must also thank Vinothan Manoharan for directing me to the Shakhnovich group in the first place and also for teaching me statistical physics at Harvard.

I thank all the current and former members of the Shakhnovich group for providing a supportive research environment for these past three years. In particular, I want to thank Yuanchi (Victor) Zhao and Rostam Razban for the many conversations we have had about science and its sociology, and for their help editing my various writings including the introduction and discussion of this thesis. I would like to thank Amy Gilson who was my desk neighbor for my first semester in the Shakhnovich group, and who, through our many conversations about society and philosophy, helped me realize I did not need to ignore those things in order to work in science. Finally, I would like to thank Roel Torres for our many discussions about life, the Chemistry department, and comics and his help with all group logistics.

I thank Jacob Barandes, Lisa Cacciabadou, and Carol Davis for their support over my five years in the physics department. Jacob Barandes counseled me during my transition out of high energy physics and started me on a trajectory of conversations which ultimately led me to Eugene Shakhnovich. At various points during my time at Harvard, Jacob was my teacher, head instructor, and discussion partner, and I am thankful for the opportunity to get to know him in all of these different capacities. Lisa was the first person I met in the department about six years ago when I was an undergraduate at MIT, and since then she has been a friendly voice which made the department feel much warmer than it would

have otherwise. I met Carol much later, around the third year of my graduate career, but from that time she has been a supportive and patient force in helping me with the logistics of department finance and travel. I also had the pleasure of traveling to the 2017 National Society of Black Physicists conference with Jacob, Lisa, and Carol, and I am glad I had the good sense to accept their invitation to attend.

Finally, I thank my academic advisor Matthew Reece. If my trajectory through Harvard had been slightly different, I would have likely been his student, and although I was not, he still treated me as if I was. He was free to talk whenever I had a question or concern about graduate school, and he provided much useful advice on research philosophy and how to prepare a research statement for post-doctoral applications.

"Combinatorics is an honest subject. No adèles, no sigma-algebras. You count balls in a box, and you either have the right number or you haven't. You get the feeling that the result you have discovered is forever, because it's concrete."

–Gian-Carlo Rota

Dedicated to my sister Ajoke Williams,
and my parents Elizabeth and Gbadetole Williams

Chapter 1

Introduction

"You're trying to predict the behavior of [complicated system]? Just model it as a [simple object], and then add some secondary terms to account for [complications I just thought of]. Easy, right? So why does [your field] need a whole journal anyway?"

–Physicist encountering a new subject, *xkcd*, Randall Munroe.

1.1 Overview

The research field of biophysics has existed since the mid-20th century, and for much of that time its practitioners have viewed physics as a tool that provided quantitative questions and methods to a discipline traditionally more focused on qualitative analysis. These physics-derived tools ultimately proved useful to biology not only because they gave the subject a new vocabulary and technology, but also because they led to important problems and solutions that biologists might not have found on their own. A few examples from this history: Luria and Delbrück used mathematical and probabilistic methods to affirm Darwin's theory of evolution by natural selection (Luria and Delbrück, 1943; Luria, 1984; Kay, 1985); Crick, Franklin, and Watson took from physics a reductionist philosophy and X-ray crystallography methods and thereby resolved the sub-cellular structures responsible for genetic inheritance (Watson and Crick, 1953; Sayre, 2000); Berg and Purcell used

1

electromagnetism and the theory of diffusion to establish limits on how accurately bacteria can determine surrounding food concentrations (Berg and Purcell, 1977).

Due to this history, more traditional physicists have considered biophysics to be a part of applied physics rather than physics proper, which is to say that they saw the subject as being concerned with problems less fundamental to our understanding of the physical world than those explored in cosmology, high energy physics, or condensed matter physics. According to this perspective, although one could use an understanding of physics to contribute to problems of biological interest, one could not use problems in biology to contribute to an understanding of physics. One of the purposes of this thesis is to argue that this view is wrong by showing that there are models motivated by biological systems which nevertheless still have properties of interest to physicists.

To this end the thesis presents three statistical physics models: The first motivated by the role permutations play in computational relationships between protein structure and sequence, the second a disordered extension to the first, and the third motivated by the general properties of correctly and incorrectly interacting monomers in protein and DNA systems. Although all models begin from principally biological concerns, they also ultimately bear features of interests to physicists. From the first model, we find multiple phases andmultiple transition temperatures, and from the second model we find a new context in which to explore quenched disorder. From the third model, we find explicit equilibrium conditions defining how a system with many interacting particles can self-organize into a more ordered configuration.

All models are "exactly solvable" in Baxter's sense of the phrase (Baxter, 2016), that is, the initial sum over states defining their partition functions can be reduced to analytical expressions from which observables can be computed. Exactly solvable models are useful in physics because they provide analytically simple frameworks for understanding properties found in more realistic systems. Thus, another purpose of this thesis is to study an unexplored intersection between biomolecular systems and exactly-solved models in statistical physics (Fig. 1.1).
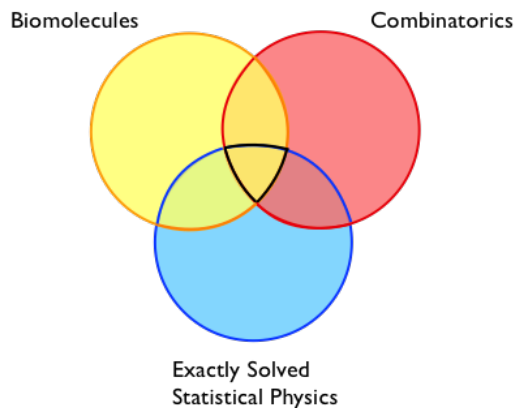
FIGURE 1.1: The problems considered in this thesis are found in the intersection between exactly-solved statistical physics, biomolecular systems, and combinatorics.

The key mathematical techniques used to study this intersection are drawn from combinatorics, and the basic approach we take to building and studying our models is as follows: We begin with a biomolecular system or a problem associated with biomolecular systems. This starting point has properties that can be reduced to well-understood calculations from combinatorics. After representing the problem combinatorially, we then use this representation to define the microstates of a statistical physics model whose exact partition function is primarily either an interesting mathematical model in of itself or a useful toy model for gaining insight into the motivating biomolecular system.

In this regard, the thesis can be divided into two parts. The first part, starting in Chapter 2, begins by considering a computational solution to the "protein design problem" problem. Protein design refers to the task of determining what sequences of amino acids are needed to obtain specific 3D protein structures (Shakhnovich, 1998). In certain computational solutions to this problem (Shakhnovich and Gutin, 1993a), one seeks the correct orderings of a particular collection of amino acids, and, motivated by such solutions, we present and analyze the properties of a model whose state space is defined by permutations of an ordered list. In Chapter 2 we analyze the simplest mean-field versions of the model, and in Chapter 3 we study the model in the context of quenched disorder and thereby define what we term a "permutation glass". In both chapters, after introducing the problem, the focus is largely mathematical and the resulting model does not make reference to the protein design problem that motivated it.

The second part, represented by Chapter 4, also uses a biomolecular system to motivate an exactly-solved statistical physics model, but after analyzing the properties of the model, we use our results to develop new ways to understand the motivating system. In this way the model we develop provides physics with an exactly-solved model of a self-organized system and also provides molecular biology with a new way to characterize systems of interacting biomolecules.

All of the presented models, whether they focus on the abstract properties of mathematical models or on what such models suggest about their motivating biomolecular systems, are united in the ways that they use combinatorics to define and explore their questions of interest. In the final chapter, we consider where else this theme might lead us by extending the prior models to ones associated with a more general or different set of combinatorics problems. The hope is that this final chapter itself provides an entryway into a new set of exactly-solved models in statistical physics.

1.2   Supplementary Literature Review

The review of the literature relevant to the respective problems in Chapters 2 through 4 is presented at the start of each chapter. In this section we review the literature relevant to the larger message of this work. In particular we review some of the important work constituting the intersection between exactly-solved statistical physics models and biomolecules, and we conclude by suggesting how incorporating combinatorics into this intersection can expand the existing models that physicists draw from in understanding biological phenomena. This review exists outside the specific collection of topics discussed in the body of this thesis, and therefore can be excluded without a significant cost to later understanding.

We will limit our subsequent discussion to models in the *physics* of biomolecules by which we mean models derived from the equilibrium statistical physics of microstates and partition functions. Therefore, we will not discuss the many important problem-solutions in evolutionary dynamics nor will we discuss famous results in biochemistry.

Finally, we will focus on models in equilibrium statistical physics rather than in non-equilibrium statistical physics. This choice is not necessarily limiting since the set of systems for which there are exactly-solved non-equilibrium models, exists within the set of systems for which there are exactly-solved equilibrium models.

1.2.1   Reign of the Ising Model

In equilibrium statistical physics, the study of a physical problem often begins with the partition function, and if the partition function can be written as a closed-form analytical expression[1] (or even be analytically approximated), we call the associated model "exactly-solved" or "exactly-solvable." Therefore, we can say that the field of exactly-solved statistical physics began in 1924, when Max Planck introduced the partition function to physics and gave it its alphabetic symbol. Calling it "Zustandsumme" (the German word for "state sum"), Planck applied the theoretical construct to study a gas of hydrogen atoms. (Mehra, 2001). One year later, in his PhD thesis, Ernst Ising used the partition function to study a simple model of ferromagnetism proposed by his advisor (Ising, 1925; Brush, 1967). In the model, microstates are defined by a linear chain of spins, each of which can point in two directions. The spins interact with their nearest neighbors and an external magnetic field. In modern notation, the energy of a particular spin microstate is written as

$$E(\{\sigma_i\}) = -J \sum_{i=1}^{N-1} \sigma_i \sigma_{i+1} - h \sum_{i=1}^{N} \sigma_i, \tag{1.1}$$

where σ_i (which can be $+1$ or -1) is the spin value at lattice site i, J is the energy of a spin-spin coupling, and h is the energy from an external magnetic field. Ising computed the partition function and the order-parameter for this system and showed that no phase-transition existed for this one-dimensional case. Over the next two decades, various physicists refined elements of Ising's analysis and by the time Onsager, in 1948 (Onsager, 1944; Brush, 1967) wrote the partition function for the two-dimensional case, the Ising model was the most famous exactly-solved model in statistical physics.

---

[1]The mathematical meaning of "closed-form" is somewhat ambiguous (see (Weisstein, 2002a)). We take it to mean an analytical expression which is simpler than the original sum-over-states defining the partition function. But one could of course ask what does "simpler" mean.

After the 1950s discovery of the structure of DNA, chemists and physicists sought physical explanations for the structural properties of all biomolecules. Given the Ising model's renown in physics, it is not surprising that many of the first attempts in these directions found their inspiration in this famous model of locally interacting spins. In particular, there are a number of features in the Ising model which make it an attractive metaphor for different systems. First, it is a model in which local interactions over an extended volume lead to macroscopic changes in the properties of the system. Second, these macroscopic changes can be induced by changing the temperature of the system. Third, since local interactions are the source of non-local changes, the Ising model is consistent with the reductionist philosophy of physics and allows macroscopic properties to be encoded by parameters defining local interactions. Applying these features to biomolecular systems, one could hope to connect the properties of individually interacting amino acids and nucleotide bases to the larger structural properties of proteins and DNA, respectively.

Over the second-half of the 20th century, many scientists chased this hope, and we will consider three problems representative of their efforts to use the Ising model to build exactly-solved models of biophysical phenomena.

- **Helix-Coil Formation**

  DNA denaturation is the process in which the nucleotide base pairs in double-stranded DNA break apart leading to a partial or full separation of the two DNA strands. In 1960, Zimm borrowed transfer-method techniques from the Ising model to study a physical model of DNA denaturation (Zimm, 1960). In Zimm's proposed model, the nucleotide bases along a chain of DNA could exist in one of two states (bonded or unbonded), and the bases could exist at the free ends between complementary DNA strands, as bound base pairs, or as part of bubbles of unbound base pairs between bound segments.

  Zimm's model of DNA denaturation was similar to one he published with Bragg a year earlier concerning alpha helix-random coil transitions in polypeptides (Zimm and Bragg, 1959). In certain polypeptides, the low-energy structure consists exclusively of a series of alpha-helices, but when the surrounding system increases in

temperature, these helices lose their structure and become random coils. In 1970, Poland and Scheraga showed that Zimm's models of alpha helix-random coil formation could be expressed as an Ising model (Poland and Scheraga, 1970), and that ever more general helix-coil models could be represented as Ising Model's where magnetic moments had more than two spin states (i.e., as "Potts models"). Nelson's text (Nelson, 2004) has a particularly readable discussion of Poland's and Scheraga's model. Taking a polymer chain to consist of monomeric units in either a helical ($\sigma = -1$) or random-coil ($\sigma = +1$) state, the energy of such a polymer can be modeled as

$$E_{\text{helix-coil}}(\{\sigma_i\}) = -\alpha k_B T \sum_{i=1}^{N} \sigma_i - \gamma k_B T \sum_{i=1}^{N-1} \sigma_i \sigma_{i+1}, \tag{1.2}$$

where α is a parameter associated with the difference in energy between helix and coil free energies, and γ is a parameter associated with the cost of immobilizing the bonds that make up the helix. Studying the statistical mechanics of a polymer made up of helices and coils with the energy function Eq.(1.2) is equivalent to studying the Ising model with energy function Eq.(1.1), and, therefore, many of the methods of the latter can be transferred to the former. From these methods one finds that from computing the partition function for Eq.(1.2), the fraction of the polymer in the helical state is found to be

$$\theta = \frac{1}{2} \left(1 + \frac{\sinh \alpha}{\sqrt{\sinh^2 \alpha + e^{-4\gamma}}} \right), \tag{1.3}$$

which for sufficiently large values of N, and appropriate interpretation of the parameters α and γ, well matches the experimental data (Zimm, Doty, and Iso, 1959; Nelson, 2004).

- **DNA Force-Extension**

  DNA consists of a long chain of molecules and, when it exists in an aqueous solution, microstates where the chain is long and straight are entropically disfavored. Thus, a force is required to stretch DNA. How one analytically computes this force clearly depends on how one models the DNA chain, and given DNA's long polymer-like

structure, it is also clear that any such model should include a connected chain of monomers. However, it has not always been clear what interaction and continuity properties one should assume about those monomers.

The Freely Jointed Chain (FJC), the simplest of the DNA models, was developed by Werner Kuhn (Kuhn, 1934) for more general purposes. In the model the chain is defined by a sequence of monomers in three dimensions where each monomer can point in any direction relative to the previous one. Kuhn introduced the model to study rubber, but the results were later used to describe molecular chains like DNA (Schellman, 1974).

The Worm-Like Chain (WLC), introduced after the FJC, took DNA to be a continuous flexible rod whose energy arose from the bending of the rod away from parallel. The model was proposed in (Saitô, Takahashi, and Yunoki, 1967) and analyzed experimentally for DNA in (Marko and Siggia, 1995), where Marko and Siggia showed it had force v. extension curves (for forces $\mathcal{O}(10^2\,\mathrm{pN})$) more accurate than those of the FJC.

Conceptually poised between the FJC and the WLC is the Discrete Persistent Chain (DPC), also known as the three-dimensional cooperative chain. Proposed by C. storm and P. Nelson (Storm and Nelson, 2003), the model is a three-dimensional Ising Model along a one-dimensional chain. Taking the chain to consist of N segments of length ℓ, where the ith segment points in the three-dimensional direction $\hat{\mathbf{t}}_i$, a particular microstate of the chain is given by $\{\hat{\mathbf{t}}_i\}$ and the associated energy is

$$E_{\mathrm{DPC}}(\{\hat{\mathbf{t}}_i\}) = -f\ell \sum_{i=1}^{N} \hat{\mathbf{z}} \cdot \hat{\mathbf{t}}_i - A\frac{k_B T}{\ell} \sum_{i=1}^{N-1} \hat{\mathbf{t}}_i \cdot \hat{\mathbf{t}}_{i+1}, \tag{1.4}$$

where f is the external force on the chain, and A is an effective-length parameter. In (Storm and Nelson, 2003), Storm and Nelson found that the high-force ($\sim 10^3\,\mathrm{pN}$) stretching predictions for the DPC provided better fits to the experimental stretching curves of DNA than both the FJC and WLC. Moreover, taking $A \to 0$ reduces the DPC to the FJC, and taking $N \to \infty$ transitions the DPC to the WLC. Therefore, in

various limiting cases the "Ising-like" Eq.(1.4) contains the previous models associated with DNA force-extension.

- **Protein Folding Problem**

  The "protein-folding problem" refers to the task of determining the three-dimensional structure of a protein from its sequence of amino acids. Mapping a one-dimensional sequence to a three-dimensional structure seems intractable enough, but further complicating the problem are the many strange properties of folded proteins. By the 1980s, proteins were known to fold completely or not at all which suggested that folding was akin to a first-order phase transition (Go, 1983). Proteins were also known to fold on very different time scales varying across protein species from 1ms to 100s. And the longer times for folding were believed to be due to the system passing through many free-energy local minima (Paine and Scheraga, 1985).

  Many of these protein-folding properties are shared by spin glasses. A spin glass is a model of spins much like the Ising model except, instead of having a fixed interaction parameter for all spins, the interaction parameter is drawn from a specified distribution. In 1987, theoretical spin glasses, like real proteins, were known to exhibit first-order phase transitions, long relaxation time scales and many local minima. Pursuing the analogy between these two disparate systems, Bryngelson and Wolynes transferred much of the then current spin-glass formalism to describe the phase properties of proteins (Bryngelson and Wolynes, 1987).

  Their main inspiration was Derrida's analysis of the spin-glass version of the infinite-range Ising model (Derrida, 1980). The energy function for the model is

  $$E_{\text{spin-glass}} = - \sum_{i_1 \leq \cdots i_r} J_{i_1, \ldots, i_r} \sigma_{i_1} \cdots \sigma_{i_r}, \tag{1.5}$$

  where $J_{i_1, \ldots, i_r}$ are coupling constants drawn from a Gaussian distribution with mean 0 and standard deviation $r!/N^{r-1}$. Motivated by Derrida's extrapolation of Eq.(1.5) to a more general model written in terms of energy, Bryngelson and Wolynes showed

FIGURE 1.2: Many of the famous exactly-solved models in the physics of biomolecules have been inspired by the Ising model Eq.(1.1). In this thesis, we hope to introduce a new inspirational model into the study of exactly-solved biophysics models, one grounded in a state space of permutations (and other combinatorial sets) rather than a state space of independent spins.

how the primary, secondary, and tertiary-energy distributions of an amino acid sequence could lead to the "glassy" properties of protein folding. The resulting analysis produced a qualitative phase diagram for protein folding and solidified a new language and metaphor for describing the associated problem Stein, 1992.

1.2.2 Concluding Remarks

From the above list, we see that many of the famous models comprising the intersection of exactly-solved statistical mechanics and biomolecules are Ising-like in that microstates

are defined by a list of independent "spin-sites" with a Hamiltonian consisting of local interactions between the spins (Fig. 1.2). The Ising model was useful for the purposes of modeling helix-coil transitions, computing force-extension curves, and understanding theoretical properties of protein folding. However, the Ising-model as metaphor and theoretical construct inevitably limits the types of problems physicists seek to solve as well as the chosen methods of solution. In particular, using the Ising-model as a theoretical motivation only works if the space of states for each degree of freedom in the system is independent of the spaces for the other degrees of freedom.

For some biomolecules systems, like the dimer system we will discuss in Chapter 4, the degrees of freedom are not independent since a particle interacting in one way limits the interaction possibilities of other particles. More specifically, in such systems, the microstates are related combinatorially. An objective of this thesis is to introduce a different type of model into theoretical biophysics, one which can handle problems in which the microstates of a system better resemble the elements of a combinatorial set rather than a list of independent spin-states. The ultimate hope is to provide a new metaphor for understanding biomolecular systems which are different, but no less important, than those documented above.

Chapter 2

From Protein Design to the Symmetric Group

"...I suppose the justification for studying these lattice models is very simple: they are relevant and they can be solved, so why not do so and see what they tell us? "

–Exactly Solved Models in Statistical Mechanics, R. J. Baxter.

2.1   Introduction

Chains of amino acids are important components of biological cells, and for such chains the specific ordering of the amino acids is often so fundamental to the resulting function and stability of the folded chain that if major deviations from the correct ordering were to occur, the final chain could fail to perform its requisite function within the cell, proving fatal to the organism.

More specifically, we see the relevance of correct ordering in the study of protein structure, which is often divided into the protein folding and protein design problem. While the protein *folding* problem concerns finding the three-dimensional structure associated with a given amino acid sequence, the protein *design* problem (also termed the inverse-folding problem; see Fig. 2.1) concerns finding the correct amino acid sequence associated with a given protein structure.
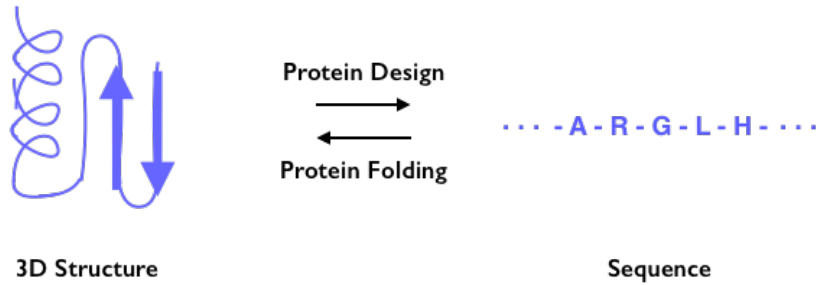
FIGURE 2.1: Folding vs. Design (or Inverse Folding) problems: The protein folding problem is concerned with determining the three dimensional structure produced by a particular sequence of amino acids. The protein design problem (which motivates the current work) is concerned with finding the sequence(s) of amino acids which yield a given three dimensional polypeptide structure. A number of approaches to the design problem are given in (Shakhnovich, 1998)

An aspect of one solution to the protein design problem is to maximize the energy difference between the low-energy folded native structure and the higher energy misfolded/denatured structures. In doing so, one takes native structure as fixed and then determines the sequence yielding the minimum energy, under the assumption (termed the "fixed amino-acid composition" assumption) that only certain quantities of amino-acids appear in the chain (Morrissey and Shakhnovich, 1996). In this resolution (specifically termed heteropolymer models (Shakhnovich and Gutin, 1993b; Shakhnovich and Gutin, 1993a)) the correct amino acid sequence is found by implementing an MC algorithm in sequence space given a certain fixed amino acid composition. This entails assuming the number of various types of amino acids does not change, and distinct states in sequence space are permutations of one another. For example, for a polypeptide chain with N residues, rather than searching over the entire sequence space (of size 20^N), one searches over a space of sequences (of size $N!/n_1!n_2! \ldots n_{20}!$) which are defined by a fixed number of each amino acid.

This aspect of the protein design problem alerts one to a gap in the statistical mechanics literature. Namely, there do not seem to be any simple and analytically soluble statistical mechanics models where the space of states is defined by permutations of a list of components.

We can take steps toward constructing such a model by considering reasonable general properties it should have. If we assume there was a specific sequence of components which defined the lowest energy sequence and was thermodynamically stable in the model, then deviations from this sequence would be less stable. Because of the role sequences of molecules play in biological systems, it is worth asking what features we expect such sequences to have from the perspective of modeling in statistical mechanics.

In Sec. 2.2 we introduce the model, and compute an exact partition function which displays what we term "quasi"-phase transitions—a transition in which the sequence of lowest energy becomes entropically disfavored above a certain temperature. In Sec. 2.3, we extend the previous model by adding a quadratic mean field interaction term and show that the resulting system displays two transition temperatures, a triple point, and a quadruple point. In Sec. 2.4, we discuss various ways we can extend this model in theoretical or more phenomenological directions.

2.2 System and Partition Function

Our larger goal is to study equilibrium thermodynamics for a system defined by permutations of a set of N components where each unique permutation is defined by a specific energy. In general, we should consider the case where the set of N components consists of L types of components for which if n_k is the number of repeated components of type k, then $\sum_{k=1}^{L} n_k = N$. For simplicity, however, we will take $n_k = 1$ for all k so that each component is of a unique type and $L = N$.

To study the equilibrium thermodynamics of such a system with a fixed N at a fixed temperature T, we need to compute its partition function. For example, for a sequence with N components (with no components repeated), there are $N!$ microstates the system can occupy and assuming we label each state $k = 1, \ldots, N! - 1, N!$, and associate an energy ϵ_k with each state, then the partition function would be

$$Z = \sum_{k=1}^{N!} e^{-\beta \epsilon_k}, \tag{2.1}$$

where ϵ_k for each state k could be reasoned from a more precise microscopic theory of how the components interact with one another. Phenomenologically, Eq.(2.1) would be the most precise way to construct a model to study the equilibrium properties of permutations, but because it bears no clear mathematical structure, it is unenlightening from a theoretical perspective.

Instead we will postulate a less precise, but theoretically more interesting model. For most ordered chains in biological cells, there is a single sequence of components which is the "correct" sequence for a particular macrostructure. Deviations from this correct sequence are often disfavored because they form less stable macrostructures or they fail to perform the original function of the "correct" sequence. With the general properties of such sequences in mind, we will abstractly represent our system as consisting of N sites which are filled with particular coordinate values denoted by ω_k. That is, we have an arbitrary but fixed coordinate vector $\vec{\omega}$ expressed in component form as

$$\vec{\omega} = (\omega_1, \ldots, \omega_N). \tag{2.2}$$

We will take the collection of components $\{\omega_k\}$ as intrinsic to our system, and thus take the state space of our system to be the set of all the vectors whose ordering of components can be obtained by permuting the components of $\vec{\omega}$, i.e., all permutations of $\omega_1, \ldots, \omega_N$. We represent an arbitrary state in this state space as $\vec{\theta} = (\theta_1, \ldots, \theta_N)$, where the θ_k are drawn without repeat from $\{\omega_k\}$. Formally, we would say our space of states is isomorphic to the symmetric group on $\vec{\omega}$ (Dixon and Mortimer, 1996). We will thus denote our state space as

$$Sym(\omega) \ := \ \text{Set of All Permutations of } (\omega_1, \ldots, \omega_N). \tag{2.3}$$

and then an arbitrary state $\vec{\theta}$ is just an element element of this set.

As a first formulation of the model, we will take $\vec{\theta}_0 = \vec{\omega}$ (the correct sequence) to represent the zero energy state in the system, and for each component θ_i of an arbitrary vector $\vec{\theta}$ which differs from the corresponding component ω_i in $\vec{\omega}$, there is an energy cost

of $\lambda_i > 0$. The Hamiltonian is then

$$\mathcal{H}_N(\{\theta_i\}) = \sum_{i=1}^{N} \lambda_i \, I_{\theta_i \neq \omega_i}, \tag{2.4}$$

where θ_i and ω_i are components of vectors $\vec{\theta}$ and $\vec{\omega}$ respectively, and I is defined by

$$I_A \equiv \begin{cases} 1 & \text{if } A \text{ is true} \\ 0 & \text{if } A \text{ is false} \end{cases}. \tag{2.5}$$

We note that although we label our general state as $\vec{\theta} = (\theta_1, \ldots, \theta_N)$, the components $\theta_1, \ldots, \theta_N$ can only take on mutually-exclusive values from the set $\{\omega_k\}$.

We want to explore the equilibrium thermodynamics of a system with a Hamiltonian of Eq.(2.4). This amounts to calculating the partition function

$$Z_N(\{\beta\lambda_i\}) = \sum_{\vec{\theta} \in Sym(\omega)} \exp\left(-\beta \sum_{i=1}^{N} \lambda_i \, I_{\theta_i \neq \omega_i}\right), \tag{2.6}$$

where $Sym(\omega)$ is again the set of all permutations of the components of $(\omega_1, \ldots, \omega_N)$. To find a closed form expression for the partition function, we group terms in Eq.(2.6) according to the number of ways to completely reorder j components in $\vec{\omega}$ while keeping the remaining components fixed. Each such reordering (i.e., each value of j) is associated with a sum over products of $e^{-\beta\lambda_i}$ terms with j factors of $e^{-\beta\lambda_i}$ (for various i) in each term. The total partition function is a sum of all such reorderings for all js from 0 to N. As can be seen from a direct expansion of Eq.(2.6), we have

$$Z_N(\{\beta\lambda_i\}) = \sum_{j=0}^{N} d_j \, \Pi_j\left(e^{-\beta\lambda_1}, \ldots, e^{-\beta\lambda_N}\right), \tag{2.7}$$

where d_j, termed the number of derangements of a list of j (Chuan-Chong and Khee-Meng, 1992), is the number of ways to completely reorder a list of j elements. The quantity $\Pi_j(x_1, \ldots, x_N)$, termed the jth elementary symmetric polynomial on n (Borwein and Erdélyi, 2012), is the sum of all ways to multiply j elements out of the N term set $\{x_1, \ldots, x_N\}$.

For example, $\Pi_2(x_1, x_2, x_3) = x_1 x_2 + x_2 x_3 + x_3 x_1$. By definition

$$\Pi_k(x_1, \ldots, x_N) = \frac{1}{k!} \left[\frac{d^k}{dq^k} \prod_{i=1}^{N} (1 + q\, x_i) \right]_{q=0}. \tag{2.8}$$

Derangements are often written as series expressions but we can use the definition of the Gamma function to write them as integrals. By definition (Weisstein, 2002c)), d_j is

$$d_j = \sum_{k=0}^{j} (-1)^k \binom{j}{k} (j-k)!. \tag{2.9}$$

Writing $(j-k)!$ as $\int_0^\infty ds\, e^{-s} s^{j-k}$, we find that Eq.(2.9) becomes

$$d_j = \int_0^\infty ds\, e^{-s} (s-1)^j. \tag{2.10}$$

Substituting this result into Eq.(2.7), we then find

$$
\begin{aligned}
Z_N(\{\beta \lambda_i\}) &= \int_0^\infty dt\, e^{-s} \sum_{j=0}^{N} (s-1)^j\, \Pi_j \left(e^{-\beta \lambda_1}, \ldots, e^{-\beta \lambda_N} \right) \\
&= \int_0^\infty ds\, e^{-s} \prod_{\ell=1}^{N} \left[1 + (s-1)e^{-\beta \lambda_\ell} \right],
\end{aligned}
\tag{2.11}
$$

which is the desired closed-form expression for the partition function of this system.

With Eq.(2.11), the problem of abstractly studying a thermal system of permutations with Hamiltonian Eq.(2.4) is, from the perspective of equilibrium statistical mechanics, now complete. However, there are still some physical and theoretical results which can be teased from this formalism. Specifically, we can ask whether this system exhibits phase transitions. To answer this question, it would prove more analytically tractable to take $\lambda_i = \lambda_0$ for all i. With this condition, we employ the identity

$$\Pi_j(\overbrace{e^{-\beta \lambda_0}, \ldots, e^{-\beta \lambda_0}}^{N \text{ elements}}) = \binom{N}{j} e^{-j\beta \lambda_0}, \tag{2.12}$$

and our partition function, Eq.(2.7), simplifies to

$$Z_N(\beta\lambda_0) = \sum_{j=0}^{N} \binom{N}{j} d_j e^{-j\beta\lambda_0} \tag{2.13}$$

$$= \int_0^\infty ds\, e^{-s} \left(1 + (s-1)e^{-\beta\lambda_0}\right)^N, \tag{2.14}$$

where we transformed our Hamiltonian as $\mathcal{H}_N(\{\theta_i\}) \to \mathcal{H}(j) = \lambda_0 j$ with j, defined as

$$j \equiv \sum_{i=1}^{N} I_{\theta_i \neq \omega_i}, \tag{2.15}$$

the number of components of $\vec{\theta}$ which are not equal to the corresponding component in $\vec{\omega}$. We call j the number of *incorrect* components of $\vec{\theta}$, and if $j = N$ we say $\vec{\theta}$ is *completely disordered*. For future reference we define the coefficient of $e^{-\beta\lambda_0 j}$ in Eq.(2.13) as $g_N(j)$ so that

$$g_N(j) = \binom{N}{j} d_j. \tag{2.16}$$

and the partition function can be written as

$$Z_N(\beta\lambda_0) = \sum_{j=0}^{N} g_N(j) e^{-j\beta\lambda_0}. \tag{2.17}$$

The quantity $g_N(j)$ is the number of ways to reorder a list of N elements so that j elements are no longer in their original position. This combinatorial definition of $g_N(j)$ will prove useful when we explore the phase behavior of more complex models of permutations.

From the form of Eq.(2.13), it is clear that, physically, its associated Hamiltonian is not realistic as it places distinct permutations (which in any true physical system most likely have quite different energy properties) in the same degenerate energy state. Still, from a theoretical perspective, the simplicity of this model makes it a suitable starting point for studying the general properties of systems of permutations.

2.2.1 Phase-like Behavior of "Non-Interacting" System

We can investigate the phase-like behavior of the system defined by the Hamiltonian Eq.(2.4) (for constant λ_i across i), by applying steepest descent (Kardar, 2007a) to Eq.(2.14) in the $N \gg 1$ limit. Performing the steepest descent approximation, solving for the critical value of s, and re-substituting it into the result, we find the approximate free energy of the system is

$$\beta F = -\ln Z_N(\beta\lambda_0) \simeq N\beta\lambda_0 - \left(e^{\beta\lambda_0} - N - 1\right) + F_0(N), \tag{2.18}$$

where $F_0(N) \sim N \ln N$ is a $\beta\lambda_0$ independent term. Noting that $\langle j \rangle = -\partial \ln Z_N / \partial(\beta\lambda_0) = \partial\beta F / \partial(\beta\lambda_0)$, we find the average number of incorrect components satisfies the following equation of state:

$$\langle j \rangle \simeq N - e^{\beta\lambda_0}. \tag{2.19}$$

By Eq.(2.15), we can infer that $\langle j \rangle$ must be greater than or equal to 0. However, the right-hand-side of Eq.(2.19) exhibits no such explicit constraint. Thus we can infer there is a phase-like transition in our system at the temperature

$$k_B T_c = \frac{\lambda_0}{\ln N}. \tag{2.20}$$

Below this temperature, we must have $\langle j \rangle \simeq 0$ and thus the "correct permutation" has the lowest free energy and is thermodynamically favored; above this temperature, $\langle j \rangle > 0$ and the system is in a disordered phase where the previous lowest energy "correct-permutation" is energetically disfavored.

Interestingly, this transition arises from the naively non-interacting Hamiltonian

$$\mathcal{H}_N(\{\theta_i\}) = \lambda_0 \sum_{i=1}^{N} I_{\theta_i \neq \omega_i}. \tag{2.21}$$

We say "naively non-interacting" because Eq.(2.21) consists of a sum over linear functions of a single index i, and thus does not suggest any coupling between terms of differing index. However, statistical mechanics tells us that the energy of a system isn't the only

thing which determines the thermodynamic behavior of a system. Indeed we have to consider entropic contributions as well, and in this system the entropy (as it is a function of j) can drive thermodynamic behavior. In other words, although the Hamiltonian is depicted as non-interacting and can set-theoretically be represented as

$$\mathcal{H}_{\text{system}} = \mathcal{H}_1 \oplus \mathcal{H}_2 \oplus \cdots \oplus \mathcal{H}_N, \tag{2.22}$$

our system really exhibits interactions between components because our total space of states $\mathcal{S}$ cannot be factorized:

$$\mathcal{S}_{\text{system}} \neq \mathcal{S}_1 \otimes \mathcal{S}_2 \otimes \ldots \otimes \mathcal{S}_N. \tag{2.23}$$

Thus the "non-interacting" system exhibits a transition at Eq.(2.20) due to the coupled nature of the state space. As discussed in the subsequent section, we term this transition a "quasi-phase transition" because it does not bear all of the standard properties we expect in phase transitions.

Not a True Phase Transition

We claim the system does not exhibit true phase transition behavior because many of these results are not consistent with the traditional thermodynamic definition of phase transitions. For one, phase transitions are associated with divergences in the derivatives of the free energy, but there is no divergence in the free energy associated with the partition function Eq.(2.14) for possible parameter values. Also, the result Eq.(2.19) only naively makes $\langle j \rangle$'s temperature dependence near $\langle j \rangle = 0$ appear non-differentiable. Apparently, since Eq.(2.19) requires that $\langle j \rangle = 0$ for $T < T_c$, we have that $\partial \langle j \rangle / \partial \beta$ goes from 0 to $e^{\beta_c \lambda_0}$ at $\beta_c = 1/k_B T_c$. However, Eq.(2.19) arises from the steepest descent approximation, and the non-approximated partition function Eq.(2.14) and its derivatives are actually differentiable over their entire domain.

Finally, with Eq.(2.13) we can define a Landau free energy $F(j)$ for this system according to $Z = \sum_j e^{-\beta F(j)}$, and what we may ordinarily label as a phase transition (i.e., going
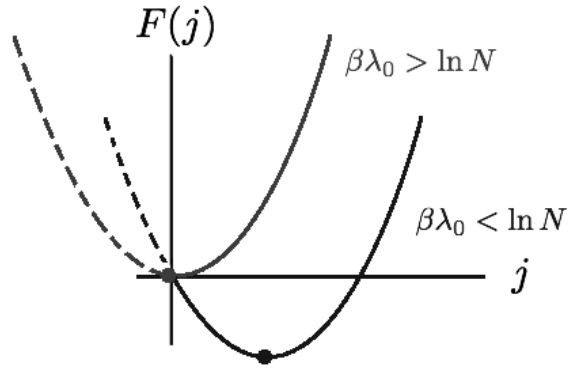
FIGURE 2.2: Free energy for "Non-Interacting Model": For $\lambda_0 > 0$, the Landau free energy of the system as a function of j, the number of incorrect components in $\vec{\theta}$, is always convex with a single global minimum. Because $j \geq 0$, the $j < 0$ domain of each plot (dashed section) is inaccessible. For sufficiently low temperatures, the minimum is at $j = 0$, but as we increase the temperature beyond Eq.(2.20), the free energy curve moves to the right (but retains its functional form) and the new minimum is at a $j > 0$ value. Actual plots of $F(j)$ for $j < 0$ require us to replace the combinatorial term $\binom{N}{j}d_j$ with its corresponding gamma function expression.

from $\langle j \rangle = 0$ to $\langle j \rangle \neq 0$) arises, not from changes in the functional form of the Landau free energy as we see in real phase transitions, but from changes in the excluded region of the Landau free energy (See Fig. 2.2). Because the functional form of the free energy remains the same we observe no true phase transition.

Alternatively, a heuristic argument for the non-existence of phase transitions in our permutation model is mathematically very similar to the Landau argument (Landau, Lifshitz, and Pitaevskii, 1980) for the non-existence of transitions in 1d Ising Models. For our permutation system with N lattice sites, the state of zero energy and zero entropy consists of every site being occupied by its correct component. To increase the energy of this system, we can choose j sites to contain incorrect components, thus giving us an energy $\mathcal{H}_j = \lambda_0 j$. The number of ways we can choose these j components is given by Eq.(2.16) Thus, upon introducing $j \neq 0$ incorrect components, the change in the Landau free energy of our system is

$$\Delta F(j) = \lambda_0 j - k_B T \ln\left[\binom{N}{j}d_j\right] \simeq j(\lambda_0 - k_B T \ln N), \tag{2.24}$$

where we took these results in the $1 \ll j \ll N$ limit and used $d_j \simeq j!/e$. In the thermodynamic ($N \to \infty$) limit, we find that $\Delta F(j) \to -\infty$ meaning there is no non-zero T at which the entropic contribution becomes subdominant to the energy. Thus the system exhibits no phase transition.

2.3   Partition Function for Interacting Model

When we first considered a model of thermal permutations, we began with a Hamiltonian where sites did not interact with one another and each had a site-dependent energy cost for being incorrectly occupied:

$$\mathcal{H}(\{\theta_i\}) = \sum_i \lambda_i\, I_{\theta_i \neq \omega_i}. \tag{2.25}$$

More generally, we can consider Hamiltonians with an arbitrary number of multiple-site interaction terms. Such a Hamiltonian could be written as

$$\mathcal{H}(\{\theta_i\}) = \sum_i \lambda_i\, I_{\theta_i \neq \omega_i} + \frac{1}{2} \sum_{i,j} \mu_{ij}\, I_{\theta_i \neq \omega_i} I_{\theta_i \neq \omega_i} + \cdots. \tag{2.26}$$

The first term in Eq.(2.26) associates an energy cost of λ_i with incorrectly occupying the component at position i. The second term models interactions between sites where the correct (or incorrect) occupation of a single site determines the energy of another. The exact values of λ_i and μ_{ij} could be chosen to ensure the "correct" state ($\theta_i = \omega_i$ for all i) is non-degenerate as in the non-interacting model. The ellipsis represent higher order interactions in this framework. Hamiltonians such as Eq.(2.26) should be more physically relevant as they would correspond to systems where the energy cost for deviating from the lowest energy permutation is not simply linear but could be represented as a tensor valued fitting function.

We can make progress in studying the thermodynamics of more general Hamiltonians like Eq.(2.26) by first only considering first- and second-order interaction terms and taking the interactions to be constants: $\lambda_i = \lambda_1$ for all i; $\mu_{ij} = \lambda_2/N$ for all i, j. The factor of

$1/N$ is chosen so that the second term matches the extensive scaling of the first term. The partition function for such parameter selections is then

$$Z_N(\beta; \lambda_1, \lambda_2) = \sum_{\vec{\theta} \in Sym(\omega)} \exp\left(-\beta\lambda_1 \sum_{i=1}^{N} I_{\theta_i \neq \omega_i} - \frac{\beta\lambda_2}{2N} \sum_{i,j=1}^{N} I_{\theta_i \neq \omega_i} I_{\theta_j \neq \omega_j}\right), \tag{2.27}$$

where λ_1 and λ_2 are interaction parameters with units of energy. We can also write this partition function in the Eq.(2.15) basis as

$$Z_N(\beta; \lambda_1, \lambda_2) = \sum_{j=0}^{N} g_N(j) e^{-\beta\mathcal{E}(j)}, \tag{2.28}$$

where $g_N(j)$ is defined in Eq.(2.16) and

$$\mathcal{E}(j) = \lambda_1 j + \frac{\lambda_2}{2N} j^2 \tag{2.29}$$

is the energy function for the system.

2.3.1 Calculating Order Parameter

Our goal is to analyze the "quasi"-phase behavior of this system in a way analogous to our analysis for the non-interacting system. To do so we begin with the Landau free energy function

$$F_N(j, \beta) = \lambda_1 j + \frac{\lambda_2}{2N} j^2 - \frac{1}{\beta} \ln g_N(j). \tag{2.30}$$

Alternative starting points for this derivation are presented in Appendix A.1. Our system is constitutively discrete, so it is not precisely correct to discuss our free energy in the language of analysis, but given our expression for Eq.(2.16) we can map this system to a continuous one which bears the same thermodynamic properties and for which analysis is appropriate. Specifically, if we take j to be continuous and use the identity $\Gamma(x+1) = x!$ and $d_j = \Gamma(j+1, -1)/e$ where the incomplete Gamma function $\Gamma(x, a)$ is defined as

$$\Gamma(x, a) = \int_a^\infty dt\, e^{-t} t^{x-1}, \tag{2.31}$$

then we can write

$$g_N(j) = \frac{\Gamma(N+1)}{\Gamma(j+1)\Gamma(N-j+1)} \frac{\Gamma(j+1,-1)}{e}, \tag{2.32}$$

With the approximation $\Gamma(j+1,-1) \simeq \Gamma(j+1)$ and the substitution Eq.(2.32), Eq.(2.30) then becomes

$$f_N(j,\beta) = \lambda_1 j + \frac{\lambda_2}{2N} j^2 + \frac{1}{\beta} \ln \Gamma(N-j+1) + f_0 \tag{2.33}$$

where we defined our approximated free energy as $f_N(j,\beta)$ and collected the j independent constants into f_0. Now Eq.(2.33) is fully continuous and amenable to analysis. To find the thermodynamic equilibrium of this system, we need to find the value of j for which $\partial f_N(j,\beta)/\partial j = 0$ and $\partial^2 f_N(j,\beta)/\partial j^2 > 0$. For the first condition we have

$$\frac{\partial}{\partial j} f_N(j,\beta) = \lambda_1 + \frac{\lambda_2}{N} j - \frac{1}{\beta} \psi_0(N-j+1) = 0. \tag{2.34}$$

As an asymptotic series, we have

$$\psi_0(x) \simeq \ln(x-1/2), \tag{2.35}$$

as can be affirmed by Taylor expansion $\psi_0(x) = \ln x + 1/2x + \mathcal{O}(x^{-2})$ (Weisstein, 2002b). Applying the approximation Eq.(2.35) to Eq.(2.34), and setting the result to be valid for the equilibrium value $j = \bar{j}$, we then find the constraint

$$e^{\beta \lambda_2 \bar{j}/N} = -e^{-\beta \lambda_1} \left(\bar{j} - N - 1/2 \right), \tag{2.36}$$

which has the solution

$$\frac{\bar{j}}{N} = 1 - \frac{1}{\beta \lambda_2} W\left(\frac{\beta \lambda_2}{N} e^{\beta \lambda_1 + \beta \lambda_2} \right) + \mathcal{O}\left(\frac{1}{N} \right), \tag{2.37}$$

where W is the (branch unspecified) Lambert W function (Weisstein, 2002d), defined by

$$W(xe^x) = x. \tag{2.38}$$

To specify the branch of the W which corresponds to a stable equilibrium we compute the second derivative of our free energy at this derived critical point. Doing so yields

$$\frac{\partial^2}{\partial j^2} f_N(j = \bar{j}, \beta) \simeq \frac{1}{N}\left(\lambda_2 + \frac{1}{\beta}\frac{1}{1 - \bar{j}/N}\right) = \frac{\lambda_2}{N}\left(1 + \frac{1}{W\left(\frac{\beta\lambda_2}{N}e^{\beta\lambda_1 + \beta\lambda_2}\right)}\right). \tag{2.39}$$

Thus Eq.(2.37) (for $\lambda_2 > 0$) yields a free energy minimum for

$$W\left(\frac{\beta\lambda_2}{N}e^{\beta\lambda_1 + \beta\lambda_2}\right) > -1, \tag{2.40}$$

and yields a maximum for the inverse condition. This amounts to stating that the stable equilibrium for $\bar{j}$ is defined by the principal branch of the Lambert W function where $W = W_0 \geq -1$, and the unstable equilibrium for $\bar{j}$ is defined by the negative branch where $W = W_{-1} < -1$.

Thus, the order parameter for this system is

$$\frac{\bar{j}_0}{N} = 1 - \frac{1}{\beta\lambda_2}W_0\left(\frac{\beta\lambda_2}{N}e^{\beta\lambda_1 + \beta\lambda_2}\right) + \mathcal{O}\left(\frac{1}{N}\right). \tag{2.41}$$

We note that taking $\lambda_2 \rightarrow 0$ and using $W(x) = x + \mathcal{O}(x^2)$ for $|x| \ll 1$ returns us to the non-interacting result Eq.(2.19).

For completeness, we define the value of j which yields a free energy maximum as $\bar{j}_{-1}$; it is related to Eq.(2.41) by replacing the principal branch function W_0 with W_{-1}.

2.3.2 Discussion of Parameter Space

In the previous section, we found that the order parameter for this system was given by Eq.(2.41). We noted that this solution represented a local minimum of the free energy as long as the Lambert W function satisfied $W = W_0 > -1$. Thus when this condition is violated, $\bar{j}_0$ is no longer a valid stable equilibrium, and our system has undergone a "quasi"-phase transition or simply a transition.

Moreover, our values of j are bounded below by $j = 0$ and bounded above by $j = N$, neither conditions of which are naturally constrained by Eq.(2.41). Thus these two
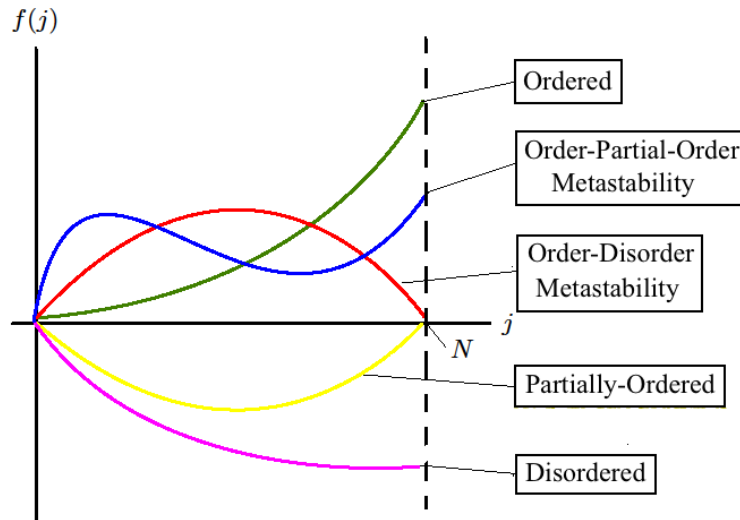
FIGURE 2.3: Possible functional forms of Eq.(2.33): We note that the stabilities that define the $j = 0$ and $j = N$ points are not thermodynamic stabilities (namely they don't arise from the $f'(j) = 0$ condition). Rather since the spectrum of j values is bounded below by 0 and above by N, owing to these boundary conditions the system can become trapped in ordinarily unstable parts of the free energy curve. The colors match the color of the associated region of parameter space in Fig. 2.4.

conditions are associated with two other transitions. In all, then, there are three conditions which define the quasi-phase boundaries in this system.

While there are three conditions which define transitions in this system, there are in fact five distinct regimes of parameter space. We can obtain a qualitative sense of these regimes by creating schematic plots of the free energy Eq.(2.33) for various parameter values of λ_1 and λ_2. The possible plots can be placed into five categories according to the plot's stable or metastable j values. We depict these possible plots in Fig. 2.3. We note that only the free energy plots with valid values of $\bar{j}_0$ contain what we normally consider a thermodynamic equilibrium; the other plots have "stable" values of j arising only from the $j = 0$ and/or $j = N$ boundary conditions.

Qualitatively, we can name the states according to the sequence space to which their equilibrium values of j correspond. We know for $j = 0$, our system is in a state with zero incorrect components in $\vec{\theta}$ and hence the system is "perfectly ordered" or just "ordered". Conversely for $j = N$ our system has N incorrect components and hence the system is "completely disordered" or just "disordered". The in-between case of $j = \bar{j}$ where $0 < \bar{j} <$

N can be given the related label of "partially-ordered". Thus, the regime names associated with our possible values of the order parameters are

- **Ordered Regime ($j = 0$ stable)**: Neither $\bar{j}_0$ nor $\bar{j}_{-1}$ exist; $f(N,\beta) > 0$.

- **Disordered Regime ($j = N$ stable)** : Neither $\bar{j}_0$ nor $\bar{j}_{-1}$ exist; $f(N,\beta) < 0$.

- **Partially-Ordered Regime ($j = \bar{j}_0$ stable)**: Only $\bar{j}_0$ exists.

- **Order and Disorder Metastable Regime ($j = 0$ and $j = N$ stable)**: Only $\bar{j}_{-1}$ exists.

- **Order and Partial-Order Metastable Regime ($j = 0$ and $j = \bar{j}_0$ stable)** : Both $\bar{j}_0$ and $\bar{j}_{-1}$ exist.

We note that it seems to be a fundamental feature (or a lack of one) of this system, that the free energy Eq.(2.33) does not admit a metastability between partial-order and disorder.

2.3.3 Monte-Carlo Generated Parameter Space

With these regime definitions, we can depict the parameter space graphically. In Fig. 2.3 we showed the possible forms of the free energy for this system where each was categorized according to the existence of the local minimum critical point $\bar{j}_0$, the existence of the local maximum critical point $\bar{j}_{-1}$, and the sign of the quantity $f_N(j,\beta)$. We can extrapolate this categorization to $\lambda_1 - \lambda_2$ parameter space, by determining which regions of parameter space correspond to specific plots in Eq.(2.33). Doing so through the Monte Carlo procedure described in Appendix A.2, we generated 10,000 points of the parameter space diagram in Fig. 2.4 for β set to 1. We note that the parameter space exhibits five regimes separated by three lines cited in Table 2.1 each of which correspond to the three conditions mentioned at the beginning of this section. These lines can be derived analytically (as shown in Appendix A.3) by considering the conditions in turn and which regimes they serve to connect.

2.3.4 Triple and Quadruple Points and Transition Temperatures

From Fig. 2.4 we see that our system is characterized by two points where there is a coexistence between multiple regimes. Given that $W_{-1}(-e^{-1}) = -1$, we have that the Ordered,
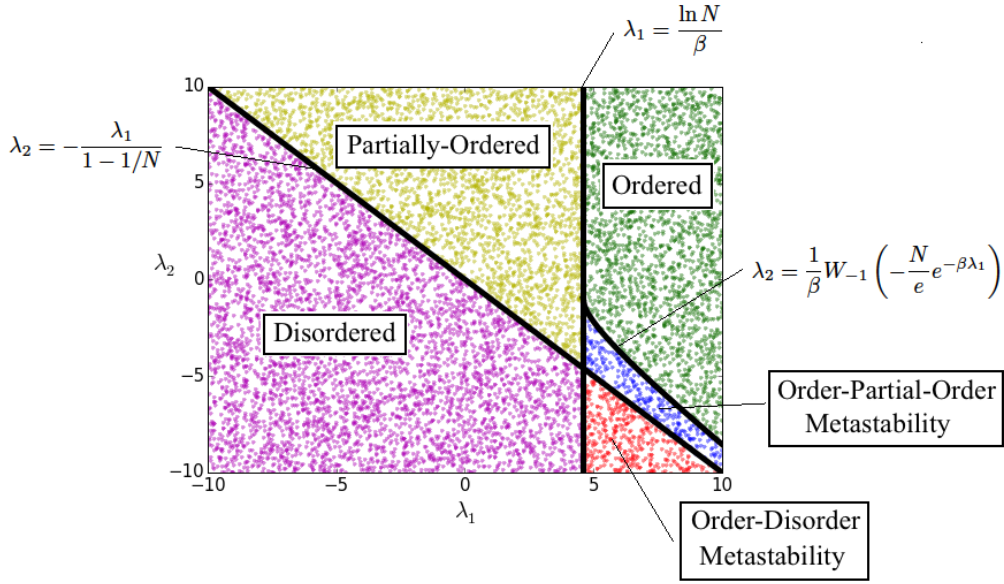
FIGURE 2.4: The $\lambda_1 - \lambda_2$ Parameter Space for Interacting Mean Field System: We set $\beta = 1$ and $N = 100$. We followed the Monte Carlo procedure outlined in the notes for 10,000 points. In the figure we also denoted the analytic lines (i.e., Eq.(A.36), Eq.(A.40), and Eq.(A.43)) which define the separation between the phases. The colors correspond to the colors of the free energy curve in Fig. 2.3.

Partially-Ordered, and Order-Partially-Ordered Metastability coexistence point is characterized by the condition

$$\lambda_1 = \ln N/\beta \quad \text{and} \quad \lambda_2 = -1/\beta. \tag{2.42}$$

These conditions characterize the system's triple point.

Similarly, for $N \gg 1$, the Partially-Ordered, Disordered, Order-Partially-Ordered Metastability, and Order-Disorder Metastability coexistence point is characterized by the condition

$$\lambda_1 = \ln N/\beta \simeq -\lambda_2. \tag{2.43}$$

This condition characterizes the quadruple point of the system.

Fig. 2.4 also depicts the possible regimes of our system for a given temperature and various Hamiltonian parameters λ_1 and λ_2. More physically, we may be interested in knowing what are the "quasi" phase properties of a system with a fixed λ_1 and λ_2 and a variable temperature. That is, what are the temperatures which define the various transitions between regimes in the system?

TABLE 2.1: Functions defining boundaries between parameter regimes.

Regime Transition	Boundary in Parameter Space
Order/Partial-Order	$\beta\lambda_1 = \ln N$
Order/Order-Partial-Order Metastability	$\beta\lambda_2 = W_{-1}\left[-(N/e)e^{-\beta\lambda_1}\right]$
Order/Disorder	$\beta\lambda_2 = -\dfrac{\beta\lambda_1}{1 - 1/N}$

An arbitrary permutation system for a fixed N and at a variable temperature is characterized by a specific energy function Eq.(2.29). Such a system is therefore defined by a specific λ_1 and λ_2, and the system can be associated with a particular point (and hence region) in the parameter space of Fig. 2.4. As we vary the temperature of this system, the temperature dependent regime-coexistence lines change and if they change in such a way as to extend the region of a regime to newly encompass our original point then our system has undergone a transition. In this way, we can define the temperatures which characterize various possible transitions of this system.

First, from Fig. 2.4 and Eq.(A.43) we note the regime-coexistence line between the partially-ordered and disordered regime is independent of temperature, and so there is no critical temperature defining a partial-order to disorder transition.

From Eq.(A.36), we can infer that the partial-order to order transition is characterized by moving below the temperature

$$k_B T_{c1} = \frac{\lambda_1}{\ln N}. \tag{2.44}$$

Contingent on which region of parameter space the system lies, this temperature also characterizes the disorder to order-disorder metastability transition and the partial-order to order-partial-order metastability transition.

And from Eq.(A.39), we can solve for the associated transition temperature given fixed λ_1 and λ_2 to find

$$k_B T_{c2} = (\lambda_1 + \lambda_2)\left[W_0\left(-\frac{N}{e\lambda_2}(\lambda_1 + \lambda_2)\right)\right]^{-1} \tag{2.45}$$

where this expression is only relevant for $-\lambda_1 < \lambda_2 < 0$ and $\lambda_1 > k_B T \ln N$. Moving above this temperature leads to the order to order-partial-order metastability transition.

2.4 Discussion

In this work, motivated by an abstraction of a foundational problem in protein design, we posited and analyzed the basic properties of a statistical physics model of permutations. Formally, we considered a simple statistical physics model where the space of states for N lattice sites was isomorphic to the symmetric group of degree N (Dixon and Mortimer, 1996), and where the energy of each permutation was a function of how much the permutation deviates from the identity permutation.

In this model, we found that due to a state space which could not be factorized in a basis defined by lattice sites, even the superficially non-interacting system can exhibit phase-like transitions, i.e., temperature dependent changes in the value of the order parameter which do note exhibit the properties typically associated which phase transitions in infinite systems. When interactions are introduced through a quadratic mean field term, the system is capable of exhibiting five regimes of thermal behavior, and is characterized by two transition-temperatures corresponding to various quasi-phase transitions.

The introduced model provides us with a basic exactly soluble system for certain interaction assumptions and thus provides a concrete model-based understanding of a system with a non-factorizable state space. Because of its utility and the type of results obtained, the model deserves to be subject to the standard extensions of typical canonical models in statistical mechanics. In particular we hope to extend it to non-trivial site dependent interactions. For example, a nearest neighbor interaction Hamiltonian of the kind which characterize the Ising Model,

$$\mathcal{H}(\{\theta_i\}) = -q \sum_{i=1}^{N} I_{\theta_i \neq \omega_i} I_{\theta_{i+1} \neq \omega_{i+1}}, \tag{2.46}$$

would be an alternative physical extreme to the mean-field interactions considered in Section 2.3.

We could also consider a generalized chain of components where the interactions between sites or the cost for an incorrectly filled site is not constant but is drawn from a distribution of values. Such a system of quenched disorder would characterize a permutation glass which may contain interesting results due to the unique nature of the state space.

Supposing it is possible to define more interesting interactions models, a natural investigation would concern the renormalization group properties of the system. Specifically, we would be interested in how would one sum over specific states (as characteristic of a renormalization group transformation) when the state space of a system looks like,

$$\mathcal{S}_{\text{system}} = \prod_{i=1}^{N} \otimes \, \mathcal{S}_i \qquad (2.47)$$

i.e., is not factorizable along lattice sites.

Finally, to connect this model of permutations to problems more relevant to protein design it would prove necessary to incorporate the possibility of repeated components or the background geometry of a lattice chain.

Chapter 3

Permutation Glass

"'Order and disorder', said the speaker, 'they each have their beauty.' "

–Speaker for the Dead, Orson Scott Card.

3.1 Introduction

In statistical physics, spin glasses exist as archetypical models of disorder due both to their solubility and to the fact that they lend intuition to systems outside of physics which nonetheless exhibit properties common to many spin glasses. Soon after the first spin glass models were solved, physicists sought to apply the lessons of frustration, quenched disorder, and multiple equilibria to biological systems like neural networks (Hopfield, 1982; Hopfield, 1984) and proteins (Bryngelson and Wolynes, 1987). But because biological systems integrate structure, function, and dynamics in ways not mirrored by any canonical model of physics, the utility of these spin glass models existed not in providing detailed predictions about biology but in supplying a quantitative framework in which to develop new ways of understanding and describing biological problems (Stein, 1992) .

In a previous work (Williams, 2017), we moved in the opposite direction: Rather than using our understanding of physics to develop new questions about biology, we used a biological question to motivate the inquiry into a physical system. Motivated by a computational examination of the protein design problem (Shakhnovich, 1998), we considered a

statistical physics model of permutations in which the state space was isomorphic to the symmetric group. Significantly, the model's motivation came, not from a physical system, but from a Monte Carlo study of a problem of biochemistry, and to establish intuition for it we considered lattice models where the energy costs were uniform across the system. But even with this simple assumption, the resulting permutation model had interesting thermal behavior because the non-factorizable nature of the state space conferred entropic disorder to a system which was nominally non-interacting. Thus the system exhibited thermal transitions among units which were coupled through state space even though they were not coupled in the Hamiltonian.

In this paper, we connect our study of the statistical physics of the symmetric group to disordered systems by considering the properties of a system with a state space of permutations and a quenched distribution of energy parameters. Given the unique nature of the state space and the solubility of the non-disordered analog, such a permutation glass[1] offers opportunities to explore the relationship between equilibria and disorder in simple exactly soluble physical systems.

In Sec. 3.2 of this paper, we discuss the original permutation model, provide schematic depictions of the systems to which it applies, and derive equations defining the thermal equilibrium of the permutation glass. In Sec. 3.3 we consider the permutation glass for various distributions of energy costs and derive transition temperatures for each case noting their overall consistency with the general result that $k_B T_c \leq \overline{\lambda} / \ln N$, where $\overline{\lambda}$ is the mean of the energy-cost distribution and N is the number of components in the system. That is, the transition temperature of a permutation glass is always less than the transition temperature of the non-disordered system with energy cost given by $\overline{\lambda}$. In Sec. 3.4 we compare the computed transition temperatures and a general expression for the order parameter of the permutation glass to results from simulations. In Sec. 3.5 we derive a distribution-independent result requiring that the "completely correct" state can only be a thermodynamic equilibrium of the system if $P_{\lambda<0} < 1/N$ where $P_{\lambda<0}$ is the probability that

---

[1]The phrase "permutation glass" seems to have first been used in (Collins, 2014) in a context different from that in this chapter. In that first use, the phrase referred to systems with a single ground state and with $N!$ degenerate low-energy microstates.
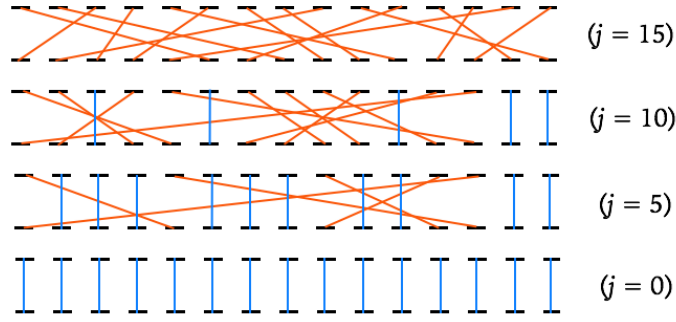
FIGURE 3.1: The permutation graph depiction of four microstates in a permutation system with $N = 15$. In each graph, j is equivalent to the number of diagonal lines in the permutation graph. The number of "correct" connections are shown as vertical lines. If we associate a Boltzmann factor $e^{-\beta \lambda_k}$ with each bottom slot k which is not connected to its corresponding top slot, multiply all Boltzmann factors for a graph, and then sum over all possible permutation graphs weighted by their net Boltzmann factor, we obtain Eq.(3.3).

an incorrectly-ordered component is energetically favored. In Sec. 3.6 we use our derived results to define a glassy regime which cannot be found in the non-disordered system. In Sec. 3.7 we conclude by discussing ways to extend this simple model of a permutation glass to more complicated models that could exhibit replica symmetry breaking, and we present an analogy between this system and a system of fermions.

3.2 Equilibrium of Permutation Glass

In the statistical physics of permutations presented in (Williams, 2017), we considered a state space defined by a list of N unique components $(\omega_1, \omega_2, \ldots, \omega_N)$. Taking the states of the system to be the various $N!$ orderings of the components, and defining the zero-energy state as the state where the components are in the order $(\omega_1, \omega_2, \ldots, \omega_N)$, we can postulate a simple Hamiltonian in which there is an energy cost λ_k for each state where ω_k is not in the position given by its zero-energy ordering:

$$\mathcal{H}_N(\{\theta_i\}) = \sum_{i=1}^{N} \lambda_i I_{\theta_i \neq \omega_i}, \tag{3.1}$$

where $I_A = 1$ if A is true and $I_A = 0$ otherwise, and $(\theta_1, \theta_2, \ldots, \theta_N) \in \text{perm}(\omega_1, \omega_2, \ldots, \omega_N)$. We term the state $\vec{\theta} = \vec{\omega}$ the "completely correct state," and we say component k of $\vec{\theta}$ is "incorrectly ordered" if it is not equal to ω_k. The order parameter of our system is $\sum_{i=1}^{N} \langle I_{\theta_i \neq \omega_i} \rangle$,
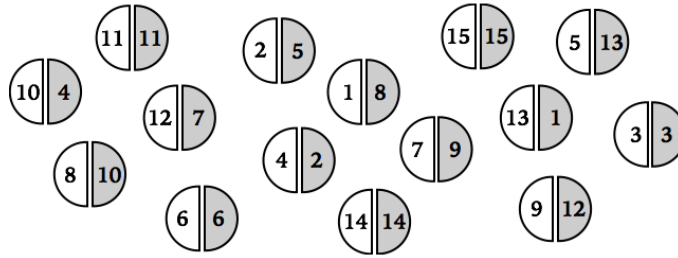
FIGURE 3.2: "Matching problem" depiction of a $j = 10$ microstate for a $2N = 30$ permutation system. The spatial location of each pair is not important in determining the energy of the state. For this state, the matching pairs are 3, 6, 11, 14, and 15. If we associate a Boltzmann factor $e^{-\beta\lambda_k}$ with each shaded circle k which is not paired with the corresponding unshaded circle k, multiply all Boltzmann factors for all pairings within a state, and sum over all possible pairings weighted by the net Boltzmann factor for each collection of pairings, we obtain Eq.(3.3).

the average number of incorrectly ordered components of $\vec{\theta}$. We denote this average more succinctly as $\langle j \rangle$.

We can depict the various microstates of this system as a permutation graph, shown in Fig. 3.1 for the case $N = 15$. In each graph, whenever there is not a line connecting a lattice site k to its vertical complement, the system gains a Boltzmann factor $e^{-\beta\lambda_k}$. The parameter j is defined as the number of diagonal lines, and when $j = 0$ we say the system is in the completely correct state.

Beyond a straightforward permutation interpretation of this model, there is an alternative (but formally equivalent) system which is defined by the Hamiltonian Eq.(3.1). Consider a collection of $2N$ subunits which only exist in N labeled pairs where each pair consists of a black subunit and a white subunit, e.g., $(B_1, W_1), (B_2, W_2), \ldots (B_{2N}, W_{2N})$. The various microstates of the system (an example of which is shown in Fig. 3.2) are defined as the various ways the pairings could be arranged while ensuring that each pair has one black and one white subunit. If we associate an energy cost λ_k with any pairing where B_k is not paired with its associated W_k, then the statistical physics of the system would be identical to the statistical physics of the permutation model governed by Eq.(3.1). This amounts to the statistical physics of the "matching hat" problem (Blitzstein and Hwang, 2014).

In (Williams, 2017), we found that the statistical physics of such simple systems was

quite interesting because even though their properties were governed by the Hamiltonian Eq.(3.1) in which distinct lattice sites did not interact, we could still have qualitative thermodynamically-driven changes in the properties of our system due to the nature of the state space. More quantitatively, for the system defined by the non-interacting Hamiltonian Eq.(3.1) with the global energy cost $\lambda_i = \lambda_0$ for all i, we can show (Appendix B.1) that the correlation between the incorrectness of two sites i and k (with $i \neq k$) is

$$\sigma_{ik}^2 \simeq \frac{1}{N-1}\left(\frac{e^{\beta\lambda_0}}{N}\right)^2,\tag{3.2}$$

for $\beta\lambda_0 < \ln N$. Thus, as the temperature of our system decreases, the likelihood that component i is incorrectly ordered given that k is incorrectly ordered increases. Therefore, the sites are correlated in spite of the non-interacting Hamiltonian. For systems with correlated degrees of freedom, introducing disorder results in qualitative changes in the system's thermal properties. So we can naturally wonder how disorder would affect a model in which the correlation arises at the level of the state space rather than the Hamiltonian.

We explore these ideas in a simple model of a permutation glass. We define a permutation glass as a statistical physics system with a state space consisting of various permutations of a list and with a Hamiltonian defined by a quenched distribution of parameter values. In a previous model, we set $\lambda_i = \lambda_0$ for analytic simplicity, but now we will maintain our distribution of λ_i values. By (Williams, 2017), the partition function for the system with Hamiltonian Eq.(3.1) is

$$Z_N(\{\beta\lambda_i\}) = \int_0^\infty ds\, e^{-s} \prod_{\ell=1}^N \left[1 + (s-1)e^{-\beta\lambda_\ell}\right].\tag{3.3}$$

Applying Laplace's method to Eq.(3.3), we can define the approximate free energy $\mathcal{F}(s_0)$ (modulo a thermodynamically irrelevant factor) according to

$$Z_N(\{\beta\lambda_i\}) \simeq \exp\left[-\beta\mathcal{F}(s_0)\right]\tag{3.4}$$

where

$$\beta \mathcal{F}(s_0) = s_0 - \sum_{\ell=1}^{N} \ln\left(1 + (s_0 - 1)e^{-\beta\lambda_\ell}\right), \tag{3.5}$$

and where $s_0 = s_0(\beta\lambda_1, \cdots, \beta\lambda_N)$ is defined by the critical point condition

$$\sum_{\ell=1}^{N} \frac{1}{e^{\beta\lambda_\ell} + s_0 - 1} = 1. \tag{3.6}$$

We note that the second derivative of the argument of Eq.(3.5) yields

$$\beta \mathcal{F}''(s_0) = \sum_{\ell=1}^{N} \frac{e^{-2\beta\lambda_\ell}}{(1 + (s_0 - 1)e^{-\beta\lambda_\ell})^2}, \tag{3.7}$$

which is always greater than zero. Thus any critical point solution of Eq.(3.6) is also a stable thermal equilibrium.

Also, although Eq.(3.5) is in fact an approximation of the true free energy $\beta F = -\ln Z_N(\{\beta\lambda_i\})$, henceforth, we will work within our approximation and take Eq.(3.5) to be the free energy from which all thermodynamic quantities are computed. The validity of this approximation is coarsely constrained by parameter regimes over which s_0 yields a stable equilibrium for $\mathcal{F}$, and, by Eq.(3.7), this stability is itself only constrained by the physical relevance of the solutions to Eq.(3.6).

We can write Eq.(3.6) in a more physically transparent form. Noting that the average number of incorrect components $\langle j \rangle$ is the sum of $\langle I_{\theta_i \neq \omega_i} \rangle$ over all components, we have

$$\langle j \rangle = \sum_{k=1}^{N} \left\langle \frac{\partial(\beta\mathcal{F})}{\partial(\beta\lambda_k)} \right\rangle = \sum_{k=1}^{N} \frac{(s_0 - 1)e^{-\beta\lambda_k}}{1 + (s_0 - 1)e^{-\beta\lambda_k}}. \tag{3.8}$$

Thus, we find

$\langle j \rangle = s_0 - 1$, and so Eq.(3.6) becomes

$$\sum_{\ell=1}^{N} \frac{1}{e^{\beta\lambda_\ell} + \langle j \rangle} = 1, \tag{3.9}$$

where $\langle j \rangle$ is the order parameter of our permutation system. Therefore, Eq.(3.9) defines the equilibrium of our system given the set of energy costs $\{\lambda_k\}$.

3.3 Transition to the Correct Microstate

In order to find the equilibrium behavior governed by Eq.(3.9), it is useful to introduce a specific distribution of λ_ℓ values and convert Eq.(3.9) into an integral. For a sum over a general function $f(\lambda_\ell)$, where the λ_ℓ are drawn from a normalized distribution $\rho_0(\lambda)$, we can write

$$\frac{1}{N}\sum_{\ell=1}^{N} f(\lambda_\ell) = \int_{-\infty}^{\infty} d\lambda f(\lambda)\left[\frac{1}{N}\sum_{\ell=1}^{N}\delta(\lambda-\lambda_\ell)\right] \equiv \int_{-\infty}^{\infty} d\lambda\, f(\lambda)\rho_0(\lambda). \qquad (3.10)$$

Thus, with each λ_j having the distribution $\rho_0(\lambda)$, Eq.(3.9) can be written as

$$\int_{-\infty}^{\infty} d\lambda\, \frac{\rho_0(\lambda)}{e^{\beta\lambda} + \langle j \rangle} = \frac{1}{N}. \qquad (3.11)$$

This is not the typical way we start an analysis of glassy systems. Motivated by (Sherrington and Kirkpatrick, 1975), the typical approach is to use the replica formalism to simplify the partition function and then use a stability analysis to check the validity of the simplification. Fortunately, as shown in Appendix B.2, the result Eq.(3.11) is consistent with the condition for the existence of the replica symmetric ansatz of the quenched free energy. More encouragingly, as our distribution $\rho_0(\lambda)$ becomes more centered around a single value $\lambda = \lambda_1$, we have $\rho_0(\lambda) \to \delta(\lambda - \lambda_1)$, which leads to Eq.(3.11) reproducing the non-disordered behavior $\langle j \rangle \simeq N - e^{\beta\lambda_1}$ found in (Williams, 2017).

Eq.(3.11) does not appear any more soluble than Eq.(3.9), but we can use it to derive a general result characterizing one type of temperature-dependent behavior in this system: the thermal transition from $\langle j \rangle \neq 0$ to $\langle j \rangle = 0$. Setting $\langle j \rangle = 0$ in Eq.(3.11) for some β_c, we have

$$\int_{-\infty}^{\infty} d\lambda\, \rho_0(\lambda)e^{-\beta_c\lambda} = \frac{1}{N}. \qquad (3.12)$$

For a given distribution $\rho_0(\lambda)$, Eq.(3.12) can be computed and then inverted to find the temperature $k_B T_c = 1/\beta_c$ at which the permutation glass achieves the $\langle j \rangle = 0$ state. But even without detailed knowledge of the distribution, we can use Jensen's inequality (Chandler, 1987) to find an upper limit on this temperature. Given that e^x is convex,

and defining $\overline{f(\lambda)} \equiv \int d\lambda \rho_0(\lambda) f(\lambda)$ we have $\overline{e^{-\beta_c \lambda}} \geq e^{-\beta_c \overline{\lambda}}$, and thus by Eq.(3.12) we find

$$k_B T_c \leq \frac{\overline{\lambda}}{\ln N}. \tag{3.13}$$

Eq.(3.13) states that the temperature at which the permutation glass achieves the completely correct $\langle j \rangle = 0$ state is always less than the corresponding temperature predicted from the permutation system in which all interaction terms have the value $\lambda_i = \overline{\lambda}$. In essence, incorporating disorder into the interaction terms leads to a reduced tolerance for thermal disorder in achieving the $\langle j \rangle = 0$ state. Moreover, Eq.(3.13) indicates that the $\langle j \rangle = 0$ state is achievable only if the mean of the λ distribution is positive.

We can derive an approximate expression for this transition temperature in the limit of small disorder. By the fact that the Fourier transform of $\rho_0(\lambda)$ is the exponential of the cumulant generating function (Kardar, 2007b), we find that Eq.(3.12) implies

$$\sum_{n=1}^{\infty} \frac{(-\beta_c)^n}{n!} \overline{\lambda^n}_c + \ln N = 0 \tag{3.14}$$

where $\overline{\lambda^n}_c$ is the nth cumulant of the distribution $\rho_0(\lambda)$. Eq.(3.14) does not allow us to exactly solve for β_c in terms of the cumulants, but it does allow us to solve for β_c perturbatively assuming the series is dominated by the first and second cumulant. Noting the first cumulant is the mean $\overline{\lambda}$, the second cumulant is the variance σ_λ^2, and assuming $(\beta_c \sigma_\lambda)^2 \gg \beta_c^k \langle \lambda^k \rangle_c$ for $k > 2$, we can approximately solve Eq.(3.14) to obtain

$$\beta_c = \frac{\overline{\lambda}}{\sigma_\lambda^2} \left(1 - \sqrt{1 - \frac{2\sigma_\lambda^2}{\overline{\lambda}^2} \ln N} \right) + \cdots, \tag{3.15}$$

where we dropped the extraneous solution which yields $\beta_c \to \infty$ as $\sigma_\lambda \to 0$. Eq.(3.15) is a general result giving the temperature at which $\langle j \rangle = 0$ transitions to $\langle j \rangle \neq 0$ (or vice-versa) for any distribution $\rho_0(\lambda)$, contingent on the assumption that the cumulants of order higher order than 2 are subdominant. In spite of its limited validity, this result affords us some intuition into how small amounts of disorder affect the transition temperature of our system. If we take our distribution of energy costs to be highly peaked at $\overline{\lambda}$ with a small

width $\sigma_\lambda \sqrt{2 \ln N} \ll \bar{\lambda}$, we can expand Eq.(3.15) to find

$$\frac{T_c(\sigma_\lambda)}{T_c(0)} = 1 - \frac{\sigma_\lambda^2}{2\bar{\lambda}^2} \ln N + \mathcal{O}\left(\sigma_\lambda^4/\bar{\lambda}^4\right), \tag{3.16}$$

where $T_c(0) \equiv T_c(\sigma_\lambda = 0) = \bar{\lambda}/\ln N$ is the transition temperature for the non-disordered system. Consistent with Eq.(3.13), Eq.(3.16) shows that the effect of making our permutation system slightly glassy (i.e., imbuing it with nonzero σ_λ) is to lower the temperature at which the system transitions from $\langle j \rangle \neq 0$ to $\langle j \rangle = 0$.

The qualitative explanation for this result is straightforward. Introducing disorder at the level of interactions effectively increases the entropy of our system, and the system then compensates for this additional entropy by making the thermal disorder limit for achieving the $\langle j \rangle = 0$ state more stringent. In a sense, because of the interaction disorder, the free energy equilibrium of the system becomes less tolerant of thermal disorder. Thus, the transition temperature, a proxy for limiting thermal disorder, is reduced. A heuristic derivation employing this intuition and reproducing an order of magnitude estimate of Eq.(3.16) is provided in Appendix B.3.

To generalize this result, we cannot make direct use of the expansion Eq.(3.14): Since Eq.(3.15) and Eq.(3.16) do not apply when higher-order cumulants cannot be neglected, a perturbative analysis is not generally useful. Therefore when higher order cumulants are relevant, we have to calculate Eq.(3.11) analytically or numerically and then determine how the value and existence of β_c depend on the properties of the chosen $\rho_0(\lambda)$. In the next section, we discuss how such properties affect β_c by calculating the transition temperature for different energy-cost distributions.

3.3.1 Example distributions

The result Eq.(3.16) predicts the value of the transition temperature presuming the width of the energy-cost distribution is small. More generally, to find the transition temperature we would need to evaluate Eq.(3.12) exactly. We will perform this calculation by considering example distributions of $\rho_0(\lambda)$: a Gaussian distribution, a uniform distribution, and a symmetric Bernoulli distribution.

In analogy to Eq.(3.15), we will compute the transition temperature, and, additionally, the conditions for the existence of the transition temperature for each of these distributions. In a later section, we will show that in spite of the diversity of these conditions, they can all be subsumed into a single inequality which places an upper limit on the probability that our energy cost for an incorrect component is less than zero (i.e., the probability that the energy cost is actually an energy benefit).

Gaussian distribution

We consider a Gaussian distribution. Given mean λ_0 and variance σ_0^2, we have the energy-costs density

$$\rho_0(\lambda) = \frac{1}{\sqrt{2\pi\sigma_0^2}} e^{-(\lambda - \lambda_0)^2/2\sigma_0^2}. \tag{3.17}$$

With this distribution, we would like to use Eq.(3.11) to find a closed-form analytic expression for $\langle j \rangle$, but, due to the insolubility of the resulting integral, we will instead use Eq.(3.14) to find a value for β_c. Because Eq.(3.17) is Gaussian, the cumulants of order higher than 2 are zero, and Eq.(3.14) reduces to

$$-\beta_c\lambda_0 + \frac{1}{2}\beta_c^2\sigma_\lambda^2 + \ln N = 0. \tag{3.18}$$

Therefore we find our β_c is exactly identical to Eq.(3.15) without the additional higher order terms:

$$\beta_c = \frac{\lambda_0}{\sigma_0^2}\left(1 - \sqrt{1 - \frac{2\sigma_0^2}{\lambda_0^2}\ln N}\right). \tag{3.19}$$

A corollary of Eq.(3.19) is that β_c exists and the system is able to achieve the $\langle j \rangle = 0$ state only if the mean and variance of the Gaussian satisfy

$$\frac{\lambda_0}{\sigma_0} \geq \sqrt{2\ln N}. \tag{3.20}$$

Eq.(3.20) indicates that as $N \to \infty$ and the number of incorrect microstates in the system increases, the mean of the Gaussian distribution of energy costs must increase with N, although sub-logarithmically so, in order for the $\langle j \rangle = 0$ state to be achievable.

Uniform distribution

We consider a uniform distribution with a finite domain. The distribution of λ values is defined as

$$\rho_0(\lambda) = \begin{cases} \dfrac{1}{2\sqrt{3}\sigma_0} & \text{for } \lambda_0 - \sigma_0\sqrt{3} \leq \lambda \leq \lambda_0 + \sigma_0\sqrt{3} \\ 0 & \text{otherwise.} \end{cases} \tag{3.21}$$

Eq.(3.21) defines a system in which each λ_k in Eq.(3.1) has a constant probability $\Delta\lambda/2\sqrt{3}\sigma_0$ to be found within an energy width $\Delta\lambda$ as long as this width is within the domain $[\lambda_0 - \sigma_0\sqrt{3}, \lambda_0 + \sigma_0\sqrt{3}]$. The form of Eq.(3.21) was chosen so that the mean is λ_0 and the variance is σ_0^2. For this distribution, we cannot compute $\langle j \rangle$ exactly given Eq.(3.11), but we can establish an implicit condition on the existence of $\langle j \rangle = 0$. Computing Eq.(3.12) given Eq.(3.21), and, taking the logarithm of the result, we find the condition

$$-\beta_c\lambda_0 + \ln\left[\frac{\sinh(\beta_c\sigma_0\sqrt{3})}{\beta_c\sigma_0\sqrt{3}}\right] + \ln N = 0. \tag{3.22}$$

We note that as $\sigma_0 \to 0$ in Eq.(3.22), $\beta_c \to \ln N/\lambda_0$, and thus this result is consistent with the zero-disorder limit. Moreover, if we were to expand Eq.(3.22) in the limit $\beta_c\sigma_0 \ll 1$, we would obtain a quadratic equation the solution of which matches Eq.(3.15). Considering the large-disorder limit $\beta_c\sigma_0 \gg 1$, we find that Eq.(3.22) has the solution

$$\beta_c \simeq \frac{1}{\lambda_0 - \sigma_0\sqrt{3}} W_0\left(\frac{N}{2\sigma_0\sqrt{3}}(\lambda_0 - \sigma_0\sqrt{3})\right), \tag{3.23}$$

where $W_0(x)$ is the principal branch of the Lambert-W function (Weisstein, 2002d). Since the sign of W_0 matches the sign of its argument, Eq.(3.23) is always positive for valid ranges of the distribution parameters. Thus the parameters are only constrained by the existence of a real W_0, which is in turn constrained by the condition that its argument is greater than or equal to $-e^{-1}$. We therefore find that for Eq.(3.23) to exist (and hence for the system to be able to achieve the $\langle j \rangle = 0$ state), the mean and variance must satisfy

$$\frac{\lambda_0}{\sigma_0} \geq \sqrt{3}\left(1 - \frac{2}{Ne}\right). \tag{3.24}$$

We note that Eq.(3.24), in contrast to Eq.(3.20), becomes independent of N in the $N \gg 1$ limit. Namely, as $N \to \infty$, the mean of the uniform distribution just needs to exceed a fixed multiple of the variance in order for the $\langle j \rangle = 0$ state to be achievable.

Symmetric Bernoulli distribution

We consider a symmetric Bernoulli distribution. The energy costs are distributed according to

$$\rho_0(\lambda) = q\delta(\lambda - \lambda_+) + (1-q)\delta(\lambda + \lambda_+), \tag{3.25}$$

where q is a dimensionless number satisfying $0 \leq q \leq 1$, and we take $\lambda_+ > 0$. Conceptually, Eq.(3.25) defines a system in which each λ_k in Eq.(3.1) has a probability q of being λ_+ and a probability $1 - q$ of being $-\lambda_+$. It is possible to solve Eq.(3.11) for $\langle j \rangle$ given the distribution Eq.(3.25) (Appendix B.4), but here we are more concerned with the conditions which allow for the existence of $\langle j \rangle = 0$.

For Eq.(3.25), the conditions for the existence of a β_c satisfying Eq.(3.15) are

$$qe^{-\beta_c\lambda_+} + (1-q)e^{\beta_c\lambda_+} = \frac{1}{N}. \tag{3.26}$$

As a check, we note that taking $q \to 1$ in Eq.(3.26) yields the solution $\beta_c = \ln N / \lambda_+$ as expected. Also, taking the logarithm of both sides of Eq.(3.26) and expanding the right hand side to second order in β_c yields a quadratic equation which reproduces Eq.(3.15) upon solution.

Eq.(3.26) can be solved exactly for β_c. Doing so (and dropping the solution which does not yield a finite β_c in the $q \to 1$ limit) yields

$$\beta_c\lambda_+ = \ln\left[\frac{1}{2N(1-q)}\left(1 - \sqrt{1 - 4N^2q(1-q)}\right)\right]. \tag{3.27}$$

It is possible to show that the argument of the logarithm in Eq.(3.27) is always greater than 1 provided $N > 1$. Thus, the only constraint on the existence of a real and positive β_c is the sign of the argument in the square root. Mandating the argument of the square root is

positive semidefinite, we find the condition

$$q \geq \frac{1}{2}\left(1 + \sqrt{1 - \frac{1}{N^2}}\right), \tag{3.28}$$

where we dropped the inequality which allowed for an extraneous $q = 0$ solution. In the limit $N \gg 1$, Eq.(3.28) tells us that the distribution Eq.(3.25) only yields the completely correct $\langle j \rangle = 0$ equilibrium if the probability of getting $\lambda = \lambda_+$ is very close to 1.

The minimal q predicted by Eq.(3.28) can be understood from the form of Eq.(3.25). The two λ values permitted by Eq.(3.25) are symmetric about $\lambda = 0$, but because the existence of the equilibrium $\langle j \rangle = 0$ depends only on the existence of an energy cost (rather than an energy benefit) of deviating from the correctly ordered microstate, only the positive λ value ensures the possibility of the $\langle j \rangle = 0$ equilibrium. As N increases, the possible number of incorrectly-ordered states in the system increases, and thus to ensure that all components are on average correctly ordered (i.e., that $\langle j \rangle = 0$ is satisfied), there needs to be a greater probability of having an energy cost and a corresponding lower probability of having an energy benefit. Thus we find q must approach 1 as $N \to \infty$.

To compare Eq.(3.28) with the results for our other distributions, we rewrite it in terms of the mean λ_0 and variance σ_0^2. From Eq.(3.25), we find

$$\lambda_0 = \lambda_+(2q - 1), \quad \sigma_0^2 = \lambda_+^2 4q(1 - q). \tag{3.29}$$

Using Eq.(3.29) to translate the inequality Eq.(3.28) into a constraint on λ_0 and σ_0, we find that β_c in Eq.(3.27) only exists if

$$\frac{\lambda_0}{\sigma_0} \geq \sqrt{N^2 - 1}. \tag{3.30}$$

In other words, Eq.(3.30) establishes the condition the distribution Eq.(3.25) must satisfy in order for the system to admit a $\langle j \rangle = 0$ equilibrium. Comparing Eq.(3.30), Eq.(3.20), and Eq.(3.24) we note that Eq.(3.30) establishes the most stringent constraint for the existence of this equilibrium: As $N \to \infty$, the mean energy costs must increase linearly with N in order for the $\langle j \rangle = 0$ state to be achievable.
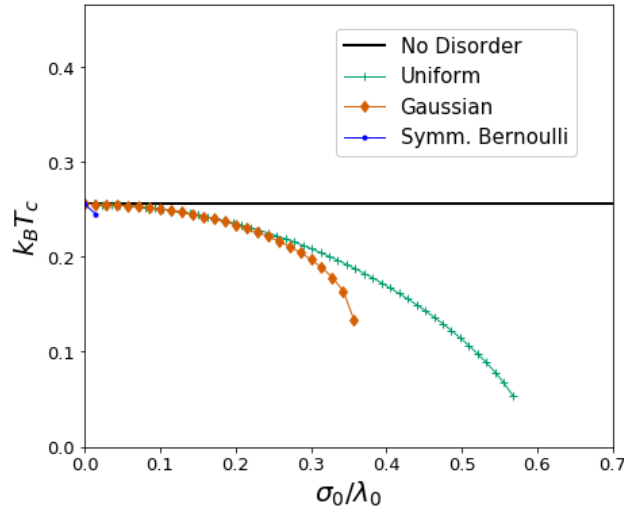
FIGURE 3.3: Plots of transition temperature vs mean-normalized standard deviation for $N = 50$. The horizontal axis is a proxy for disorder in the energy-cost distribution, and the vertical axis gives the corresponding thermal disorder the system can tolerate while still allowing $\langle j \rangle = 0$ to be accessible. The $k_B T_c$ curves for the Gaussian, uniform, and symmetric Bernoulli distribution are found from Eq.(3.19), Eq.(3.22), and Eq.(3.27), respectively. Each curve is only plotted for the domain of σ_0 / λ_0 which yields real values for $k_B T_c$, and thus the relative end points of the curves allow us to compare which distributions are most tolerant of disorder in the energy-cost distribution.

3.3.2 Comparison of transition temperatures

In Fig. 3.3 we plot the derived transition temperatures Eq.(3.19), Eq.(3.22), and Eq.(3.27) (with λ_+ and q computed from Eq.(3.29)) as functions of σ_0 / λ_0. We see that the symmetric Bernoulli distribution curve ends at $\sigma_0 / \lambda_0 \approx 0.02$ and thus admits the smallest amount of energy-cost disorder before the $\langle j \rangle = 0$ state is unachievable. Conversely, the uniform distribution ends at $\sigma_0 / \lambda_0 \approx 0.56$ and thus admits the largest amount of energy-cost disorder.

Consistent with Eq.(3.13) and the intuition underlying Eq.(3.16), we find that each distribution predicts a transition temperature satisfying

$$k_B T_c \leq \frac{\lambda_0}{\ln N} \tag{3.31}$$

and thus predicts a lower transition temperature than the corresponding non-disordered prediction. In the same way that the transition temperature results Eq.(3.19), Eq.(3.27), and Eq.(3.22) must be consistent with Eq.(3.31), in a future section, we will show how each of
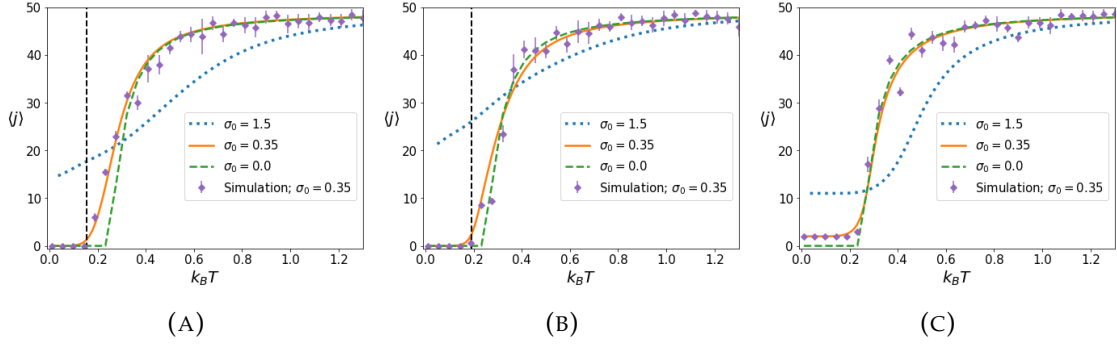
FIGURE 3.4: Theory and simulation comparison for $N = 50$. (a) Gaussian distribution. (b) Uniform distribution. (c) Symmetric Bernoulli distribution. All distributions were defined with $\lambda_0 = 1.0$. As the theoretical (i.e., non-simulated) results, in each figure, we have dashed, dotted, and solid line curves which were all computed from Eq.(3.34). The dashed curve corresponds to the zero-disorder ($\sigma_0 = 0.0$) solution Eq.(3.32). The dotted curve corresponds to the high-disorder ($\sigma_0/\lambda_0 = 1.5$) solution. The solid curve defines our intermediate-disorder ($\sigma_0 = 0.35$) solution. The vertical dashed lines in (a) and (b) are the transition temperatures computed from Eq.(3.19) and Eq.(3.23), respectively, at $(\lambda_0, \sigma_0) = (1.0, 0.35)$; there is no transition temperature for Fig. 3.4c because $\sigma_0/\lambda_0 = 0.35$ violates Eq.(3.30). The points in each plot are the simulated results for the $\sigma_0 = 0.35$ solution. We note that for (a), (b), and (c), Eq.(3.34) matches the simulated results, and for (a) and (b), the temperatures computed from Eq.(3.19) and Eq.(3.23) correctly match the temperature value at which the simulation transitions from $\langle j \rangle = 0$ to $\langle j \rangle > 0$.

the previous distribution-specific constraints on λ_0/σ_0 can be unified into a distribution-independent result expressed in terms of $P_{\lambda<0}$, the probability that an incorrectly-ordered component is energetically favored. But first, in the next section, we compare these analytic results to results from simulations.

3.4 Simulation Comparison

We seek to affirm the theoretical transition temperatures of the previous section by comparing them to simulation results. Doing so requires us to simulate how $\langle j \rangle$ varies as a function of temperature when the $\{\lambda_i\}$ are drawn from the Gaussian, uniform, and symmetric Bernoulli distributions.

First, we derive a more general theoretical prediction to which we will compare the simulations. For the statistical physics of the non-disordered model where the Hamiltonian is $\mathcal{H} = \lambda_0 \sum_i I_{\theta_i \neq \omega_i}$, we know the order parameter has the simple form

$$\langle j \rangle \simeq N - e^{\beta\lambda_0} \qquad \text{(non-disordered result)}. \tag{3.32}$$

We would like to find analogous results for our permutation glasses defined by various distributions of energy costs. This would amount to computing Eq.(3.12) for a given distribution and inverting it to find $\langle j \rangle$ as a function of temperature and the parameters of the distribution. This procedure can be implemented exactly for the symmetric Bernoulli distribution, but there seems to be no analytic solution for the Gaussian or the uniform distribution. So, we will instead use a more general expression for $\langle j \rangle$ which allows us to reduce all the distribution-dependent order parameters to a common form.

Given the Hamiltonian Eq.(3.1) and that $\langle j \rangle$ is the sum of $\langle I_{\theta_i \neq \omega_i} \rangle$ across all components, we have

$$\langle j \rangle = -\sum_{i=1}^{N} \frac{\partial}{\partial(\beta\lambda_i)} \ln Z_N(\{\beta\lambda_i\}). \tag{3.33}$$

Then, using Eq.(3.3), yields the general result

$$\langle j \rangle = N - \frac{1}{Z_N(\{\beta\lambda_i\})} \sum_{k=1}^{N} Z_{N-1}(\{\beta\lambda_i\}_{i\neq k}), \tag{3.34}$$

where $Z_{N-1}(\{\beta\lambda_i\}_{i\neq k})$ is defined by Eq.(3.3) with the product taken over the $N-1$ elements of $\{\lambda_i\}$ not including λ_k. The utility of Eq.(3.34) is that it gives us the exact temperature dependence of the order parameter contingent on a particular distribution of energy costs. The caveat is that, rather than being a function of distribution parameters like means and variances, Eq.(3.34) requires us to draw the explicit set of $\{\lambda_i\}$ from the given distribution.

With Eq.(3.34), we have our theoretical prediction and can now discuss the simulation. The simulation was set up as follows: First, the vector $\vec{\omega} = (1, 2, \ldots, N)$ was defined to be the completely correct permutation. This was the initial state in the simulation. Single-step state transitions were enacted by exchanging two randomly chosen elements of the current vector contingent on the Metropolis acceptance criterion, i.e., that $e^{-(E_f - E_i)/T} < u$ where E_f and E_i were the final and initial state energies, respectively, T was the temperature, and u was a number drawn uniformly from $[0, 1)$. The initial and final state energies were computed from Eq.(3.1) where the $\{\lambda_i\}$ were drawn from the given distribution defined by a mean λ_0 and variance σ_0^2. The simulation was run for 5×10^4 steps of which

the last 10^3 steps were used to define the ensemble of states. From this ensemble of states, we computed j (the number of elements in the state which did not match the corresponding element in $\vec{\omega}$) for each state and then averaged this value of j across all states in the ensemble to find the simulation prediction of $\langle j \rangle$ at a specific temperature. We chose 30 temperature values between 0.1 and 1.3. Finally, for a given distribution, the drawn set of $\{\lambda_i\}$ was used in Eq.(3.34) to obtain the corresponding theoretical prediction.

In Figures 4a, 4b, and 4c, we show simulation results for the parameter values $(N, \lambda_0, \sigma_0) = (50, 1.0, 0.35)$; respectively, these figures correspond to the Gaussian, uniform, and symmetric Bernoulli distribution of energy costs. As theory comparisons, for each distribution, we also plotted Eq.(3.34) for the same parameter values as in the simulation. We note that in all three cases, the theory curves well match the simulated results. As zero-disorder and high-disorder comparisons, we included theory curves of the order parameter for the standard deviation values $\sigma_0 = 0.0$ and 1.5 with N and λ_0 the same in all cases. From the differences in the curves among the plots, we see that at high disorder, the temperature behavior of Eq.(3.34) is greatly dependent on the distribution from which the $\{\lambda_i\}$ are drawn.

Finally, for Fig. 3.4a and Fig. 3.4b, we computed the transition temperatures obtained from Eq.(3.19) and Eq.(3.23), respectively, and displayed the predictions as vertical dashed lines. Consistent with the simulation results, these lines correspond to the temperature values at which $\langle j \rangle$ transitions from zero to non-zero values or vice versa. Moreover, we note that, consistent with Fig. 3.3, a disorder of $\sigma_0/\lambda_0 = 0.35$ allows the order parameter for the Gaussian and uniform distributions to reach $\langle j \rangle = 0$ at sufficiently low temperatures, but, at this level of disorder, the order parameter for the symmetric Bernoulli distribution remains non-zero over its entire temperature range because its $k_B T_c$ does not exist.

The similarity between the theoretical and the simulation results is reassuring, but what still remains is the task of finding a unified interpretation for the constraints Eq.(3.20), Eq.(3.24), and Eq.(3.30). We turn to developing such an interpretation in the following section.

3.5   Understanding Parameter Constraints

What is strange about the parameter conditions given by Eq.(3.20), Eq.(3.24), and Eq.(3.30) is their variety. Although each represents the conditions the mean and variance of the respective distribution must satisfy in order for the $\langle j \rangle = 0$ state to be an equilibrium, they all have quite different scaling behaviors as functions of N. Perhaps most interestingly, the condition Eq.(3.24) becomes independent of N in the $N \gg 1$ limit, thus suggesting that at large N the amount of interaction disorder a system with a uniform distribution of energy costs can tolerate is independent of the number of microstates available to it.

However, underlying this variety in parameter conditions is a unity of the situations giving rise to them. Specifically, the conditions Eq.(3.20), Eq.(3.24), and Eq.(3.30) are the translations into distribution-parameter language of something which bears a common form when written as a probability. We can understand this by determining how the derived conditions place upper limits on the probability of obtaining an energy benefit, i.e., of drawing $\lambda < 0$ from the distribution.

We begin with our previous constraint which must be satisfied in order for β_c to exist:

$$\int_{-\infty}^{\infty} d\lambda \, \rho_0(\lambda) e^{-\beta_c \lambda} = \frac{1}{N}.$$

(3.35)

Next, we define

$$P_{\lambda < 0} \equiv \int_{-\infty}^{0} d\lambda \, \rho_0(\lambda),$$

(3.36)

which represents the probability that a λ_k in Eq.(3.1) is less than zero (i.e., yields an energy benefit for an incorrectly ordered component rather than an energy cost). With the fact that $f(x) < e^x f(x)$ for $x > 0$ and from Eq.(3.35), we can infer that in order for β_c to exist (and, in turn, for the completely correct equilibrium $\langle j \rangle = 0$ to be a physical state) we must have

$$P_{\lambda < 0} < \frac{1}{N}.$$

(3.37)

Thus as $N \to \infty$, the probability of each lattice site having $\lambda < 0$ must go to zero. Physically, we can interpret this result with the same intuition used to interpret Eq.(3.28). As

the number of sites N in our system increases, the number of potential incorrectly ordered microstates also increases, and thus to combat the entropic disorder from these microstates and to ensure the existence of the $\langle j \rangle = 0$ equilibrium, the system must be ever more likely to have an energy cost (rather than an energy benefit) for incorrectly occupying a single site. Thus as N increases, the system must become less tolerant of $\lambda < 0$ values, and $P_{\lambda < 0}$ goes to zero. Finally, the probability limit Eq.(3.37) is consistent with temperature limit Eq.(3.13) since both inequalities are derived from the same equilibrium condition.

Eq.(3.37) is a general result which must be true regardless of the distribution we choose, but what we find is that our previously derived mean-variance conditions are simply representations of Eq.(3.37) in the language of the parameters which define each specific distribution. To better understand how our mean-variance conditions Eq.(3.20), Eq.(3.24), and Eq.(3.30) are related to Eq.(3.37), we interpret them as placing upper limits on how much variance σ_0^2 the system can tolerate before the $\langle j \rangle = 0$ state is no longer an equilibrium. Given that the $\langle j \rangle = 0$ state is only achieved through the positive λ domain of the distribution $\rho_0(\lambda)$, the upper limit on σ_0 must be tantamount to a lower limit on $\int_0^\infty d\lambda\, \rho_0(\lambda)$, or, equivalently an upper limit on $\int_{-\infty}^0 d\lambda\, \rho_0(\lambda)$. Such an upper limit implies that if too much of the distribution is contained within the negative λ domain, then the $\langle j \rangle = 0$ state is not possible. Thus interpreting Eq.(3.20), Eq.(3.24), and Eq.(3.30) as upper limits on the variances of their respective distributions, we can compute corresponding upper limits on the probability of obtaining a negative value of λ. For the relevant distributions we find (Appendix B.5)

$$P_{\lambda<0}^{\text{uniform}} \leq \frac{1}{Ne} \tag{3.38}$$

$$P_{\lambda<0}^{\text{gauss}} \lesssim \frac{1}{2N\sqrt{\pi \ln N}} \tag{3.39}$$

$$P_{\lambda<0}^{\text{bernoulli}} \lesssim \frac{1}{4N^2} \tag{3.40}$$

The above expressions represent the maximum probability of having an energy benefit in the system and still being able to achieve the $\langle j \rangle = 0$ state at a certain temperature. All of these results are unified by their inverse scaling with N and, as shown in Fig. 3.5, their
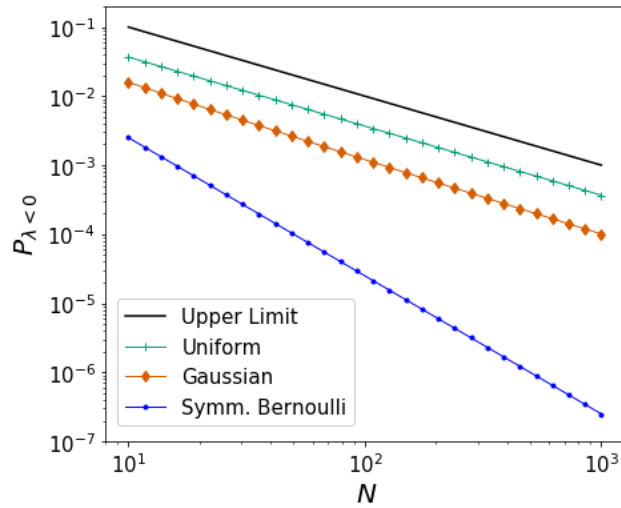
FIGURE 3.5: Log-log plot of the critical probabilities Eq.(3.37), Eq.(3.38), Eq.(3.39), and Eq.(3.40) as functions of N. The curves give the critical probability above which the $\langle j \rangle = 0$ equilibrium cannot be achieved for the given distribution. The solid curve represents the upper limit on critical probabilities established by Eq.(3.37). The closer the probability curve is to this upper limit, the more disorder it can admit before the $\langle j \rangle = 0$ equilibrium is unachievable. Consistent with Eq.(3.37), each critical probability curve exists below this $1/N$ limit.

consistency with the limit established by Eq.(3.37).

The results Eq.(3.38), Eq.(3.39), and Eq.(3.40) afford us a new interpretation of the results in Fig. 3.3. We previously noted that the uniform distribution admitted the most amount of disorder before the $\langle j \rangle = 0$ state was inaccessible and that the symmetric Bernoulli distribution admitted the least amount of disorder. From Fig. 3.5 we see why: The uniform distribution allows the most amount of disorder because it admits the largest probability of energy benefits for incorrectly ordered components. By admitting a larger probability of energetically beneficial incorrect components, the distribution need not be tightly concentrated about the mean and can therefore have a higher standard deviation. Conversely, the symmetric Bernoulli distribution allows the least amount of disorder because it admits the smallest probability of energy benefits for incorrectly ordered components. The Gaussian distribution admits an intermediate value of disorder because its limiting probability exists between the limiting probabilities of the two other distributions.

Arguably, this explanation simply translates the old question into a new one: Why, conceptually, do the various distributions have the limiting probabilities shown in Fig.

3.5? Their relative ordering could be understood by considering the $\lambda < 0$ tails of each distribution. In order for the $\langle j \rangle = 0$ state to be accessible, the distribution needs to be dominated by positive values of λ. We can roughly understand this by noting that in the non-disordered result Eq.(3.32), $\langle j \rangle = 0$ is not accessible if $\lambda_0 < 0$. For the uniform distribution Eq.(3.21), it is possible to completely eliminate $\lambda < 0$ values by simply increasing the ratio λ_0/σ_0 with σ_0 finite; thus for the uniform distribution, σ_0 can be finite and possibly large while the $\langle j \rangle = 0$ state is still accessible. However, the long tail of the Gaussian Eq.(3.17) implies there will always be $\lambda < 0$ values for non-zero σ_0. This is even more so for the symmetric Bernoulli distribution Eq.(3.25) since its probability density is not defined by an exponential fall off. Thus, in order to limit the $\lambda < 0$ values, the Gaussian distribution needs to be less tolerant of large spreads than the uniform distribution, and the symmetric Bernoulli distribution must be even less tolerant than the Gaussian distribution. This relative tolerance of disorder leads to the sequence shown in Fig. 3.5.

Lastly, noting that the results Eq.(3.38), Eq.(3.39), and Eq.(3.40) all scale at least as $\sim 1/N$ with corrections to the power of N contingent on the distribution, we could guess there exists a stronger limit than Eq.(3.37) which any distribution must satisfy in order for β_c to exist. Namely, in order for the $\langle j \rangle = 0$ state to be achieved, we could conjecture that the probability of obtaining an energy benefit must satisfy, in the $N \gg 1$ limit,

$$P_{\lambda<0} \lesssim \frac{1}{N^{1+\alpha(N)}}, \quad \text{[Conjecture]} \tag{3.41}$$

where $\alpha(N) > 0$ is dependent on the properties of the distribution. Thus the variety of results in the conditions placing limits on the distribution parameters is somewhat misleading because what is important is not the parameters themselves but the probabilities (specifically the probability of an energy benefit) they are associated with.

3.6 Glassy Regime

In the previous sections, we considered the conditions defining a permutations glass which allow for the existence of the $\langle j \rangle = 0$ equilibrium. We pursued this analysis in analogy to
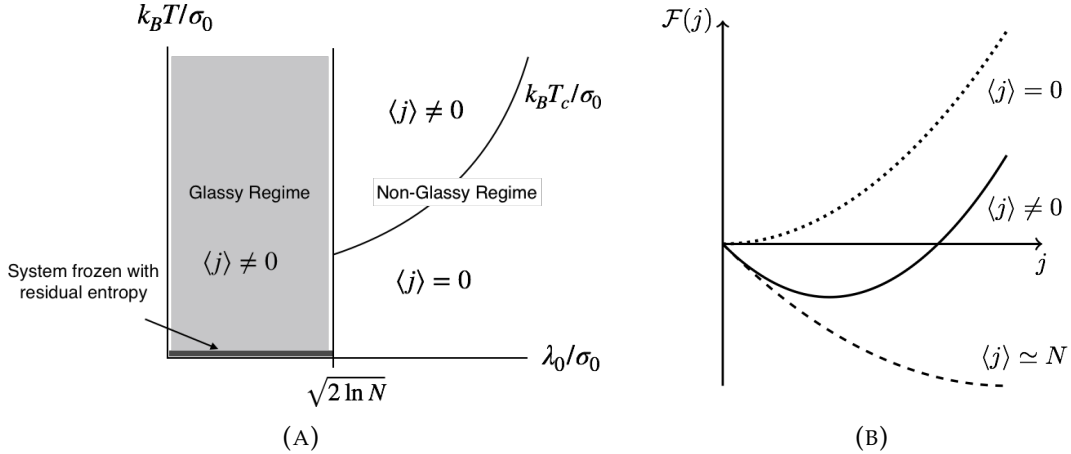
FIGURE 3.6: (a) Glassy and non-glassy regime for a quenched Gaussian distribution of energy costs. Although the order parameter in the non-glassy regime has behavior similar to that in the non-disordered system, the order parameter in the glassy regime is always non-zero and the corresponding system becomes frozen at zero-temperature and exhibits a residual entropy. (b) Schematic of Landau free energy plots of Eq.(3.46). The free energy is shifted so that $\beta \mathcal{F}(j = 0) = 0$. Much like the possible free energies for the non-disordered system where $\rho(\lambda) = \delta(\lambda - \lambda_0)$, we find the disordered system defined by the Hamiltonian Eq.(3.1) has three possible free energy curves each defined by a single equilibrium $\langle j \rangle$ which falls within $[0, N]$. However, for a system in the glassy regime, the free energy with a global minimum at $\langle j \rangle = 0$ cannot be achieved at any temperature even if the average energy cost $\overline{\lambda}$ is positive. Thus the glassy regime is characterized by a non-zero entropy even at zero-temperature.

the non-disordered system where the $\langle j \rangle = 0$ state (found at temperatures below $\lambda_0 / \ln N$) defined the only thermal transition in the system. From the discussion in Sec. 3.5, we see that the permutation glass differs from the non-disordered system in that for the permutation glass it is possible to have a positive mean energy cost $\overline{\lambda}$ with the system still not transitioning to $\langle j \rangle = 0$ at a physical temperature. The $\langle j \rangle = 0$ macrostate is significant because it is the only macrostate for which the system has a single microstate and hence an entropy of zero. The number of microstates associated with a general j is given by Williams, 2017

$$\Omega_N(j) = \binom{N}{j} d_j, \tag{3.42}$$

where d_j is the number of derangements of a list with j elements. We only find $\Omega_N = 1$, when $j = 0$ and thus if Eq.(3.35) cannot be satisfied at a physical temperature $k_B T_c$, the system always has a non-zero entropy.

Using Eq.(3.35), there are two results which are important in defining a glassy regime for this system. First, we recall the derived inequality

$$k_B T_c \leq \frac{\overline{\lambda}}{\ln N}, \tag{3.43}$$

Eq.(3.43) requires that any temperature at which $\langle j \rangle = 0$ is achieved to fall below $\overline{\lambda}/\ln N$ and, importantly, a necessary condition for such a temperature to exist is for $\overline{\lambda} > 0$. For the case without quenched disorder (i.e., $\rho_0(\lambda) = \delta(\lambda - \overline{\lambda})$), the inequality in Eq.(3.43) becomes an equality, and the system always assumes the $\langle j \rangle = 0$ macrostate when $k_B T$ falls below the stated value.

However, for quenched distributions an additional constraint must be satisfied. For the Gaussian, symmetric Bernoulli, and uniform two-parameter distributions analyzed in Sec 3.3.1, the critical temperature takes on the general schematic form of $k_B T_c(\lambda_0, \sigma_0, N)$, where λ_0 and σ_0 are the mean and standard deviation of the distributions. For all of these analyzed distributions, we found that there was a minimum value of λ_0/σ_0 below which $k_B T_c(\lambda_0, \sigma_0, N)$ was no-longer physical. Namely, Eq.(3.35) only had a real solution for β_c, if

$$\frac{\lambda_0}{\sigma_0} \geq f(N), \tag{3.44}$$

for some function $f(N)$ that depends on the properties of the distribution. In other words, even if $\overline{\lambda} > 0$ and there are temperatures $k_B T$ that exist below $\overline{\lambda}/\ln N$, none of these temperatures would yield the $\langle j \rangle = 0$ equilibrium unless Eq.(3.44) is satisfied as well. If Eq.(3.44) is violated, then even at zero-temperature we would have $\langle j \rangle \neq 0$ and, by Eq.(3.42), the entropy of the system would be non-zero. Therefore, when Eq.(3.44) is violated the system exhibits a zero-temperature residual entropy typical of glassy systems (Nemilov, 2009) and we can take a violation of Eq.(3.44) together with a positive $\overline{\lambda}$ to be definitive of the "glassy regime" of the system.

These ideas become clearer with a concrete example and a figure. For a quenched distribution of energy-costs drawn from a Gaussian distribution, we found the critical temperature.

$$\frac{k_B T_c}{\sigma_0} = \left(\frac{\lambda_0}{\sigma_0} - \sqrt{\frac{\lambda_0^2}{\sigma_0^2} - 2 \ln N} \right)^{-1}. \tag{3.45}$$

The phase diagram associated with this result is shown in Fig. 3.6a. The figure depicts the fact that, for $\lambda_0/\sigma_0 < \sqrt{2 \ln N}$, Eq.(3.45) becomes imaginary and the system enters the glassy regime and that although both the non-glassy and glassy regime have $\langle j \rangle \neq 0$ macrostates, unlike the non-glassy regime, the glassy regime never achieves $\langle j \rangle = 0$ at a physical temperature.

We have already derived a more general condition for establishing the existence of the glassy regime. We can found that a necessary, but not sufficient, condition for the $\langle j \rangle = 0$ macrostate to exist is that $P_{\lambda<0} < 1/N$. Therefore, a sufficient, but not necessary, condition for the system to exist in a glassy regime is for this inequality to be violated, namely for $P_{\lambda<0} \geq \frac{1}{N}$. Because $P_{\lambda<0} < 1/N$ is a weaker condition for the existence of the $\langle j \rangle = 0$ state than the condition derived directly from an analysis of the critical temperature, the condition $P_{\lambda<0} \geq \frac{1}{N}$ is stronger than necessary for establishing the existence of the glassy regime.

Looking beyond this result, we might expect the introduction of disorder into our permutation system to come with the multiple equilibria and ultrametricity of SK spin glasses. However, for the class of permutation glasses considered here, this is not the case. We can see this by computing the Landau free energy for this disordered system. By Eq.(3.5), Eq.(3.10), and the substitution $s - 1 \rightarrow j$, we find

$$\beta \mathcal{F}(j) = 1 + j - N \int_{-\infty}^{\infty} d\lambda \, \rho_0(\lambda) \ln \left(1 + j e^{-\beta \lambda} \right), \tag{3.46}$$

In Fig. 3.6b, we schematically plot this free energy, noting that it exhibits all of the functional forms of the free energy for the non-disordered case $\rho_0(\lambda) = \delta(\lambda - \lambda_0)$. Mathematically, this arises due to its stability conditions: Because the free energy for the glassy system is always convex, it can have at most one minimum and, by the constraints of this system,

this minimum must occur somewhere in the range of $0 \leq j \leq N$. However, not all forms of this free energy are accessible for all parameter values in the system. In particular, for the glassy regime in which Eq.(3.35) has no solution, the free-energy curve with a global minimum at $\langle j \rangle = 0$ cannot be achieved and the system has $\langle j \rangle \neq 0$ for all temperatures.

Thus, for the simple permutation glass considered in this paper, we say the system exists in the "glassy regime" if Eq.(3.35) does not admit a solution for β_c even when the mean energy costs $\overline{\lambda}$ is greater than zero. This simplest version of a permutation glass does not exhibit the replica symmetry breaking and ultrametricity characteristic of SK glasses, but we argue for the labeling of a particular regime as "glassy" due to its differing properties from the non-glassy regime: In the non-glassy regime, the disorder is not large enough to lead to phase behavior different from that for the non-disordered system. However, in the glassy regime, the disorder is so large that even at zero-temperature the system can exist in multiple microstates even if there is only a single free energy minima as a function of j. Therefore, the simplest permutation glass does exhibit glassy behavior.

3.7 Discussion

Motivated by the importance of the orderings of amino acid sequences in the structure and function of proteins, a model was previously proposed to study the equilibrium thermodynamics of a system where particular permutations of an ordered list defined various energy states of the system. In that model, for simplicity and solubility, it was imposed that all lattice sites had the same energy cost for an incorrectly ordered component. However, more generally, it would have been useful to consider a system of permutations where the energy cost for each lattice site was drawn from a quenched distribution of energy costs.

We considered such permutation glasses here. The replica symmetric ansatz of such glasses yielded a result consistent with the thermodynamically stable state computed by applying Laplace's method to the partition function. We found that this simplest permutation glass exhibits a glassy regime–characterized by $\langle j \rangle \neq 0$ for all temperatures–if Eq.(3.35) cannot be satisfied even when $\overline{\lambda} > 0$. In the non-glassy regime, the $\langle j \rangle = 0$ state

can be achieved but the transition temperature satisfies $k_B T_c \leq \overline{\lambda}/\ln N$, and thus the system is less tolerant of thermal disorder than is the non-disordered system in moving to the $\langle j \rangle = 0$ state.

From this analysis we found that we must have $P_{\lambda < 0} < 1/N$ in order for $\langle j \rangle = 0$ to be a possible macrostate, that is, in order for the completely correct ordering to be an achievable thermal equilibrium and for the system to be in the non-glassy regime, the probability of having an energy benefit for an incorrectly ordered component must be less than the inverse of the number of components in the system.

But having considered the permutation glass defined by the "non-interacting" Hamiltonian Eq.(3.1), a natural extension would be to consider a permutation glass with the typical spin glass-like Hamiltonian

$$\mathcal{H} = \sum_{i<j} \mu_{ij} I_{\theta_i \neq \omega_i} I_{\theta_j \neq \omega_j}, \tag{3.47}$$

where μ_{ij} is drawn from a distribution of interaction energies. Such a Hamiltonian associates an energy cost μ_{ij} with a permutation where both component i and component j are in an incorrect position. When the global analog of Eq.(3.47) was studied in (Williams, 2017), we found very non-trivial regime behavior including multiple metastable states, multiple transition temperatures, and quadruple and triple points. Thus, considering the disordered behavior of a system with Hamiltonian Eq.(3.47), should yield some novel results (such as replica symmetry breaking) over the simpler phase behavior depicted in Fig. 3.6a.

Also, it is well known that spin glasses and other disordered systems often exhibit non-exponential relaxation behavior and memory effects (Binder and Young, 1986), thus an interesting question would be whether such properties exist in kinetic permutation glasses. Answering such a question would likely require studying glasses defined by Eq.(3.47) rather than Eq.(3.1). In spin glass models, the glass transition temperature is important in defining the onset of such non-exponential relaxations. However, the analog of such a temperature does not seem to exist in the model defined by Eq.(3.1). Thus, before a kinetic analysis of permutation glasses can yield additional insights into the non-equilibrium

properties of disordered systems, it would likely prove necessary to consider more complex glass models than the one considered in this paper.

Finally, we mention that our free energy Eq.(3.46) is reminiscent of a solution to a canonical problem in statistical mechanics. If we have a fermion system with a countably finite (but large) number of energy levels N_{lvl} where each level is labeled ε_k for some integer k, the grand canonical potential of the system would be (Landau, Lifshitz, and Pitaevskii, 1980)

$$\beta \Omega_{\text{Fermi}} = -\sum_k \ln\left(1 + e^{\beta(\mu - \varepsilon_k)}\right)$$
$$= -N_{lvl} \int_{-\infty}^{\infty} d\varepsilon\, g(\varepsilon)\, \ln\left(1 + e^{\beta(\mu - \varepsilon)}\right) \tag{3.48}$$

where μ is the chemical potential, $g(\varepsilon)$ is an energy density, and we used the heuristic Eq.(3.10) to replace the discrete sum with an integral. Comparing Eq.(3.46) and Eq.(3.48), we can transform the former into the latter by making the substitutions $\beta F(j) - 1 - j \to \beta \Omega_{\text{Fermi}}$, $N \to N_{\text{lvl.}}$, and $j \to e^{\beta \mu}$. Now, considering the constraint Eq.(3.11) for the thermal equilibrium of the permutation glass, we find that the analogous constraint for the fermion system is

$$\langle n_{\text{Fermi}} \rangle = e^{\beta \mu} \tag{3.49}$$

where the average number of fermions is given by

$$\langle n_{\text{Fermi}} \rangle = N_{\text{lvl.}} \int_{-\infty}^{\infty} d\varepsilon \frac{g(\varepsilon)}{e^{\beta(\varepsilon - \mu)} + 1}. \tag{3.50}$$

Given the transformation $j \to e^{\beta \mu}$, we see that Eq.(3.49) implies that in translating the equilibrium permutation glass results to a system of fermions, we should interpret the order parameter $\langle j \rangle$ as the average number of fermions $\langle n_{\text{Fermi}} \rangle$. The fact that $0 \leq \langle j \rangle / N \leq 1$ in the permutation glass, therefore correctly implies that $0 \leq \langle n_{\text{Fermi}} \rangle / N_{\text{lvl.}} \leq 1$ in the fermion system. Thus, the model considered in this paper (the canonical ensemble of a simple permutation glass) seems to match the grand canonical ensemble of a fermion system with a large number of energy levels and where the chemical potential is given by

$$\beta\mu = \ln\langle n_{\text{Fermi}}\rangle.$$

Perhaps such a correspondence is not so surprising since permutations are central to the formalisms of both systems. Still, it is worth asking whether this relationship can allow the understanding of one system to yield insights into the other.

Chapter 4

Self-Assembly of a Dimer System

"Faced with the same natural phenomena, my experience is that physicists and biologists will ask different questions, but by the time we find answers, we ought to be able to convince one another that we have accomplished something."

– William Bialek, *Biophysics: A Search for Principles*

4.1   Introduction

Self-assembly occurs in many microbiological systems, driving the formation of bilayer membranes, micelles, and virus capsids (Nelson, 2004). For a macromolecular system to be able to undergo self-assembly, its components must be able to find one another within their larger volume and also be able to distinguish correct from incorrect contacts. In self-assembly, the number of possible incorrect contacts is always much greater than the number of correct contacts, a fact which makes the physical and mathematical problem of self-assembly a combinatorial one.

As a brute force resolution to this combinatorial problem, researchers have often used computational methods to study the specific properties of self-assembled systems (Wales, 2005; Nguyen, Reddy, and Brooks, 2007; Johnston, Louis, and Doye, 2010). Conversely, analytical studies of self-assembly often avoid combinatorics all together and begin under

the infinite volume-infinite particle number assumptions of the law of mass action (Israelachvili, Mitchell, and Ninham, 1976; Marsh, 2012; Perlmutter and Hagan, 2015) or, in order to avoid the complications associated with analyzing a specific system, have focused on more phenomenological properties of self-assembly (Nguyen and Vaikuntanathan, 2016; Norn and André, 2016).

However, it is possible to study self-assembly analytically and specifically in the context of a model whose combinatorial properties are simple enough to admit an exact expression for the partition function. Although the typical examples of self-assembly involve the creation of large macromolecular structures on time scales relevant for cellular function, a simple kind of self-assembly is exemplified in the way single-stranded DNA fragments attach to their complementary strands, transcription factors find their correct DNA binding sites, and proteins seek their optimal binding partners (Fig. 4.1). In all of these systems, as in all systems capable of self-assembly, monomers only assemble into a functional set of interactions if the monomers can find one another and bind correctly.

We can capture the basic features of these systems with a simple model. Say we have $2N$ distinct monomers $\alpha_1, \alpha_2, \dots, \alpha_{2N}$ which form correct or incorrect contacts with one another according to the reaction equation

$$\alpha_i + \alpha_j \rightleftharpoons \alpha_i \alpha_j. \tag{4.1}$$
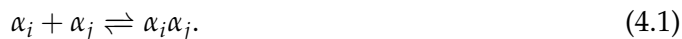
With $2N$ monomers, there are $N(2N-1)$ possible (α_k, α_ℓ) pairs, and we define N of these pairs as correct contacts that have a lower binding energy than that of the remaining $2N(N-1)$ incorrect contacts; $-(E_0 + \Delta)$ for correct contacts compared to $-E_0$ for incorrect ones, where $E_0, \Delta > 0$. We say the system has undergone "fully-correct assembly" when all monomers are bound to their correct partners.

In spite of the apparent simplicity of this model, the correct and incorrect interactions are defined by non-trivial combinatorics which lead to a unique partition function and interesting phase behavior of the self-assembled system. In particular, for a system of monomers contained in a volume V and satisfying $N \gg 1$, we find that the two necessary (but not sufficient) conditions the system must satisfy in order to be capable of fully-correct

(A) ssDNA-ssDNA   (B) TF-DNA   (C) Protein-Protein
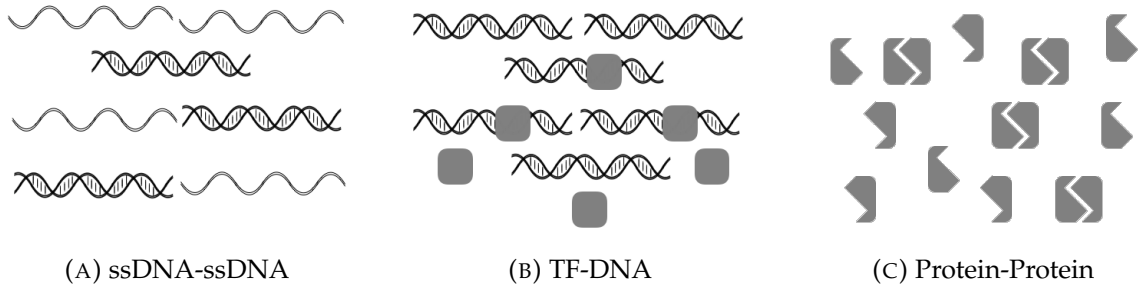
FIGURE 4.1: Example self-assembling biomolecular dimer systems. In (a), distinct single-stranded DNA (ssDNA) strands exist in a system with their complementary strands and with other double-stranded DNA (dsDNA). In (b), transcription factors (TFs) exist in a system with their DNA binding partners and with already bound TF-DNA dimers. Since the binding sites for the DNA are embedded in the much longer strand of an entire DNA molecule, the effective DNA molecules to which the TFs bind are much less motile than their TF partners. In (c), distinct protein monomers exist in a system with the heterodimers formed from them. In all systems, we consider "fully-correct assembly" as the state where all monomers are bound to their correct monomer or binding site.

assembly are

$$2N < e^{\beta \Delta}, \qquad NV < \sqrt{2}\, \lambda_0^3\, e^{\beta(E_0 + \Delta)}, \qquad (4.2)$$

where $\beta = 1/k_B T$ and λ_0 is the de Broglie thermal wavelength of a monomer. The first condition in Eq.(4.2) ensures that the energy advantage for correct contacts can overcome their combinatorial disadvantage. The second condition ensures that the monomers are able to find one another in their volume and bind together. What is interesting about these dual conditions is that, although one might think that number density is a relevant quantity in defining the possibility of self-assembly, the ratio of N and V does not appear, and instead it is their product and N alone which are constrained. Moreover, both conditions in Eq.(4.2) can only clearly be satisfied under finite number and finite volume assumptions and thus a precise statistical physics formulation is required to obtain them.

This problem of building models of correct and incorrect dimers has a few antecedents in the study of protein interactions. The authors of (Deeds et al., 2007) computationally studied the diffusion of dimer-forming lattice proteins in a three-dimensional grid and inferred that low-energy specific dimers dominate higher-energy non-specific dimers, only if the system temperature is low enough that specific dimers are stable but high enough that non-specific dimers are unstable. The authors of (Zhang, Maslov, and Shakhnovich, 2008)

used the law of mass action (Sethna, 2006) to study specific and non-specific protein interactions and establish approximate bounds on the minimum protein concentration and maximum protein diversity a cell requires to be in a safe zone, i.e., a parameter regime where non-functional interactions comprise fewer than 50% of the total interactions. In (Johnson and Hummer, 2010), the authors employed a computational evolutionary model of protein interactions to show how selection pressure that seeks to minimize non-specific interactions can determine the way the energy gap between specific and non-specific interactions depends on the number of protein interfaces.

What distinguishes the current work from these previous approaches is that it begins with simple assumptions concerning how correct and incorrect dimers can form from monomers that are not necessarily proteins and embeds these assumptions in an analytical statistical mechanics framework. Using an analytical statistical mechanics framework, rather than the law of mass action or a computational framework, allows us to both respect the finite-number properties key to defining the combinatorics of the system and to derive general equations governing dimer assembly rather than having to infer such equations from computational trends.

The purpose of this work is to use statistical physics to better understand the properties of dimer self-assembly. In Sec. 4.2, we present the premises of our model, connect these premises to a combinatorial problem we term the "Dance Hall Problem", and then use the solution of this problem to compute the partition function of the system. In Sec. 4.3, we approximate the partition function through Laplace's method and obtain the equilibrium conditions relating the average number of correct dimers to the total number of dimers in the system. In Sec. 4.4, we define the condition under which the dimer system undergoes fully-correct assembly, and use this condition to categorize dimer systems as one of two approximate types. In this section, we also numerically solve and plot the equilibrium conditions, compare the results to simulations, and depict the dimer system in parameter space. In Sec. 4.5, we derive the necessary conditions for the system to be capable of fully-correct assembly, and interpret the two types as corresponding to "search" or "combinatorics" limited on fully-correct assembly. In Sec. 4.6, we apply the derived

results to biomolecular systems of ssDNA-ssDNA interactions, TF-DNA interactions, and protein-protein interactions ultimately finding that all such systems appear to be of the search-limited type. In the final sections, we outline the limitations of the model and consider ways to extend it to better reflect the properties of real dimer systems.

4.2 Non-Gendered Partition Function

In this section, we build the partition function for a system of distinguishable monomers that can form incorrect or correct dimers contingent on the dimer's constituent monomers. To match the physical conditions of self-assembly, we impose that the binding energy for the correct dimer is lower than the binding energy of the incorrect dimer, and thus that correct dimers are energetically preferred. However, the combinatorics of the dimer assembly is such that there are many more incorrect dimer microstates than correct dimer microstates, and so incorrect dimers are entropically preferred. We refer to this as the "combinatorial disadvantage" of correct dimers.

We complete the calculation in steps: After outlining the particle and energy properties of the model, we present the partition function, reframe its computation in terms of a combinatorial sub-problem, and finally use the solution to this sub-problem to obtain an exact integral expression for the partition function.

The system studied in this section (and presented throughout the main body of the paper) is termed "non-gendered" to emphasize the fact that there is only one type of monomer and each monomer can bind to any other monomer. Such systems well describe the conditions of ssDNA-ssDNA interactions and some protein-protein interactions. But in TF-DNA interactions, there are two types of "monomers" each of which only binds to the other type; we call this system "gendered." In Appendix D, we outline the mathematical and physical properties of a "gendered" dimer model.

4.2.1 Naive Partition Function

Say that our system contains $2N$ distinguishable monomers labeled $\alpha_1, \alpha_2, \ldots, \alpha_{2N}$. Each monomer has a mass m_0, and the monomers exist at thermal equilibrium temperature T in

a volume V. Each monomer can bind to any other monomer, and when monomer α_k binds to monomer α_ℓ, the two form the dimer (α_k, α_ℓ) where the ordering within the pair is not important.

We define correct dimers as those consisting of an α_k binding with α_{N+k} where $k \leq N$; all other dimers are considered incorrect. Thus each monomer has one other monomer to which it binds to yield a correct dimer, and, more generally, there are N possible correct dimers and $2N(2N-1)/2 - N = 2N(N-1)$ possible incorrect dimers. We take the incorrect dimers to form with binding energy $-E_0$, and the correct dimers to form with binding energy $-(E_0 + \Delta)$ where $E_0, \Delta > 0$. Summarily, the binding energy for a dimer (α_i, α_j) is

$$
\mathcal{E}(\alpha_i, \alpha_j) = \begin{cases} -(E_0 + \Delta) & \text{if } |j - i| = N \\ -E_0 & \text{if } |j - i| \neq N. \end{cases} \tag{4.3}
$$

We term E_0 the "offset binding energy", and Δ the "energy advantage" of correct dimers. For simplicity, we will assume that the monomers and dimers are point particles with no rotational or vibrational properties. Also, apart from their binding, the monomers and the dimers are free particles which do not interact with one another. Therefore, the total energy of a microstate comes from the kinetic energies of the monomers and the kinetic energies and binding energies of the dimers. An example microstate for a non-gendered dimer system is shown in Fig. 4.2.

In order to study the thermal equilibrium properties of such a system, we need to construct its partition function. To build the partition function we must define the microstates of the system, the energy of a microstate, the various degeneracy factors relevant to defining a microstate, and how we will sum over all microstates. Given the definition of our system, a naive choice for how to characterize the system microstate is to use a $2N \times 2N$ contact matrix $\mathcal{C}$ whose elements are defined according to

$$
\mathcal{C}_{ij} = \begin{cases} 1 & \text{if dimer } (\alpha_i, \alpha_j) \text{ exists in system,} \\ 0 & \text{otherwise.} \end{cases} \tag{4.4}
$$

With the elements $\mathcal{C}_{ij}$, we can then specify which monomers exist in isolation and which
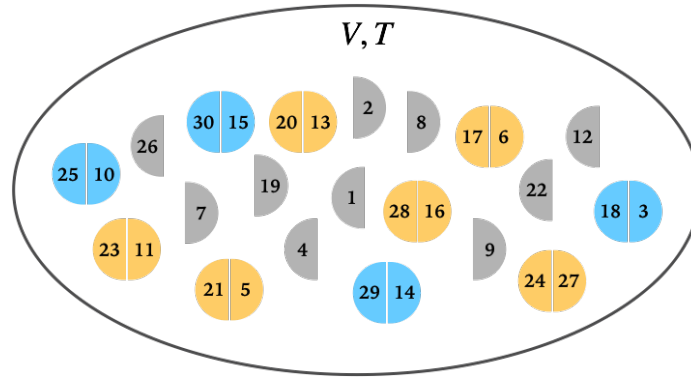
FIGURE 4.2: Example microstate of the non-gendered system with $2N = 30$ monomers. Correct dimers consist of binding k to $k + 15$ and have binding energy $-(E_0 + \Delta)$. All other dimers are incorrect and have binding energy $-E_0$. This microstate has four correct dimers (in blue), six incorrect dimers (in yellow), and ten monomers (in grey). For pictorial clarity, the figure represents monomers as half-circles, but monomers are taken to be point particles in the model. To which half-circle the individual monomers correspond is not important. The total binding energy for this microstate is $-(10E_0 + 4\Delta)$.

are bound together. From the constraints of the system, we can also infer that $\mathcal{C}_{ij}$ has no diagonal elements, is symmetric, and only has a single non-zero entry of 1 in each column or row. Given Eq.(4.3) and Eq.(4.4), the energy of a particular microstate would then be

$$E(\{\mathcal{C}_{ij}\}) = \sum_{i<j}^{2N} \mathcal{C}_{ij}\mathcal{E}(\alpha_i, \alpha_j) = -E_0 \sum_{i<j}^{2N} \mathcal{C}_{ij} - \Delta \sum_{i<j}^{2N} \mathcal{C}_{ij}\,\delta_{N,\,j-i}. \tag{4.5}$$

By the definition of the contact matrix in Eq.(4.4), the total number of dimers in the system is $\sum_{i<j} \mathcal{C}_{ij}$, and the total number of monomers is $2N - 2\sum_{i<j} \mathcal{C}_{ij}$. Presuming we are working under dilute-solution conditions, the monomers and dimers are non-interacting, and the degeneracy of a particular microstate $\mathcal{C}_{ij}$ can be accounted for by including factors of the ideal-gas partition functions for the appropriate number of monomers and dimers. If we have N distinguishable and non-interacting point particles of mass m_0, the free-particle contribution to the partition function is

$$Z_{\text{free}} = \left(\frac{V}{\lambda_0^3}\right)^N, \tag{4.6}$$

where V is the volume of the system, and $\lambda_0 = h/\sqrt{2\pi m_0 k_B T}$ is the thermal de Broglie wavelength of a single monomer. There is no permutation correction in Eq.(4.6) because

our particles are distinguishable. From Eq.(4.5) and Eq.(4.6), the partition function for the dimer system can be expressed as

$$
Z_N(V, T, E_0, \Delta) = \sum_{\{\mathcal{C}_{ij}\}} \exp\left[\beta \sum_{i<j}^{2N} \mathcal{C}_{ij}\mathcal{E}(\alpha_i, \alpha_j)\right] \left(\frac{V}{\lambda_0^3}\right)^{2N - 2\sum \mathcal{C}_{ij}} \left(\frac{V}{(\lambda_0/\sqrt{2})^3}\right)^{\sum \mathcal{C}_{ij}} \tag{4.7}
$$

where $\beta = 1/k_B T$, the dimers have mass $2m_0$, $\sum \mathcal{C}_{ij}$ sums over indices $i < j$, and the microstate summation runs over all valid contact matrices for this system.

Our larger objective is to derive an analytic form for the partition function and to then use this partition function to derive the thermal equilibrium conditions. But according to Eq.(4.7), in order to compute the partition function we have to enumerate and then sum over all valid contact matrices for this system. The set of possible contact matrices are all $2N \times 2N$ matrices that are symmetric, have no diagonal elements, and where each row's and each column's only non-zero element is 1. Finding a systematic way to enumerate such matrices is challenging enough, but further complicating the calculation is the way the binding energy Eq.(4.5) changes contingent on which elements in $\mathcal{C}$ are non-zero.

We can bypass these complications by expressing Eq.(4.7) as a summation over states defined by the number of total dimers and number of correct dimers in the system. In terms of the contact matrix, we have

$$
k = \sum_{i<j}^{2N} \mathcal{C}_{ij}, \qquad m = \sum_{i<j}^{2N} \mathcal{C}_{ij}\, \delta_{N, j-i}, \tag{4.8}
$$

as the number of total dimers and the number of correct dimers, respectively. Then, rather than defining and summing over all possible contact matrices, we need only sum over the possible values of k and m with the appropriate Boltzmann and degeneracy factors. In constructing the partition function, we define a state by a particular value of k and m. Eq.(4.5) indicates that the binding energy for such a state is $-kE_0 - m\Delta$. Therefore, the partition function Eq.(4.7) can be written as

$$
Z_N(V, T, E_0, \Delta) = \sum_{k=0}^{N} \sum_{m=0}^{k} \Omega_N(k, m)\, e^{\beta(kE_0 + m\Delta)} \left(\frac{V}{\lambda_0^3}\right)^{2N - 2k} \left(\frac{V}{(\lambda_0/\sqrt{2})^3}\right)^{k} \tag{4.9}
$$
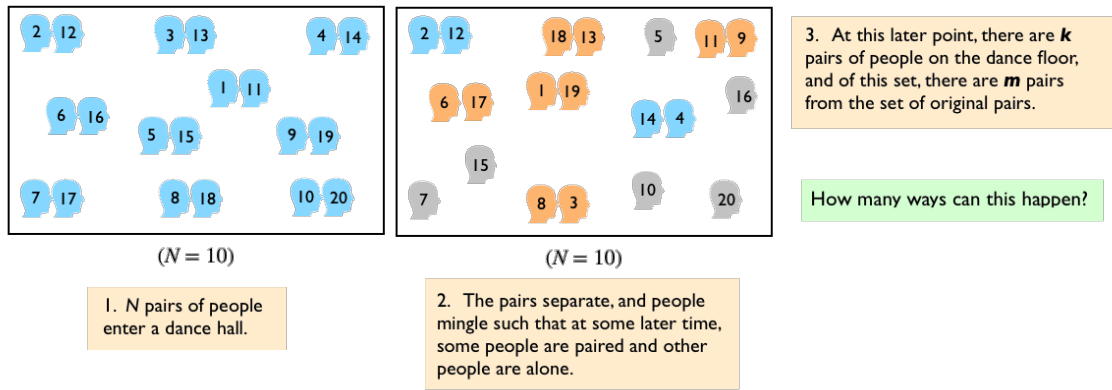
FIGURE 4.3: Depiction of the dance-hall problem for $N = 10$.

where $\Omega_N(k, m)$ is the number of ways to construct a microstate with k dimers, of which only m are correct dimers. The task of computing the partition function now reduces to the task of computing the degeneracy factor $\Omega_N(k, m)$, and this calculation amounts to a problem of combinatorics.

4.2.2 Dance-Hall Problem

Determining $\Omega_N(k, m)$ generalizes beyond the constraints of this problem, and we can embed its definition in the answer to a less abstract problem. We phrase the problem as follows:

> N pairs of people enter a dance hall. All people in the pairs separate, and people mingle with one another such that at some later time, some people are paired and other people are alone. At this later time, there are k pairs of people on the dance floor, and of this set, there are m pairs from the set of original pairs. How many ways can this happen? (See Fig. 4.3 for depiction)

The quantity $\Omega_N(k, m)$ is the answer to this question. To determine this quantity, we break it up into two factors: $\Omega_N(k, m)$ can be written as a product between the number of ways to select m of the original pairs from the initial set of N pairs and the number of ways to create, from the remaining $2(N - m)$ people, $k - m$ pairs which are not amongst

the remaining $N - m$ original pairs. We thus have

$$\Omega_N(k, m) = \binom{N}{m} a_{N-m,k-m},\tag{4.10}$$

where $a_{n,\ell}$ is the number of ways to form ℓ pairs from a set of $2n$ originally paired elements such that none of these ℓ pairs coincides with any of the original n pairs.

The quantity $\Omega_N(k, m)$ must also satisfy a summation identity which we can use to check our final result. The total number of ways to form k pairs out of a collection of $2N$ people (each of which can form a pair with any other person) is the number of ways to select $2k$ people to be amongst the pairs multiplied by $(2k - 1)!! = (2k)!/(2^k k!)$, the number of ways to rearrange the selected people amongst the pairs (Chuan-Chong and Khee-Meng, 1992). Thus, summing Eq.(4.10) over all possible values of k, we should find

$$\binom{2N}{2k}(2k - 1)!! = \sum_{m=0}^{k} \binom{N}{m} a_{N-k,k-m}.\tag{4.11}$$

To check this result, we need only determine $a_{n,\ell}$.

It is easy to calculate $a_{n,\ell}$ for a few representative values. For $\ell = 1$, $a_{n,1}$ is the number of ways to create a single pair that is not among the original n pairs. In other words, $a_{n,1}$ is the difference between the number of ways to pair $2n$ objects and the number of original pairs:

$$a_{n,1} = \frac{2n(2n - 1)}{2} - n = 2n(n - 1),\tag{4.12}$$

For $\ell = n$, $a_{n,\ell}$ reduces to a solution to the "bridge couples problem" (Margolius, 2001): The number of ways to completely rearrange n paired people into n new pairs such that none of these pairs is amongst the original collection is

$$a_{n,n} = \sum_{j=0}^{n} (-1)^j \binom{n}{j}(2n - 2j - 1)!!.\tag{4.13}$$

For general ℓ, we can find $a_{n,\ell}$ by applying the principle of inclusion-exclusion (Chuan-Chong and Khee-Meng, 1992). We work through this derivation in Appendix C.2 and

ultimately find

$$a_{n,\ell} = \sum_{j=0}^{\ell} (-1)^j \binom{n}{j} \binom{2n-2j}{2\ell-2j} (2\ell - 2j - 1)!!. \tag{4.14}$$

It is simple to check that Eq.(4.14) satisfies Eq.(4.13) and straightforward to check that it satisfies Eq.(4.12). To check Eq.(4.11), it is necessary to express Eq.(4.14) in terms of an integral as is done at the end of *SM Sec. 2*.

4.2.3 Final Partition Function

Expressing Eq.(4.10) in terms of the derived result Eq.(4.14), we find that Eq.(4.9) provides an exact partition function for our system of dimer-forming non-gendered monomers. However Eq.(4.9) is not yet in its most reduced form because it is still written as a summation over discrete indices. We can write this partition function in a form more responsive to the methods of calculus by using additional integration and combinatorial identities (see Appendix C.3 for details). In the end, we find the partition function

$$Z_N(V, T, E_0, \Delta) = \frac{1}{2\sqrt{\pi}\,\Gamma\,(N+1/2)} \left(\frac{V}{\lambda_0^3}\right)^{2N} \int_0^{\infty} \int_0^{\infty} dx\, dy\, \frac{e^{-x-y}}{\sqrt{xy}} \left(\mathcal{M}_+^{2N} + \mathcal{M}_-^{2N}\right), \tag{4.15}$$

where

$$\mathcal{M}_{\pm} \equiv \sqrt{x} \pm \left(\frac{2\sqrt{2}\,\lambda_0^3}{V}\right)^{1/2} e^{\beta E_0/2} \sqrt{y\,\Phi(x; \beta\Delta)}, \tag{4.16}$$

and

$$\Phi(x; \beta\Delta) \equiv e^{\beta\Delta} + 2x - 1, \tag{4.17}$$

with Γ being the Gamma function. Eq.(4.15) is an exact result and no mathematical approximations have been made in obtaining it. In particular, the integration variables x and y are not the $N \gg 1$ extrapolations of the summation variables k and m, but rather the former are variables introduced by using integration identities to express combinatorial factors as integrals. Thus Eq.(4.15) is valid for all N.

The advantage in expressing our original partition function Eq.(4.7) as Eq.(4.15) is that, as an exponential integral, Eq.(4.15) is now amenable to approximation via Laplace's method, and we can use this method to obtain the equilibrium conditions of the system. First, given the appearance of k and m in Eq.(4.7), we can compute the average number of dimers with

$$\langle k \rangle = \frac{\partial}{\partial(\beta E_0)} \ln Z_N, \tag{4.18}$$

and the average number of correct dimers with

$$\langle m \rangle = \frac{\partial}{\partial(\beta \Delta)} \ln Z_N. \tag{4.19}$$

We can use similar derivatives to compute the various elements of the covariance matrix for k and m:

$$\begin{pmatrix} \sigma_k^2 & \sigma_{km}^2 \\ \sigma_{mk}^2 & \sigma_m^2 \end{pmatrix} = \begin{pmatrix} \partial_{\beta E_0}^2 & \partial_{\beta E_0} \partial_{\beta \Delta} \\ \partial_{\beta \Delta} \partial_{\beta E_0} & \partial_{\beta \Delta}^2 \end{pmatrix} \ln Z_N, \tag{4.20}$$

where σ_k^2 is the variance of the total number of dimers, σ_m^2 is the variance of the number of correct dimers, and $\sigma_{km}^2 = \sigma_{mk}^2$ is the covariance between the total number of dimers and the number of correct dimers.

Eq.(4.18), Eq.(4.19), and Eq.(4.20) represent the main physical observables of this model, and computing these quantities will allow us to better characterize the various properties of the self-assembling dimer system. For example, we should be able to determine the conditions under which the energetic benefit for having a state of all correct dimers outweighs the entropic cost of not only having dimers rather than monomers but also of selecting the N correct dimers out of a much larger set of incorrect dimers. Such conditions would constitute "regime" conditions for this system, and in order to find these conditions we first need to more specifically characterize the equilibrium properties of the system.

4.3   Equilibrium Conditions of Non-Gendered System

With the partition function Eq.(4.15), we now have the main theoretical tool we need to explore the equilibrium properties of our system of non-gendered monomers. Our next task is to extract from this partition function physical information concerning the number of total dimers and the number of correct dimers. However, keeping Eq.(4.15) as an integral in the subsequent analysis would result in cumbersome integral expressions for both $\langle k \rangle$ and $\langle m \rangle$. It would be far simpler to approximate Eq.(4.15) as a function without an integral, and to then use this new function as a proxy for the partition function.

Working towards this goal, we first rewrite Eq.(4.15) in a more suggestive form. Defining the effective free energy as

$$\beta F_N(x, y; V, T, E_0, \Delta) = x + y + \frac{1}{2}\ln(xy) - \ln\left(\mathcal{M}_+^{2N} + \mathcal{M}_-^{2N}\right) + \beta F_0(N, V, T), \quad (4.21)$$

where $\beta F_0(N, V, T)$ represents terms that are independent of the variables x and y, we have

$$Z_N(V, T, E_0, \Delta) = \int_0^\infty \int_0^\infty dx\, dy\, \exp\left[-\beta F_N(x, y; V, T, E_0, \Delta)\right]. \quad (4.22)$$

Next, by Laplace's method (Breitung, 2006), we can take Z_N in the $N \gg 1$ limit to be dominated by the local maximum of its exponential integrand. We can then make the approximation

$$Z_N(V, T, E_0, \Delta) \simeq 2\pi \left(\det H\right)^{-1/2} \exp\left(-\beta F_N\right)\Big|_{x=\bar{x}, y=\bar{y}}, \quad (4.23)$$

where $\bar{x}$ and $\bar{y}$ are the critical points of Eq.(4.21) defined by

$$\partial_i(\beta F_N)\Big|_{x=\bar{x}, y=\bar{y}} = 0, \quad (4.24)$$

for $i = x, y$, and H is the Hessian matrix with the elements

$$H_{ij} = \partial_i \partial_j(\beta F_N)\Big|_{x=\bar{x}, y=\bar{y}}. \quad (4.25)$$

In order for Eq.(4.23) to be a valid approximation (and have an error of at most $\mathcal{O}(N^{-1})$), then $\bar{x}$ and $\bar{y}$ must not only satisfy Eq.(4.24), but the Hessian matrix at these critical points must also be positive definite (Hubbard and Hubbard, 2015), namely, it must satisfy

$$\det H > 0, \quad \operatorname{Tr} H > 0. \tag{4.26}$$

The two conditions Eq.(4.24) and Eq.(4.26) together ensure that βF_N is at a local minimum at the critical points $\bar{x}$ and $\bar{y}$ and thus that it properly defines the thermodynamic equilibrium of the system.

With the right side of Eq.(4.23) we now have a theoretically closed form expression that we can use as a proxy for a our partition function. We can transcribe the mostly mathematical conditions defining βF_N into physical results by using Eq.(4.23), Eq.(4.19), and Eq.(4.18) to establish a system of equations between $\langle k \rangle$, $\langle m \rangle$, $\bar{x}$, and $\bar{y}$. In deriving these equations, we take Eq.(4.21) evaluated at $x = \bar{x}$ and $y = \bar{y}$ to be the true free energy of this system [1] Solving this system, we obtain equilibrium conditions written exclusively in terms of $\langle k \rangle$ and $\langle m \rangle$:

$$\frac{4\sqrt{2}\,\lambda_0^3}{V}\,e^{\beta E_0} = \frac{\langle k \rangle - \langle m \rangle (1 - e^{-\beta \Delta})}{\left(N - \langle k \rangle\right)^2} \tag{4.27}$$

$$\frac{e^{\beta \Delta}}{2} = \langle m \rangle \frac{N - \langle m \rangle (1 - e^{-\beta \Delta})}{\langle k \rangle - \langle m \rangle (1 - e^{-\beta \Delta})}. \tag{4.28}$$

In Appendix C.4.1, we derive the conditions Eq.(4.27) and Eq.(4.28), and in Appendix C.4.2 we ensure the validity of Laplace's method by checking that the relevant critical points satisfy Eq.(4.26). To be precise, these equilibrium conditions have errors of the order of $\mathcal{O}\left(\langle k \rangle^{-1}\right)$ and $\mathcal{O}\left(N^{-1}\right)$, but we will take them to be exact in the subsequent analysis because these errors only become relevant when we are considering few particle systems or systems which are mostly composed of monomers.

Eq.(4.27) and Eq.(4.28) tell us how the average number of dimers $\langle k \rangle$ and the average

---

[1] We acknowledge that by the definition of free energy as $-k_B T \ln Z_N(V, T, ; E_0, \Delta)$, our quantity F_N differs from the actual free energy by a constant. However, this difference makes a negligible contribution to our physical results when working in the $N \gg 1$ limit.

number of correct dimers $\langle m \rangle$ relate to each other and to system parameters like the number of particles, system volume, and the binding energies of correct and incorrect dimers. Their form is reminiscent of law of mass action equations–i.e., they have an energy dependent exponential term on one side and particle number ratios on the other–however, there are some important differences. For one, factors of $(1 - e^{-\beta \Delta})$ multiply the average number of correct dimers, a feature which we will later see is important in deriving results for the $\Delta \to 0$ limit of the system. Moreover, in Eq.(4.28) there is an N dependent term which cannot be related to the typical particle number ratios of the law of mass action, but which we will see is important in defining the state of fully-correct assembly.

With Eq.(4.20) we can calculate the covariance and variance relationships between the average number of dimers and the average number of correct dimers. From Eq.(4.20), and the approximate free energy given in the Eq.(C.30) and evaluated at $x = \bar{x}, y = \bar{y}$, we find

$$\sigma_k^2 = \frac{1}{2N} \langle k \rangle \left(N - \langle k \rangle \right), \quad \sigma_{km}^2 = \frac{1}{2N} \langle m \rangle \left(N - \langle k \rangle \right), \tag{4.29}$$

$$\sigma_m^2 = \langle m \rangle - \frac{\langle m \rangle^2}{2} \left(\frac{1}{\langle k \rangle} + \frac{1}{N} \right) \tag{4.30}$$

indicating that the thermal fluctuations in our order parameters go to zero once the system becomes completely dimerized ($\langle k \rangle \simeq N$) and completely composed of all correct dimers ($\langle m \rangle \simeq N$).

From here, we could attempt to solve the equilibrium conditions Eq.(4.27) and Eq.(4.28) and obtain explicit expressions for $\langle k \rangle$ and $\langle m \rangle$ as functions of temperature and other system parameters. However, as coupled quadratic equations, these conditions yield quartic equations for $\langle k \rangle$ and $\langle m \rangle$. There are methods for obtaining analytic solutions to quartic equations (Irving, 2013), but the general solutions are sufficiently complicated as to not be too physically useful. So we instead solve these equilibrium conditions numerically.

But before we pursue a numerical solution, we can still build understanding of the system by analytically considering two special cases: The case where correct dimers do not have a binding energy advantage over incorrect dimers, and the case where the offset binding energy is so large that all monomers have formed (not necessarily correct) dimers.

4.3.1 No Energy Advantage ($\Delta = 0$)

We consider the system without correct dimers having an energy advantage over incorrect dimers, namely the case where $\Delta = 0$. For this case, we define the system by the reaction equation

$$\alpha_i + \alpha_j \rightleftharpoons \alpha_i \alpha_j, \qquad \text{Binding Energy} = -E_0 \tag{4.31}$$
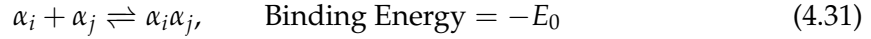
where $-E_0$ is the binding energy of the forward reaction. The partition function for such a system can easily be written down by taking the appropriate limit of the partition function Eq.(4.15). We find

$$Z_N(V, T, E_0, \Delta = 0) = \frac{1}{2\sqrt{\pi}} \left(\frac{V}{\lambda_0^3} \right)^{2N} \int_0^\infty dy\, \frac{e^{-y}}{\sqrt{y}} \left[\left(1 + \sqrt{2\delta y} \right)^{2N} + \left(1 - \sqrt{2\delta y} \right)^{2N} \right], \tag{4.32}$$

where

$$\delta \equiv \frac{2\sqrt{2}\,\lambda_0^3}{V} e^{\beta E_0}. \tag{4.33}$$

To derive the equilibrium conditions for this system, we can apply Laplace's method to Eq.(4.32) in a way similar to the method's application to Eq.(4.15). However, doing so would lead to equilibrium conditions for $\langle k \rangle$ alone, since the parameter Δ (which defines $\langle m \rangle$ through $\langle m \rangle = \partial \ln Z_N / \partial (\beta \Delta)$) is absent. Alternatively, we can simply consider Eq.(4.27) and Eq.(4.28) for $\Delta = 0$. Doing so, we find

$$\frac{4\sqrt{2}\,\lambda_0^3}{V} e^{\beta E_0} = \frac{\langle k \rangle}{\left(N - \langle k \rangle \right)^2}, \qquad \langle m \rangle = \frac{\langle k \rangle}{2N}. \tag{4.34}$$

These equations have straightforward interpretations from the perspective of the law of mass action and counting, respectively.

Identifying the concentration of monomers as $[\text{monomers}] = (2N - 2\langle k \rangle)/V$ and the concentration of dimers as $[\text{dimers}] = \langle k \rangle / V$, we can write the first equation in Eq.(4.34) as

$$\sqrt{2}\,\lambda_0^3 e^{\beta E_0} = \frac{[\text{dimers}]}{[\text{monomers}]^2}, \tag{4.35}$$

(A) $E = -5\Delta$ (B) $E = -2\Delta$ (C) $E = 0$
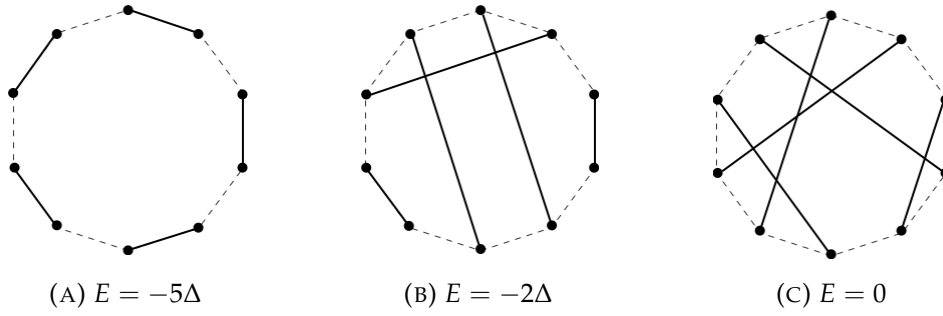
FIGURE 4.4: Example microstates of a graph system with $2N = 10$ vertices each of which has degree 1. We let (a) define the lowest energy microstate with energy $E = -5\Delta$. Each graph that has an edge not found in the lowest energy graph incurs an energy penalty $+\Delta$. Studying the equilibrium statistical physics of such a collection of graphs leads to the partition function in Eq.(4.37) without the factor of c^N and the additional corrections. Eq.(4.38) indicates that the system assumes its lowest energy graph at or below the non-zero temperature $\Delta / \ln(10)$.

which is reminiscent of a law of mass action interpretation of Eq.(4.31). The left side of Eq.(4.35) is off by a factor of 2 from what we would precisely calculate using the law of mass action because a foundational assumption of our dimer system is that each α_i occurs once and is distinguishable from α_j for $j \neq i$, and such an assumption of distinguishability is not manifest in the simple "monomer + monomer $\rightleftharpoons$ dimer" rendering of Eq.(4.31).

The second equation in Eq.(4.34) can be understood with a simple argument. If there is no energy difference between correct dimers and incorrect dimers, then the ratio between the average number of correct dimers and the average number of dimers should be equal to the ratio between the possible values of each. Given that there are N possible correct dimers and $2N(2N-1)/2$ possible dimers, we should find that the ratio between the average number of correct dimers and the average number of dimers at thermal equilibrium is

$$\frac{\langle m \rangle}{\langle k \rangle} = \frac{N}{2N(2N-1)2/2} = \frac{1}{2N-1}, \tag{4.36}$$

which, in the $N \gg 1$ limit, is consistent with the second equation of Eq.(4.34).

4.3.2 Complete Dimerization ($E_0 \gg k_B T$)

If our dimer system had an offset binding energy that was much larger than the energy scale of thermal fluctuations, then the system would be entirely composed of dimers, and

the corresponding thermodynamics would be determined by the combinatorics of correct and incorrect interactions. In such a situation, the only energy parameter relevant in defining the microstate of the system would be Δ. In this $E_0 \gg k_B T$ limit, the partition function Eq.(4.15) reduces to

$$Z_N(V, T, E_0 \gg k_B T, \Delta) = \frac{c^N}{\sqrt{\pi}} \int_0^\infty dx \, \frac{e^{-x}}{\sqrt{x}} \left(e^{\beta \Delta} + 2x - 1 \right)^N + \mathcal{O}(c^{-1}), \qquad (4.37)$$

where $c = (V/\lambda_0^3)e^{\beta E_0}$. Given that $\langle k \rangle = \partial \ln Z_N / \partial(\beta E_0)$, Eq.(4.37) implies that $\langle k \rangle \simeq N$. Analyzing Eq.(4.27) in this limit is difficult because of the divergence that occurs as $\langle k \rangle$ approaches N, but the second equation suffers no such divergence. Using $\langle k \rangle \simeq N$ in Eq.(4.28) yields for $\langle m \rangle$

$$\langle m \rangle \simeq \frac{e^{\beta \Delta}}{2}. \qquad (4.38)$$

At the highest temperatures, Eq.(4.38) gives us the expected result that the system reduces to one of virtually no correct dimers, $\langle m \rangle \simeq 1/2$. However, given that $\langle m \rangle$ cannot exceed N, Eq.(4.38) also implies that there is a finite temperature below which $\langle m \rangle \simeq N$, and hence at which all of the dimers in the system are correct. This temperature is $k_B T \simeq \Delta / \ln(2N)$. The fact that this temperature is non-zero for finite N is important since such a result contradicts a potential expectation that complete order is only possible at zero temperature. We do not call this behavior a phase transition since it disappears in the thermodynamic $N \to \infty$ limit, but it is clear that, like a phase transition, moving below this temperature results in behavior that cannot be fully captured by our analytic approximations. In the next section, we will define the temperature at which fully-correct assembly occurs for arbitrary Δ and E_0, and we will see that $k_B T = \Delta / \ln(2N)$ is a special case of a more general result.

Finally, Eq.(4.37) has a simple interpretation from the perspective of the statistical physics of graphs. We consider the set of graphs with N edges and $2N$ vertices where each vertex has degree 1. If we define one graph in this set as the lowest energy graph (with $E = -N\Delta$), and say that the system incurs an energy penalty $+\Delta$ whenever a graph has an edge not amongst the lowest energy graph, then the partition function for the system is given by

the first term in Eq.(4.37) without the factor of c^N. Moreover, Eq.(4.38) indicates that below a temperature $\Delta/\ln(2N)$, the system settles into its lowest energy graph (Fig. 4.4).

4.4   Types and Regimes of Dimer Systems

We say that our dimer system has undergone fully-correct assembly when the average number of dimers is equal to the average number of correct dimers, $\langle k \rangle = \langle m \rangle$. In this section, we use this definition to show that the dimer system can be categorized as one of two types. This categorization is based on analytic approximations for the temperature at which fully-correct assembly is achieved, but by plotting simulations and numerical solutions to Eq.(4.27) and Eq.(4.28) for these two system types, we find that the categorization also reflects a qualitative difference in the relationship between $\langle k \rangle$ and $\langle m \rangle$. With the intuition from these numerical analyses, we then define different physical regimes of the system (e.g., complete assembly, partial assembly, negligible assembly etc.) and use parameters spaces in $\beta E_0 - \beta \Delta$ and $2N - V/\lambda_0^3$ space to show that the two system types can access different regimes of self-assembly.

4.4.1   Type I and Type II Dimer Systems

When our system is at high T we can expect most of the monomers to exist alone such that $\langle m \rangle$, the average number of correct dimers, and $\langle k \rangle$, the average number of total dimers, are both much less than $\mathcal{O}(1)$. However, as we decrease the system temperature, we could expect there to be a point at which $\langle m \rangle = \langle k \rangle$. At this point, we would say the system is in the regime of fully-correct assembly. At what temperature does the system enter this regime?

Imposing $\langle m \rangle = \langle k \rangle$ on both equations Eq.(4.27) and Eq.(4.28), and presuming that this condition is valid at a temperature T_c, we find that T_c must satisfy

$$\frac{\sqrt{2}\,\lambda_{0,c}^3}{V}\, e^{\beta_c(E_0+\Delta)} \frac{\left(1-2Ne^{-\beta_c\Delta}\right)^2}{1-e^{-\beta_c\Delta}} = N - 1/2 \tag{4.39}$$

where $\lambda_{0,c} = h/\sqrt{2\pi m_0 k_B T_c}$ and $\beta_c = 1/k_B T_c$. Moreover, at this temperature, $\langle m \rangle$ and $\langle k \rangle$ assume the common value

$$\langle m \rangle = \langle k \rangle = \frac{N - 1/2}{1 - e^{-\beta_c \Delta}}. \tag{4.40}$$

From Eq.(4.39), we can show that $k_B T_c$ is bounded above by $\Delta/\ln(2N)$ which, together with Eq.(4.40), implies that, at $T = T_c$, $\langle k \rangle$ and $\langle m \rangle$ have a value between $N - 1/2$ and N. Therefore, for this regime of fully-correct assembly, not only do all the dimers consist entirely of correct dimers, but all the monomers have formed dimers.

For general parameter values, Eq.(4.39) requires numerical methods to solve, but it is possible to find approximate analytical solutions in two limiting cases. In the case of large energy advantage for correct dimers ($\beta_c \Delta \gg 1$), the terms proportional to $e^{-\beta_c \Delta}$ go to zero, and we can solve for T_c explicitly to find

$$k_B T_c \simeq \frac{2}{3}(E_0 + \Delta) \left[W_0 \left(\frac{E_0 + \Delta}{3 E_V} (2N)^{2/3} \right) \right]^{-1} + \mathcal{O}(N^{-1}) \equiv k_B T_{\mathrm{I}}, \tag{4.41}$$

where we defined

$$E_V \equiv \frac{h^2}{2\pi m_0 V^{2/3}}, \tag{4.42}$$

as an effective energy a free monomer of mass m_0 in a volume V, and where W_0 is the principal branch of the Lambert W function defined by the condition $W_0(xe^x) = x$ for $x > -1$ (Weisstein, 2002d). Alternatively, in the case where the offset binding energy is large ($\beta_c E_0 \gg 1$), the squared quantity must approach 0 to compensate for its large coefficient, and we find

$$k_B T_c \simeq \frac{\Delta}{\ln(2N)} \equiv k_B T_{\mathrm{II}}. \tag{4.43}$$

In practice, the solution to Eq.(4.39) cannot always be approximated by either T_{I} or T_{II}, but in cases when it can, the corresponding thermal dependences for $\langle k \rangle$ and $\langle m \rangle$ are sufficiently different between these two limiting cases that it is appropriate to categorize these

cases as two different system types. We define these two system types approximately as

$$
\text{System Type} = \begin{cases} \text{Type I} & \text{for } T_c \simeq T_{\mathrm{I}}, \\[2mm] \text{Type II} & \text{for } T_c \simeq T_{\mathrm{II}}. \end{cases} \tag{4.44}
$$

For systems where T_c cannot be approximated by either T_{I} or T_{II}, we call the system type "indeterminate".

In the following sub-sections, we explore this system categorization and the implications of Eq.(4.39) in two ways: First, using Eq.(4.44) to categorize numerical solutions to Eq.(4.27) and Eq.(4.28); second, constructing a parameter space plot of the solutions and using the system categorization to understand which spaces are accessible to Type I and Type II systems.

4.4.2 Numerical Solutions and Simulations

In Fig. 4.5, we plot the numerical solutions to the equilibrium conditions Eq.(4.27) and Eq.(4.28) and compare the results to simulation results for Type I, Type II, and indeterminate systems. The error bars in the plots are computed from Eq.(4.29) and Eq.(4.30), and the system is simulated using a Metropolis-Hastings Monte Carlo algorithm with a set of moves chosen to ensure efficient exploration of the state space (see Appendix C.5 for details).

The qualitative difference between Type I and Type II systems is apparent from comparing how $\langle k \rangle$ and $\langle m \rangle$ relate to one another for each system type. In both system types, when $T < T_c$, the equilibrium equations Eq.(4.27) and Eq.(4.28) break down and $\langle k \rangle$ and $\langle m \rangle$ assume the value given by Eq.(4.40). But for Type I systems, as we increase the temperature above T_c, the $\langle m \rangle$ curve closely shadows the $\langle k \rangle$ curve, indicating that most of the dimers in such systems are correct. Conversely, for Type II systems, as we increase the temperature above T_c, the $\langle m \rangle$ curve quickly drops away from the $\langle k \rangle$ curve, with the $\langle k \rangle$ curve remaining near N, indicating that most of the dimers are incorrect. This is the essential qualitative difference between Type I and Type II dimer systems: Above the critical temperature T_c, Type I systems have dimers which are generally dominated by correct
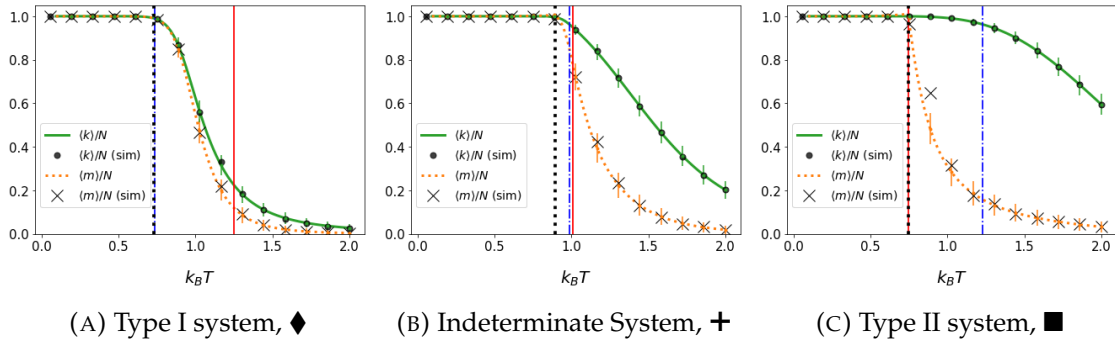
(A) Type I system, ◆   (B) Indeterminate System, ✚   (C) Type II system, ■

FIGURE 4.5: Numerical solutions to Eq.(4.27) and Eq.(4.28) and corresponding simulation results. We set $E_V = 10^{-3}$, $N = 50$, and defined all energies in units of $k_B T = 1.0$. The error bars are the standard deviations in k and m computed from Eq.(4.29) and Eq.(4.30). In (a), $E_0 = 4.15$ and $\Delta = 5.75$; In (b), $E_0 = 9.05$ and $\Delta = 4.65$; In (c), $E_0 = 14.00$ and $\Delta = 3.75$. The $\langle k \rangle$ and $\langle m \rangle$ numerical solutions are represented by solid green and dotted orange curves, respectively. The $\langle k \rangle$ and $\langle m \rangle$ simulation results are denoted by "●" and "×", respectively, and each point represents the average of 50 simulations where, for each simulation, the last 600 time steps of 30,000 were used to compute the ensemble average (see Appendix C.5 for details). Vertical lines correspond to T_c (black dotted), T_I (blue dashdotted), and T_{II} (red solid). For Type I systems, $T_c \simeq T_I$, and for Type II systems, $T_c \simeq T_{II}$. The characteristic feature of a Type I system is a soft transition from $\langle m \rangle \simeq N$ to $\langle m \rangle < N$ after which $\langle m \rangle$ closely shadows the behavior of $\langle k \rangle$. The characteristic feature of a Type II system is a sharp transition for $\langle m \rangle$ at $T \simeq \Delta / \ln(2N)$ followed by an exponential decline which drops $\langle m \rangle$ far away from the $\langle k \rangle$ value. The sharpness of the transition leads to relatively large fluctuations in m as shown by the larger discrepancy between simulation and analytic results in (c) versus those in (a) and (b). In Type I systems, partially dimerized states can have mostly correct contacts, and in Type II systems partially dimerized states always have mostly incorrect contacts.

contacts while Type II systems have dimers which are generally dominated by incorrect contacts.

4.4.3 Parameter Space Plots

In Eq.(4.40), we took the relationship $\langle m \rangle = \langle k \rangle$ to define the fully-correct assembly regime of the dimer system. This regime is evident in all the plots in Fig. 4.5 for $T \leq T_c$, but these plots also show that there are many different relationships between $\langle k \rangle$ and $\langle m \rangle$ that we can use to define various regimes of dimer assembly. It is easiest to get a sense of these regimes with parameter space plots.

Fig. 4.6a and Fig. 4.6b depict, respectively, $\beta E_0 - \beta \Delta$ and $2N - V / \lambda_0^3$ parameter spaces for the dimer system with N and V fixed in the former and E_0 and Δ fixed in the latter. A system at a particular temperature and with particular parameter values is located at a
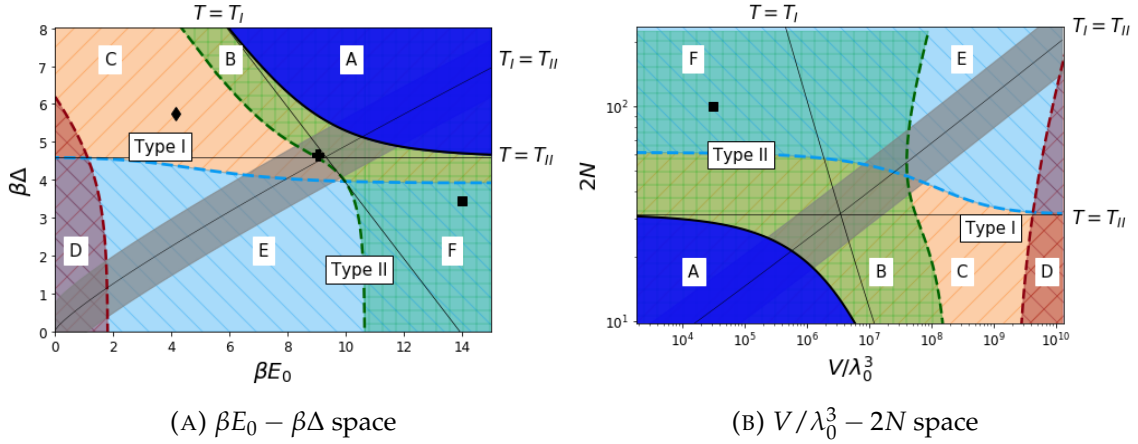
(A) $\beta E_0 - \beta\Delta$ space

(B) $V/\lambda_0^3 - 2N$ space

FIGURE 4.6: Parameter space regimes of dimer system. In (a), we set $E_V = 10^{-3}$ and $N = 50$. In (b), we set $E_0 = 14.00$ and $\Delta = 3.45$. In both (a) and (b), we set $k_B T = 1.0$. Each region is defined by solutions to Eq.(4.27) and Eq.(4.28) satisfying the following: (A) fully-correct assembly (Eq.(4.40)); (B) nearly-complete assembly with mostly correct contacts $(\langle k \rangle/N > 0.95$ and $\langle m \rangle/\langle k \rangle > 0.5)$; (C) partial dimerization with mostly correct contacts $(\langle k \rangle/N < 0.95$ and $\langle m \rangle/\langle k \rangle > 0.5)$; (D) negligible dimerization $(\langle k \rangle/N < 0.05)$; (E) partial dimerization with mostly incorrect contacts $(\langle k \rangle/N < 0.95$ and $\langle m \rangle/\langle k \rangle < 0.5)$; (F) nearly-complete assembly with mostly incorrect contacts $(\langle k \rangle/N > 0.95$ and $\langle m \rangle/\langle k \rangle >< 0.5)$. The black curve bounding region A in (a) and (b) is, respectively, the function $\beta\Delta(\beta E_0)$ and the function $2N(V/\lambda_0^3)$ found from analytic solutions to Eq.(4.39). The solid lines are functions computed from their respectively labeled conditions. The grey diagonal strip in (a) and (b) defines a region in which the system type is indeterminate; above or below the strip, the system is more clearly of Type I or Type II. The markers ♦, +, and ■ correspond, respectively, to (a), (b), and (c) in Fig. 4.5 at $T = 1.0$. All regions are common to both systems types, except for regions C and F which are unique to Type I and Type II systems, respectively. Therefore, only Type I systems can be partially dimerized and mostly correct while only Type II systems can be nearly-completely dimerized and mostly incorrect.

specific point on either parameter space plot. For example, the $T = 1.0$ values of $\langle k \rangle$ and $\langle m \rangle$ in the plots of Fig. 4.5 are represented as ♦, +, and ■ markers in Fig. 4.6a, and the $T = 1.0$ values of $\langle k \rangle$ and $\langle m \rangle$ in Fig. 4.5c are represented by ■ in Fig. 4.6b. We emphasize that because our results are derived in the $N \gg 1$ limit, the properties outlined for Fig. 4.6b become less accurate descriptions of the original system, for lower values of $2N$.

The solid straight lines are the parameter space expressions of the conditions $T = T_{\text{I}}$, $T = T_{\text{II}}$, and $T_{\text{I}} = T_{\text{II}}$ given the definitions in Eq.(4.41) and Eq.(4.43). If we take a system at a certain temperature to be defined by a point in Fig. 4.6a or Fig. 4.6b, then decreasing the system temperature brings the point closer to region A. Because the region boundaries are themselves temperature dependent, the sizes and extents of the regions also change as we change the system temperature. See Fig. C.1 in Appendix C.6 for a depiction of how the

plots in Fig. 5 change as we decrease the value of $k_B T$. We define a system as Type I or Type II according to whether decreasing the system temperature leads the point representing the system to enter region A (fully-correct assembly region) at a point at which either the T_I or T_{II} line can approximate the region A boundary. The temperatures T_I and T_{II} must be sufficiently distinct for this categorization to be non-ambiguous and so the grey regions in both plots of Fig. 4.6 define approximate regions where $T_I \simeq T_{II}$ and hence where the system type is indeterminate.

In the parameter space plots, we define six regimes that an arbitrary dimer system can be in at a given temperature.

(A) **Fully-correct assembly:** All monomers exist as dimers and all dimers are correct; Eq.(4.40), $1 - 1/2N < \langle k \rangle / N = \langle m \rangle / N < 1$.

(B) Nearly-complete assembly with mostly correct contacts: Almost all the monomers exist in dimers, and most of these dimers are correct; $\langle k \rangle / N > 0.95$; $\langle m \rangle / \langle k \rangle > 0.5$.

(C) **Partial assembly with mostly correct contacts:** Monomers have only partially dimerized, and most of these dimers are correct; $\langle k \rangle / N < 0.95$; $\langle m \rangle / \langle k \rangle > 0.5$.

(D) **Negligible assembly:** Few of the monomers exist as dimers; $\langle k \rangle / N < 0.05$.

(E) **Partial assembly with mostly incorrect contacts:** Monomers have only partially dimerized, and most of these dimers are incorrect; $\langle k \rangle / N < 0.95$; $\langle m \rangle / \langle k \rangle < 0.5$.

(F) **Nearly-complete assembly with mostly incorrect contacts:** Almost all the monomers exist in dimers, and most of these dimers are incorrect. $\langle k \rangle / N > 0.95$; $\langle m \rangle / \langle k \rangle < 0.5$.

The regimes are not necessarily mutually exclusive. For example, there is a parameter space region in which the "negligible assembly" regime (region C) satisfies the conditions of the "partial assembly with mostly correct contacts" regime (region B). This is because the dotted line boundaries in Fig. 4.6a and Fig. 4.6b are defined by somewhat arbitrary limiting values for $\langle k \rangle$ and $\langle m \rangle$ (e.g., $\langle k \rangle / N < 0.10$ and $\langle k \rangle / N > 0.90$ could respectively have been used to define negligible and nearly-complete assembly), and thus transitioning across such boundaries occurs smoothly as "crossover", rather than as "phase", transitions.

However, the boundary surrounding region A is unambiguously defined by Eq.(4.39), and transitioning across this boundary by decreasing T below T_c fixes $\langle m \rangle$ at the value given in Eq.(4.40). For Type I systems, this $T = T_c$ transition occurs smoothly (Fig. 4.5a), but for Type II systems the transition occurs sharply (Fig. 4.5c) corresponding to an apparent discontinuity in $\partial \langle m \rangle / \partial T$ and thus suggesting the appearance of a phase transition. However, this transition occurs at an N dependent temperature that goes to zero in the thermodynamic limit, and thus does not fulfill the standard definition of a phase transition.

Echoing an assertion made in the previous section, Fig. 4.6a and Fig. 4.6b show that Type I and Type II systems exhibit regimes of behavior exclusive to each type. When monomers are partially dimerized in a Type I system, most of the dimers can consist of correct contacts, while when monomers are partially dimerized in a Type II system, most of these dimers always consist of incorrect contacts.

These parameter space plots allow us to immediately see a few properties of the dimer system not evident in the solution plots. First, from the regime definitions and the line representing the $T = T_{\text{II}}$ condition in both Fig. 4.6a and Fig. 4.6b, we see that $\beta \Delta > \ln(2N)$ (or, equivalently, $2N < e^{\beta \Delta}$) appears to be a sufficient but not necessary condition for an arbitrary system's dimers to be mostly composed of correct dimers. Therefore, the dimers in a system are mostly correct if the number of distinct monomers in the system is less than $e^{\beta \Delta}$.

Second, in Fig. 4.6a we see the expected result that the system only enters the fully-correct assembly regime when $\Delta \gg k_B T$ and $E_0 \gg k_B T$. This makes qualitative sense because a value of E_0 much larger than the energy scale of thermal fluctuations is needed for dimers to be able to form, and, similarly, a large value of Δ ensures that correct dimers are privileged over incorrect dimers.

However, in Fig. 4.6b we have a possibly unexpected result: It is only the lower left corner of the $2N - V/\lambda_0^3$ parameter space that contains the fully-correct assembly regime. This suggests that it is the absolute values of both particle number and volume, rather than just their ratio encoded in number density, that determine whether fully-correct assembly is possible. This result might be unexpected since reaction equations similar to those

defining our dimer system (i.e., similar to Eq.(4.1)) are often studied by considering reactant number densities in the form of concentrations. Experience with such analyses leads one to expect that limits on number density are the only relevant criteria for constraining whether correct dimerization is achieved. But now we see that a statistical mechanics analysis suggests otherwise. We interpret this result in the next section.

4.5 Inequalities for Assembly and Type

Having constructed the parameter spaces in Fig. 4.6, we now pursue two goals: A qualitative interpretation of the analytical conditions constraining the fully-correct assembly regime, and a more precise way to define the separation between Type I and Type II systems. We pursue the first goal by finding necessary but not sufficient conditions for a system to be in the fully-correct assembly region of parameter space and then by using these conditions to motivate the more conceptual labels of "search-limited" and "combinatorics-limited" for Type I and Type II systems, respectively. We pursue the second goal by deriving and interpreting necessary but not sufficient conditions for a system to be of Type I.

4.5.1 Limits of Fully-Correct Dimerization

In Fig. 4.6a and Fig. 4.6b, region A defines the parameter space for which a dimer system is in the regime of fully-correct assembly. A necessary and sufficient condition for the system to be in this regime is $T < T_c$ where T_c is given by the solution to Eq.(4.39). The complexity of Eq.(4.39) makes this condition difficult to interpret physically, but the solid lines in the parameter space plots, corresponding to $T = T_I$ and $T = T_{II}$, allow us to state two necessary but not sufficient conditions that have clearer physical interpretations.

From Eq.(4.39), Eq.(4.41), and Eq.(4.43), we can show that $T_c < T_I, T_{II}$. Thus, a necessary condition for the achievement of the fully-correct assembly regime is that $T < T_I$ and $T < T_{II}$. Using Eq.(4.41) and Eq.(4.43) to translate the $T < T_I$ and $T < T_{II}$ inequalities into physical limits on volume and particle number, we find that they correspond, respectively,

to

$$NV < \sqrt{2}\, \lambda_0^3\, e^{\beta(E_0 + \Delta)}, \qquad (4.45)$$

and

$$2N < e^{\beta\Delta}. \qquad (4.46)$$

where, consistent with the $N \gg 1$ limit, we dropped the $\mathcal{O}(N^{-1})$ term in Eq.(4.41). In Fig. 4.6a, Eq.(4.45) and Eq.(4.46) are satisfied when a system exists to the right of the $T = T_{\mathrm{I}}$ line and above the $T = T_{\mathrm{II}}$ line. In Fig. 4.6b, Eq.(4.45) and Eq.(4.46) are satisfied when a system exists to the left of the $T = T_{\mathrm{I}}$ line and below the $T = T_{\mathrm{II}}$ line. Since the fully-correct assembly region exists within these limits in both figures, Eq.(4.45) and Eq.(4.46) are necessary but not sufficient conditions for fully-correct assembly. Also, although they both contain the parameter N, Eq.(4.45) and Eq.(4.46) are independent of one another. Using Eq.(4.46) to eliminate N from Eq.(4.45) results in an inequality for V which is sufficient but not necessary for the achievement of full-correct assembly. So, to only consider necessary conditions for fully-correct assembly, we consider Eq.(4.45) and Eq.(4.46) separately.

A system only satisfies Eq.(4.45) if it has binding energies E_0 and Δ which are strong enough for all $2N$ monomers to find and bind to one another in the volume V. We thus term Eq.(4.45) a "search-limiting" condition for the dimer system. A system only satisfies Eq.(4.46) if it has an energy advantage Δ which is strong enough that the completely correct configuration of dimers is thermodynamically preferred over all the other combinatorially more numerous incorrect configurations. We thus term Eq.(4.46) a "combinatorics-limiting" condition.

We can think of Type I systems as being "search-limited" since in such systems Δ is sufficiently large that correct dimers can overcome their combinatorial disadvantage, and, therefore, the primary limiting factor in creating correct dimers is the ability of the relevant monomers to find one another, i.e., satisfying Eq.(4.45). Similarly, we can think of Type II systems as being "combinatorics-limited" since in such systems E_0 is sufficiently large that monomers can find one another, and the primary limiting factor in creating correct dimers is the need to overcome their combinatorial disadvantage, i.e., satisfying Eq.(4.46).

It may seem strange that the inequality Eq.(4.45) is said to define the search-limits of dimer assembly and yet it makes no reference to the number density of the system. Shouldn't high number density be a requirement for monomers to be able to find one another in their volume? The answer depends on the properties of the monomers comprising the system. Number density is mainly relevant if the dimers formed from associating monomers are all identical, and the monomers exist in multiple copies which are uniformly distributed in the constituent volume. In such cases, dimerization occurs if the monomers can find one another, and since the reactants are uniformly distributed throughout their volume, the only factor constraining whether they are able to find one another is how many of these monomers are in a particular region of their larger space. Thus, only density is relevant.

But for our dimer model, each of the $2N$ monomers exists as a single-copy, and all of the dimers are distinct. In order for the system to assume the fully-correct assembly regime, each monomer must ignore the $2N - 2$ other monomers that are not its optimal binding partner and find the optimal partner in the volume V. Increasing the number of distinct monomers makes a successful search less likely since there are more spurious potential binding partners, as does increasing the system volume since there is a larger space to search within. Therefore, both N and V should have upper limit constraints. However, why is it their product NV that has an upper limit constraint given in Eq.(4.45)? One answer is that particle number and volume are not independently constrained for a successful search. For example, a large volume and a small number of particles is just as harmful to a successful search as is a small volume and a large number of particles; in both cases a monomer still has to wade through a large number of various states—defined by possible position states or potential monomer binding partners—before it finds its optimal partner. Therefore the search limits on particle number become more stringent as the volume increases as do the search limits on volume when the particle number increases. Thus, it is their product which is constrained.

4.5.2   Limits of Type I System

According to Eq.(4.44) we categorized a dimer system as Type I or Type II contingent on how close T_c was to either T_I or T_{II}. This definition was necessarily approximate since the distinction between these two system types is a qualitative one which smoothly disappears as our system moves closer to the $T_I = T_{II}$ lines in Fig. 4.6a and Fig. 4.6b. But because of how T_I and T_{II} relate to one another in the two system types, we can rephrase the definition without explicit reference to how either relates to T_c.

When T_I and T_{II} are not approximately equal, the critical temperature T_c ends up being well approximated by the lower of the two values as is seen in Fig. 4.5a and Fig. 4.5c. For Type I systems, the lower value is always T_I and for Type II systems the lower value is T_{II}. Therefore, another way to define the system types is as

$$\text{System Type} = \begin{cases} \text{Type I} & \text{for } T_I < T_{II}, \\ \text{Type II} & \text{for } T_I > T_{II}. \end{cases} \tag{4.47}$$

where this definition is only unambiguous if T_I and T_{II} are not approximately equal. It is this phrase "not approximately equal" that makes this alternative definition, like the original definition Eq.(4.44) a qualitative one. However, this definition can be used as a guide to write a necessary but not sufficient condition for whether a system is of a particular type.

Eq.(4.47) states that in order for a system to be of Type I, we must have $T_I < T_{II}$. This inequality alone is a necessary but not sufficient condition for the system to be of Type I. For example, Fig. 4.5 satisfies $T_I < T_{II}$, but its system type is ambiguous. Still, we can consider how this condition constrains the parameter space for this system. We rewrite this inequality in terms of a limit on the number of distinct monomers in the system. Using Eq.(4.41) and Eq.(4.43) in $T_I < T_{II}$ and noting that, by the monotonicity property of the Lambert W function, if $W_0(X) > k$, then $X > ke^k$, we can show that $T_I < T_{II}$ implies

$$2N < \exp\left[\frac{3\Delta}{2E_0} W_0\left(\frac{E_0}{3E_V}\right)\right]. \tag{4.48}$$

Eq.(4.48) corresponds to the region in Fig. 4.6b that is below the $T_I = T_{II}$ line. Thus, if

a dimer system can be categorized as Type I, then the number of distinct monomers it contains must satisfy Eq.(4.48).

Eq.(4.48) is equivalent to a bare statement of the $T_{\text{I}} < T_{\text{II}}$ condition. However, unlike the $T_{\text{I}} < T_{\text{II}}$ condition, it presents constraints on $2N$ in terms of a closed-form expression and is thus easier to interpret. Taking $\Delta \ll E_0$ in Eq.(4.48), leads to a lower limit on the number of particles in the system. This makes sense because a smaller energy advantage for correct contacts means the system must have a smaller number of distinct monomers in order to avoid the prevalence of incorrect contacts which would push the system to be Type II. For large volumes V, Eq.(4.48) indicates that the maximum value of $2N$ becomes proportionally larger. This result is consistent with the fact that increasing N decreases T_{II}: Since it is the positive difference between T_{I} and T_{II} that leads a system to be characterized as Type I, a decrease in T_{I} through an increase in V, can be paired with a decrease in T_{II} through an increase in N, with the system still maintaining its type. It is true that increasing N also decreases T_{I}, but because $W_0(x)$ varies more slowly than $\ln(x)$ this decrease occurs more slowly than the corresponding decrease in T_{II}.

Eq.(4.48) is as a conceptually and analytically simple criteria for determining whether a dimer-system can be categorized as Type I. Satisfying Eq.(4.48) does not guarantee that the system is Type I, but failing to satisfy it guarantees that the system is not Type I. In the next section, we will use this criteria to determine whether various biomolecular systems have biophysical properties consistent with those of Type I dimer systems.

4.6   Biomolecular Systems

In this section we consider three systems whose properties approximately match the assumptions which underly the non-gendered or the gendered dimer models, the latter of which is outlined in Appendix D: The assembly of ssDNA into dsDNA, the specific and non-specific interactions between transcription factors and DNA, and the dimerization of distinguishable monomeric proteins into dimers (Fig. 4.1).

There are some important differences between the assumptions underlying the model and the properties of these real systems.

First, we assumed that each monomer species exists in a single copy in the system. This assumption clearly does not mirror the properties of real biomolecular systems which often have multiple copies, with different copy numbers, for important biomolecules. We take our model to approximate the behavior of systems with many different monomers but where the copy-numbers of each monomer are sufficiently similar and are uniformly distributed that we can consider a small region of the system to have a single-copy of each monomer type. In Sec. 4.8 we will state a formulation of the non-gendered problem which better takes into account differences in particle number and will mention issues relevant to the solution.

Second, in developing the dimer model, we have employed the dilute-solution approximation throughout in which the monomers and dimers are presumed to be point-like and non-interacting. But, in real biomolecular systems, one would expect volume exclusion and intermolecular interactions to lead to deviations from ideal behavior. In Sec. 4.8 we will comment on how we can make up for this limitation by extending the model, but for the current analysis we just acknowledge that the model only approximates the interaction properties of the monomers and dimers in the proposed real systems.

Third, our model uses only two parameters to define the binding energy matrix of $2N$ distinct monomers, whereas actual systems of distinct interacting proteins or strands of DNA would have more complicated binding interactions even if such interactions could be cleanly divided into correct and incorrect bindings. Consequently, in order to frame the properties of biomolecular systems in terms of model parameters, we use average energy scales representative of the systems of interest as approximations for E_0 and Δ.

Finally, in real biomolecular dimer systems, there are often rotational and vibrational contributions to entropy (Finkelstein and Janin, 1989) which, in a more complete theoretical treatment, would have been accounted for in our dimer partition function Eq.(4.9). Because our model only takes into account the translational entropy of the dimers, when given biophysical data on binding free energies, we will take E_0 and $E_0 + \Delta$ to be approximated by the provided binding free energies minus an estimated translational entropy contribution to those free energies. In this sense, the binding energy parameters of

our model are "effective" binding energies obtained by averaging over the various unaccounted for internal microstates of the dimer, but are not directly associated with a measurable quantity. Carefully incorporating rotational and vibrational contributions into the partition function Eq.(4.9) would lead to equilibrium conditions with different temperature dependences than those in Eq.(4.27) and Eq.(4.28), and thus different conditions for Type I and Type II dimer systems. Thus taking E_0 and $E_0 + \Delta$ to approximate these unaccounted for entropies amounts to an additional approximation in which we are ignoring the temperature dependence of these entropies. All binding energy calculations are found in the *Supplementary Code*.

In the subsequent sections, we will have two main goals: First, to use Eq.(4.45), Eq.(4.46), and estimates of biophysical parameters for various biomolecular systems to determine how the diversity of monomers in the system would need to be constrained in order for fully-correct assembly to be accessible at physiological temperatures. Second, to determine whether the system is a Type I (search-limited) or Type II (combinatorics-limited) dimer system, and thus whether partially dimerized systems are dominated by correct contacts in these systems. Completing the first goal provides us with the information for the second goal: According to Fig. 4.6b, if a system satisfies Eq.(4.46) but not Eq.(4.45), then the system is of Type I, but if a system satisfies Eq.(4.45) but not Eq.(4.46) then the system is of Type II. We will also use Eq.(4.48) to affirm these system categorizations.

4.6.1 ssDNA-ssDNA interactions

Within a cell, dsDNA never spontaneously separates into ssDNA, but in polymerase chain reactions (PCR), solutions containing copies of a single dsDNA sequence are heated to high enough temperatures that the strands can separate. In a prepared system, consider having, instead of multiple copies of a single sequence of dsDNA as in PCR, N different sequences of dsDNA which, when heated to high enough temperatures, separate into N ssDNA segments and N associated complementary segments (Fig. 4.1a).

This system is contrived from a biological perspective but provides a simple playground in which to study the predictions of the dimer model. What insights do the physical properties of the non-gendered dimer model provide for such a system of ssDNA and dsDNA? One relevant question is whether such a system is a Type I or a Type II dimer system.

Take a single ssDNA segment to have 20-nucleotide bases, a length which is within the range of standard lengths of primers in a typical PCR (Innis and Gelfand, 1999). In the language of the model, each α_k for $k = 1, \ldots, N$, represents one ssDNA fragment and α_{N+k} represents the corresponding complementary fragment. Because each α_k is presumed distinct, we require that none of the ssDNA is self-complementary, and hence each is distinct from its complementary strand. We will assume binding occurs in an all-or-nothing fashion and that the bubbles that exist in real strands (Fei and Ha, 2013) are not present. The reaction equation for this system is

$$\text{ssDNA}_k + \text{ssDNA}_{\text{comp},k} \rightleftharpoons \text{dsDNA}_k \tag{4.49}$$

where $k = 1, \ldots, N$.

Since only complementary ssDNA fragments can form dsDNA, there is no binding energy favorability between non-complementary ssDNAs, and so we can take $E_0 = 0$. From this condition alone, Fig. 4.6a suggests that such a system of interacting ssDNA is trivially of Type I, since a non-zero value of Δ and a zero value of E_0 would place the system well above the $T_\text{I} = T_\text{II}$ line.

Still, we can consider what estimates for binding energies imply about the number of distinct ssDNA that can exist in such a system. A representative binding free energy between complementary strands was found as follows: We randomly generated 10^6 20-base sequences of ssDNA (where the bases A, G, T, and C were equally probable), computed the binding free energy for each with its corresponding complement, and averaged over all free energies . We used an experimentally calibrated and cross-referenced formula given in (SantaLucia, 1998) to compute these free energies and assumed a 50 mM Na$^+$ surrounding solution (see *Supplementary Code* for implementation details). From these free energies

we we able to estimate a binding energy parameter of $\Delta \simeq 31.5$ kcal/mol. From the fact that a nucleotide base pair has a mass of about 650 daltons, we can take the mass of a 20-base ssDNA to be $m_0 = 6.5$ kDa (Metzler, 2001). We take our system to be at temperature $T = 310.15$ K.

With these parameters Eq.(4.45) and Eq.(4.46) yield, respectively,

$$(NV)_{\text{max}} = 4.2 \times 10^4 \ \mu\text{m}^3, \qquad (2N)_{\text{max}} = 1.6 \times 10^{22}, \tag{4.50}$$

Since a 20-base pair ssDNA can have at most $4^{20} \sim 10^{12}$ distinct sequences, the combinatorial condition on $(N)_{\text{max}}$ is automatically satisfied, and it is thus the search condition $(NV)_{\text{max}}$ which limits the achievement of fully-correct assembly in this conjectured system. Moreover, taking $E_0 \rightarrow 0$ in the necessary condition Eq.(4.48), yields $2N < \exp(\Delta/2E_0) \sim \exp(10^{13})$ which is practically infinite and more than satisfied for the possible values of N in the system. Therefore, this system is indeed of Type I, and is a search-limited dimer system.

4.6.2 Transcription factor-DNA Interactions

Transcription factors (TFs) are proteins that bind to DNA and regulate a gene's transcription into mRNA and thus how much protein is produced from that gene (Alberts et al., 2013). Given their importance in gene regulation networks and the specificity of their functions, TFs must attach to precise regions of DNA which they select out of a combinatorial sea of other binding regions (Fig. 4.1b). A TF finding its intended DNA target is said to bind to it "specifically" while bindings to all other targets are considered "non-specific" (Jen-Jacobson, 1997).

Let's say we have N different TFs in a system together with their corresponding N DNA binding sites. The association and dissociation reaction for this system can be written as

$$\text{TF}_k + \text{DNA}_\ell \rightleftharpoons (\text{TF-DNA})_{k\ell} \tag{4.51}$$

where $k, \ell = 1, \dots, N$. We want to use the biophysical parameters defining TF-DNA systems to consider what our model states about the diversity constraints of these systems. First, a system of interacting TFs and DNA sites is gendered because there are two types of interacting units and because we take the interactions to occur between respective members of the two types rather than within the same type. Also, since the DNA strand is fixed relative to the TFs, the system is more like a system of free monomers interacting with fixed binding sites rather than a system of dimer forming monomers. Consequently, the reduced mass μ of the dimers becomes the mass of the motile monomer (i.e., the mass of the TF), and the qualitative picture we associate with the system is more akin to Fig. D.2 than to Fig. D.1 in Appendix D.

In (Jen-Jacobson, 1997), Jacobsen lists 12 proteins (including endonucleases, repressors, and activators) with their respective protein-DNA association constants for specific and non-specific contacts under various conditions. Converting these association constants to binding free energies, and subtracting translational entropies to estimate our binding energy parameters E_0 and Δ, we find $E_0 \simeq 22.9$ kcal/mol and $\Delta \simeq 6.4$ kcal/mol. We take the mass of a transcription factor monomer to be $m_{\mathrm{TF}} \simeq 64$ kDa, a typical protein mass (Milo and Phillips, 2015), and we take $T = 310.15$ K.

From these parameter values, we find that gendered analogs of Eq.(4.45) and Eq.(4.46) (given in Eq.(D.27) and Eq.(D.28), respectively) yield

$$(NV)_{\mathrm{max}} = 2.7 \ \mu\mathrm{m}^3, \qquad (N)_{\mathrm{max}} = 3.2 \times 10^4. \tag{4.52}$$

Both of these results establish limits on the maximum diversity of TFs needed for fully-correct assembly to be achievable at physiological temperatures, but the condition that establishes more stringent limits for a particular volume is what ultimately defines whether the system is of Type I or Type II. The authors of (Pérez-Rueda and Collado-Vides, 2000) estimate that there are about $N = 3 \times 10^2$ different TFs in *E. coli*, a value which, for the *E. coli* volume $1\mu\mathrm{m}^3$, satisfies (N_{max}) but not $(NV)_{\mathrm{max}}$. Thus, the $(NV)_{\mathrm{max}}$ limit, derived from $T < T_{\mathrm{I}}$, establishes the stronger limit on TF diversity for a 1 $\mu\mathrm{m}^3$ volume system, and we can conclude that this system is a Type I, or search-limited, dimer system. Moreover, given

our parameter values, we find that the gendered analog of Eq.(4.48) (given in Eq.(D.29)) yields $N \lesssim 10^5$, which is well satisfied for the estimate $N \sim 10^3$, and thus such a system satisfies the necessary condition to be of Type I.

The fact that $(N)_{\mathrm{max}}$ is satisfied but not $(NV)_{\mathrm{max}}$ additionally means that the system is located below the $T = T_{\mathrm{II}}$ line in a plot like Fig. 4.6b, and thus the binding energies for the system are large enough that, at equilibrium, most of the TF-DNA bindings are correct (i.e., specific) bindings. Such a claim might seem strange given what is known about how TFs bind to DNA. TFs find their correct bindings sites through a two part process in which they first bind non-specifically to DNA and then slide along the DNA molecule. In the process of searching for its specific binding site, the TF spends most of its time non-specifically bound to DNA (Hippel and Berg, 1989). This fact seems to contradict our claim that a TF-DNA system is dominated by specific rather than non-specific contacts. However, the TF's search for its correct binding site is a decidedly non-equilibrium process while our result is an equilibrium one. What our result suggests is that if the relaxation to equilibrium was not for whatever reason too slow for cellular function, TFs would still have sufficiently strong binding to their specific sites that they could successfully wade through the combinatorial sea of incorrect binding sites and find their correct ones. In other words, although real TF-DNA systems have evolved to not make use of equilibrium self-assembly, their biophysical properties appear to still afford them the ability to do so.

4.6.3   Protein-Protein Interactions

Although proteins are the ostensible conclusion of the central dogma of molecular biology, the basic unit of life is much more complex than a bag of freely diffusing proteins (Alberts, 1998). Cells have highly organized internal structures with some proteins existing freely within the cramped environment of the cytoplasm while other proteins function alongside organelles in complex-machine like interaction networks necessary for cellular metabolism or replication. But, while a "bag of proteins" is not a faithful metaphor of the cell, it still serves as a useful model for studying the constraints of protein-protein interactions.

Say we have a solution of $2N$ distinct monomeric proteins each of which, through a functional interaction, typically forms a heterodimer (and has the lowest binding energy) with one other protein, but also has the ability to bind to the other proteins through non-functional interactions (Fig. 4.1c). In terms of the dimer model, functional interactions correspond to correct dimers and non-functional interactions correspond incorrect dimers. Whether a non-gendered or a gendered dimer model is more appropriate when describing proteins depends on the interaction properties of the proteins involved. However, the two classes of models have sufficiently similar quantitative properties that we can choose the non-gendered model as representative of both. The reaction equation for such a (non-gendered) system would be

$$\text{protein}_k + \text{protein}_\ell \rightleftharpoons (\text{protein-protein})_{k\ell} \tag{4.53}$$
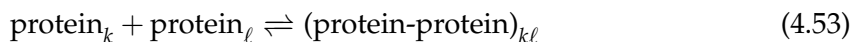
where $k, \ell = 1, \ldots, N$.

We consider again the question we asked for the previous biophysical systems: Given the approximate range of binding energies for protein dimers, are such protein-protein interactions systems of Type I or Type II?

The authors of (Kastritis et al., 2011) provide a downloadable protein-protein interaction data set consisting of a diverse collection of 144 protein complexes including antibody/inhibitor, enzyme/inhibitor, and G protein complexes. From this data set we can estimate an average binding free energy for functional (i.e., correct) protein complexes. An estimate of the binding free energy for non-functional complexes (i.e., incorrect protein interactions) is provided in (Zhang, Maslov, and Shakhnovich, 2008) by comparing the results of Yeast 2-Hybrid experiments across two data sets. Extracting our binding energy parameters E_0 and Δ from these data sets, we find $E_0 \simeq 18.9$ kcal/mol and $\Delta \simeq 7.7$ kcal/mol. We will take the mass of a monomer in this system to be the typical protein mass $m_0 \simeq 64$ kDa (Milo and Phillips, 2015), and we assume a system temperature of $T = 310.15$ K.

With these parameter values, Eq.(4.45) and Eq.(4.46) give us, respectively,

$$(NV)_{\text{max}} = 4.7 \times 10^{-1}\,\mu\text{m}^3, \qquad (2N)_{\text{max}} = 2.7 \times 10^5, \tag{4.54}$$

indicating that for a volume of $1\,\mu\text{m}^3$, the search-limiting constraint Eq.(4.45) provides a stronger limit on the number of different proteins in the system. Estimates of the number of different proteins in *E. coli* put the number to be on order of $N \sim 10^3$ (Soufi et al., 2015; Corbin et al., 2003), a result which satisfies the $(N)_{\text{max}}$ condition but not the $(NV)_{\text{max}}$ condition. Given the calculated parameter values, we can check that $N \sim 10^3$ is more than three orders of magnitude less than the maximum computed from Eq.(4.48), and thus this system indeed satisfies the necessary condition to be of Type I. Therefore, like systems of interacting TFs and DNA sites, systems of interacting proteins in an *E. coli* volume appear to be Type I, search-limited, dimer systems and thus have functional binding energies which are strong enough to overcome the combinatorial disadvantage of correct contacts at physiological temperatures.

Actual protein-protein interaction systems have numerous features not present in the model. Aside from the fact that proteins exist in multiple copies in real cells, we know that not all protein dimers are heterodimers (or even interact most strongly as heterodimers (Lukatsky, Zeldovich, and Shakhnovich, 2006)); not all protein dimers can spontaneously dissociate into their constituent monomers (e.g., HIV-1 reverse transcriptase); not all constituent monomers are stable by themselves (Nooren and Thornton, 2003); and not all proteins form dimers since many protein complexes important to cellular function (e.g., *lac* repressor) contain more than two constituent proteins.

But working within the constraints of the model, the fact that the estimated diversity of proteins in *E. coli* is much lower than $(N)_{\text{max}}$ suggests that these protein systems have energy advantages for correct contacts that are larger than what would be marginally necessary to privilege those correct contacts in an equilibrium system. This result is not surprising for the same reason that the TF-DNA results were not surprising; we know from the dynamics of TF-DNA interactions that cells do not only seek to optimize the fraction of their proteins in the so-called correct contacts, but also seek to minimize the time it takes to

System	N_{real}	$(NV)_{\text{max}}$ (μm^3)	$(2N)_{\text{max}}$	RHS of Eq.(4.48)
ssDNA-ssDNA	$\sim 10^{12}$	$\sim 10^4$	$\sim 10^{22}$	$\sim \exp(10^{13})$
TF-DNA	$\sim 10^2$	~ 1	$\sim 10^4$	$\sim 10^5$
protein-protein	$\sim 10^3$	$\sim 10^{-1}$	$\sim 10^5$	$\sim 10^7$

TABLE 4.1: The limits Eq.(4.45), Eq.(4.46), and Eq.(4.48) for various biomolecular systems at $T = 310.15$ K. The ssDNA has 20 bases. Because TF-DNA interactions constitute a gendered dimer system, we used Eq.(D.27), Eq.(D.28), and Eq.(D.29) to compute the relevant quantities in the TF-DNA row. In calculating Eq.(4.48) (or Eq.(D.29)), we assumed a volume $V = 1\,\mu m^3$. The fourth column contains real upper limits on the monomer diversity of the associated systems. We see that although the values of N_{real} exist below $(N)_{\text{max}}$ for each biomolecular system, N_{real} exceeds $(NV)_{\text{max}}$ for a volume of $1\,\mu m^3$. Together, these two comparisons indicate that all of these systems are Type I (i.e., search-limited) dimer systems for a volume of $1\,\mu m^3$. Further affirming this label is that N_{real} satisfies the Type I necessary condition Eq.(4.48) for each system. Therefore, these biomolecular systems would have equilibrium curves for $\langle k \rangle$ and $\langle m \rangle$ more akin to Fig. 4.5a than to Fig. 4.5b or Fig. 4.5c.

find such contacts (Hippel and Berg, 1989), and such minimization would likely provide stronger constraints than the equilibrium ones derived here.

4.7 Discussion and Interpretation

This work has five main analytical results: The exact partition function for dimer assembly, Eq.(4.15); the associated equilibrium conditions, Eq.(4.27) and Eq.(4.28); the temperature condition for fully-correct assembly, Eq.(4.39); the analytical definition of the two different system types, Eq.(4.44); the necessary but not sufficient inequalities for fully-correct assembly, Eq.(4.45) and Eq.(4.46); the necessary but not sufficient condition for the system to be of Type I, Eq.(4.48).

The final two results allow us to qualitatively characterize two different system types. Contingent on a dimer system's binding energy, particle number, and volume parameters it can be categorized as Type I/search-limited, Type II/combinatorics-limited, or indeterminate. In search-limited systems, the energy advantage for correct contacts is large enough to overcome the combinatorial disadvantage of such contacts, and the achievement of the fully-correct assembly regime is more constrained by the ability of the correct monomers to find one another in their surrounding volume. In combinatorics-limited systems, the opposite is the case with binding energies being large enough for the monomers

to find one another, and achieving fully-correct assembly more constrained by the ability of the correct dimers to overcome their combinatorial disadvantage. Indeterminate systems have properties that cannot be cleanly distinguished as being either search-limited or combinatorics-limited.

In terms of their binding trends, the qualitative difference between the two main types is that search-limited systems can be partially dimerized with most of their dimers consisting of correct contacts (Fig. 4.5a), but, when combinatorics-limited systems are partially dimerized, most of the dimers consist of incorrect contacts (Fig. 4.5c). Thus being able to categorize a dimer system as either Type I or II allows us to determine whether there can be mostly correct dimers in the system when the monomers are only partially dimerized.

Applying these results to the biophysical systems that motivated the model (Fig. 4.1)– and after listing numerous caveats–we found that all such systems appear to be search-limited systems (Table 4.1). Per our previous discussion, this means that the fully-correct assembly regime in these systems is more constrained by the ability of monomers to find one another in their constituent volumes than by the need to overcome the combinatorial disadvantage of correct dimers, and that these systems are capable of having partially-dimerized states that are dominated by correct contacts.

The latter result might appear obvious: Of course we should expect biomolecular systems in which functional interactions can be defined would exhibit binding energies that privilege those functional interactions over competing ones. However, in most biophysical analyses of non-functional interactions (e.g., (Deeds et al., 2007; Zhang, Maslov, and Shakhnovich, 2008; Johnson and Hummer, 2010)) emphasis is placed on how binding energies must be large enough to out compete non-functional interactions, and there is rarely any mention of how system size (in terms of volume) affects correct binding. But the interpretation behind the search-limiting condition Eq.(4.45) is that system size also constrains the ability of monomers to find one another and is just as relevant as binding energies in limiting non-functional interactions.

This interpretation leads us to a second interesting result: Eq.(4.45) indicates that in

achieving the fully-correct assembly regime, it is the product of particle number and volume, rather than their ratio encoded in density, that is constrained. This result reflects the fact that each of the monomers in a dimer system must find its optimal binding partner in the constituent volume, a task which is more difficult when said volume is large. This is because the quantity $2N$ serves two roles in this model; it defines the number of monomers in the system, but, since each monomer is distinct, it also defines the number of monomer species. Thus increasing N increases the density of the system, leading to more interactions between monomers for a given volume, but it also increases the number of different interacting monomer types and makes it more difficult for a single monomer to find its one other optimal binding partner. Similarly, increasing the volume V increases the number of position states a monomer must search through to find its optimal binding partner and makes such a search more difficult. Importantly, these effects are not independent. Eq.(4.45) indicates that the search-condition can be violated just as well for a large number of different monomers in a small volume as for a small number of monomers in a large volume. The "Dance Hall problem" discussed in Sec. 4.2.2 is useful in lending an intuitive picture to the competing relevance of N and V in achieving fully-correct assembly: It is easiest for a person to reach his or her original dance partner if both the number of other dancers and the volume of the hall is small. Increase either one and the task of reaching one's partner becomes more difficult.

4.8   Limitations and Extensions

To simplify our study of dimer self-assembly, we made a number of assumptions which limited the generality of the model and which thus point to ways to extend it.

First, we assumed that there was only a single-copy of each unique monomer in the system. This assumption greatly simplifies the combinatorial problem at the heart of the model, but does not match the properties of real biomolecular systems which almost always have many different monomer species each with a particular number of copies. However, one could consider a system where monomer species occur in multiple copies, but for which all monomers have the same copy-number. If these copies are uniformly

distributed throughout the system, then for a small region, one can take the equilibrium dynamics of the system to be defined by the consideration of only a single copy of each species.

To move beyond such a heuristic argument would require a more general formulation of the problem. For example, the non-gendered model should include $2N$ unique monomers $\alpha_1, \ldots, \alpha_{2N}$ where an α_k monomer has n_k copies in the system. For this more general system, one would need to determine the best way to model interactions between the same species and also how to consider mismatches between the number of possible correct partners and the number of available monomers in the system. Currently, it is not clear what is the best route towards attacking this more general problem.

For tractability, we did not give the monomers and dimers any sub-structure and instead defined their translational thermodynamics merely by the standard ideal-gas partition function Eq.(4.6). In protein systems, for example, we should expect the monomers and dimers to have non-zero moments of inertia and the dimers to have vibrational properties, facts we can incorporate into the preliminary partition function Eq.(4.9) by correcting the quantities raised to the power of k and m with the appropriate rotational and vibrational partition functions. The principal effect of these contributions would be to give stronger temperature dependences to $\langle k \rangle$ and $\langle m \rangle$. For example, taking the monomers to be spherical and the dimers to be vibration-less linear molecules with moments of inertia I, the factor of $\lambda_0^3 / V \sim T^{-3/2}$ in Eq.(4.27) would be replaced with

$$\lambda_0^3 \Theta / VT \sim T^{-5/2}, \tag{4.55}$$

where $\Theta = \hbar^2 / 2 I k_B$. It is apparent that for protein systems such incorporations are important because rotational and vibrational contributions to entropy have non-negligible contributions to the "price of lost freedom" (Finkelstein and Janin, 1989) experienced by monomers when they associate into dimers. However, it is not clear whether these incorporations would remove the sharp fall off in $\langle m \rangle$ exhibited by Type II systems.

Also, by giving the monomers and the dimers partition functions of the form V / λ_0^3, we assumed that they were dimensionless particles which did not interact outside of their

bindings. Such an assumption is not correct for the aqueous, and often crowded, solutions in which biomolecules actually reside (Fulton, 1982). Thus, for better correspondence with real systems, we should incorporate volume exclusion and interparticle interactions into the model by replacing the ideal gas partition function Eq.(4.6) with the appropriate first-order terms in a Virial expansion (Kardar, 2007c).

Two other limitations of the model concern length and time scales. Although the dimer model was able to capture some of the combinatorial properties of self-assembly, more often (as in the case of protein capsid or bilayer membrane assembly) the phrase "self-assembly" refers to the spontaneous construction of macromolecular structures that are much larger than their constituent parts (Israelachvili, Mitchell, and Ninham, 1976). Thus, generalizations of this model that seek to provide more insight into the statistical physics constraints of self-assembly would need to incorporate self-assembly on a hierarchy of scales without sacrificing the precision of the statistical physics treatment.

Second, since systems exhibiting self-assembly evolve towards equilibrium (rather than being perennially perched there), a mathematical model of the non-equilibrium properties of this dimer system would make a more useful archetype of self-assembly. Simulations are a good first step in this direction as long as they properly model the transition-state properties of assembly. To produce the simulations shown in Fig. 4.5, we started all of our systems in the low-entropy microstate of all correct dimers and used a non-physical transition step in which dimers could switch constituent monomers without dissociating. These unphysical choices were geared towards ensuring that our system efficiently explored the state space over our chosen simulation times. However, a more faithful simulation of self-assembly would have the system begin in a state of all monomers and would only allow monomer dissociation and association as transition steps. Our preliminary attempts to abide by these constraints reveal that for certain parameter regimes the system falls prey to the common self-assembly problem of "kinetic traps" (Hagan, Elrad, and Jack, 2011) in which even if the parameter space diagrams in Fig. 4.6 suggest that the system is in the regime of fully-correct assembly, the system can remain, for long simulation times, in a state of only partially-correct dimers. This kinetic trapping appears to be most prevalent

in Type II/combinatorics-limited systems, and reasonably disappears as $E_0 \rightarrow 0$, suggesting the Type I vs. Type II categorization can also be a qualitative categorization for the likelihood of kinetic trapping, but a more precise analytical argument would be preferred over these qualitative observations.

4.9   Concluding Statement

Motivated by the assembly of ssDNA into dsDNA, TF-DNA binding, and protein-protein interactions, we built a statistical physics model in which systems of monomers can bind together in correct or incorrect contacts. The model sought to explore how the energy benefit of correct contacts must be balanced against their corresponding combinatorial penalty in order for fully-correct assembly to still be possible. The value in exploring such a question through statistical physics rather than through the law of mass action is that the finiteness of the partition function in statistical physics allows us to respect—and hence more specifically account for—the finite-number combinatorial arrangements that are crucial in determining the possibility of self-assembly.

Chapter 5

Conclusion

"When studying something new I often used to start in the middle, using some complicated theory already developed by others. But often one sees further by starting with the simplest questions and examples, because that makes it easier to understand the basic problem and then perhaps to find a new approach to it."

– Dusa McDuff, *The Princeton Companion to Mathematics*

5.1 Summary

In the preceding chapters, we presented three statistical physics models motivated by various properties of biomolecular systems. Here we summarize the models and their associated results before discussing extensions.

- In Chapter 2, we began by considering the protein-design problem, and from the role permutations play in this problem, we proposed a model in which the state space was isomorphic to the symmetric group. By taking an arbitrary microstate of a thermal system to be $\vec{\theta} \in \mathrm{perm}(\omega_1, \ldots, \omega_N)$ and defining $j = \sum_{i=1}^{N} I_{\theta_i \neq \omega_i}$, we found that the mean-field energy function

$$\mathcal{E}_N(j) = \lambda_1 j + \frac{\lambda_2}{2N} j^2, \tag{5.1}$$

yielded (in the $N \gg 1$ limit) the equilibrium order-parameter

$$\langle j \rangle / N = 1 - \frac{1}{\beta\lambda_2} W_0 \left(\frac{\beta\lambda_2}{N} e^{\beta(\lambda_1 + \lambda_2)} \right), \tag{5.2}$$

where W_0 is the principal branch of the Lambert W function. What is significant about Eq.(5.2) is its variety of thermal behavior despite its simple energy function; the associated $\beta\lambda_1$ vs. $\beta\lambda_2$ phase plot exhibits five distinct parameter regimes, a triple and quadruple point, and two transition temperatures.

- In Chapter 3, we replaced the mean-field energy function Eq.(5.1) with one defined by quenched disorder and thereby built the basic theory of the "permutation glass." For the same space of states as in Chapter 2, we defined the energy of the system as

$$\mathcal{H}_N \left(\{\theta_i\} \right) = \sum_{k=1}^{N} \lambda_k I_{\theta_k \neq \omega_k}, \tag{5.3}$$

where $\{\lambda_k\}$ is the quenched distribution of energy-costs. Computing the partition function and equilibrium conditions (in the $N \gg 1$) for this energy function, we found that the order parameter $\langle j \rangle$ is constrained by

$$\frac{1}{N} = \int_{-\infty}^{\infty} d\lambda \, \frac{\rho_0(\lambda)}{e^{\beta\lambda} + \langle j \rangle}, \tag{5.4}$$

where $\rho_0(\lambda)$ is the distribution of λ values from which the elements $\{\lambda_i\}$ are drawn. From Eq.(5.4), we then found that the $\langle j \rangle = 0$ macrostate occurs at the temperature $k_B T_c = \beta_c^{-1}$, where

$$\frac{1}{N} = \int_{-\infty}^{\infty} d\lambda \, \rho_0(\lambda) e^{-\beta_c \lambda}. \tag{5.5}$$

Moreover, a necessary (but not sufficient) condition for the thermal equilibrium of the system to be $\langle j \rangle = 0$ was found to be

$$k_B T < k_B T_c \leq \frac{\overline{\lambda}}{\ln N}, \tag{5.6}$$

where $\overline{\lambda}$ is the average of the λ values over the distribution. From these results,

we defined the permutation glass regime of the system as one in which $\langle j \rangle = 0$ is never thermodynamically accessible even though there exists temperatures T that satisfy Eq.(5.6). Namely, for the permutation glass regime, there is no β_c that satisfies Eq.(5.5), even though $\overline{\lambda} > 0$.

Even more simply, we found that a necessary (but not sufficient) condition for the system to be able to access the $\langle j \rangle = 0$ state is

$$P_{\lambda<0} < \frac{1}{N}, \tag{5.7}$$

where $P_{\lambda<0} \equiv \int_{-\infty}^{0} d\lambda \, \rho_0(\lambda)$. Namely, for $\langle j \rangle = 0$ to be a thermodynamic state, the probability of an energy benefit for an incorrectly-ordered component must be less than the inverse of the number of components. Conversely, a sufficient (but not necessary) condition to define a system as in the permutation glass regime is the system satisfying $P_{\lambda<0} \geq 1/N$.

- In Chapter 4, we used the specific and non-specific interaction properties of protein and DNA molecules to introduce a model of dimer self-assembly. Given a system with $2N$ monomers labeled $\alpha_1, \ldots, \alpha_{2N}$ where the monomers can exist as bound dimers (α_k, α_ℓ) or as monomers, we required each monomer to have a single correct binding partner. The binding energies for these dimers were defined through

$$\mathcal{E}(\alpha_k, \alpha_\ell) = \begin{cases} -(E_0 + \Delta) & \text{for } |k - \ell| = N \\ -E_0 & \text{otherwise.} \end{cases} \tag{5.8}$$

The combinatorial properties of this model allowed us to write the associated partition function as an exact double integral from which we could analytically explore the equilibrium conditions of the system. Ultimately, we found that the equilibrium conditions were defined by the system of equations

$$\frac{4\sqrt{2}\lambda_0^3}{V}e^{\beta E_0} = \frac{\langle k \rangle - \langle m \rangle(1 - e^{-\beta\Delta})}{(N - \langle k \rangle)^2}, \qquad \frac{e^{\beta\Delta}}{2} = \langle m \rangle \frac{N - \langle m \rangle(1 - e^{-\beta\Delta})}{\langle k \rangle - \langle m \rangle(1 - e^{-\beta\Delta})}, \tag{5.9}$$

where λ_0 is the de Broglie thermal wavelength of a monomer, and $\langle k \rangle$ and $\langle m \rangle$ are the average number of dimers and average number of correct dimers, respectively. Beginning from Eq.(5.9), we found that dimer systems come in two distinct types, search-limited and combinatorics-limited, where, in the former, volume primarily constrains the achievement of the completely-correct dimers configuration, and in the latter combinatorics primarily constrains the completely-correct configuration. In particular, a biophysical analysis suggested that real systems consisting of ssDNA-ssDNA, protein-DNA, protein-protein interactions are all of the search-limited type.

The introduced models can be seen as particular examples of the intersection cited in Fig. 1.1: They are unexplored exactly-solved models in statistical physics which are defined by combinatorial questions but which have motivations extending from biomolecular contexts. One of the main purposes of this thesis was to show that one can find mathematically and qualitatively interesting exactly-solved statistical physics models in biology, and thus that biomolecular systems could be as fruitful of a context in which to find clean and useful physics models as condensed-matter systems. Moreover, by introducing the statistical physics of the symmetric group and the permutation glass to physics, we have provided examples for how the utility relationship between biology and physics is not only defined by the way the latter contributes to the former; the former, too, can contribute to the latter.

In the rest of this conclusion, we outline additional problems related to the ones in this thesis, problems which either are extensions of the frameworks we already introduced or are consistent with the tri-pronged theme of being motivated by a biomolecular context, made precise through combinatorics, and exactly-solvable.

5.2 Generalized Derangements

In Chapters 2 and 3, we studied models for which the state space consisted of permutations of a list of components, precisely defined as $(\omega_1, \omega_2, \ldots, \omega_N)$. In these models, each type of component in the component list occurred once. However, we could consider a more general scenario in which the component ω_k occurs n_k times for $k = 1, \ldots, N$. For such a

state space, the total number of inequivalent rearrangements of the components would be the multinomial

$$\frac{(n_1 + n_2 + \cdots + n_N)!}{n_1! n_2! \cdots n_N!}. \tag{5.10}$$

How would we construct a statistical physics in which the state space was defined by the permutations of such a list with repeated components? In constructing the statistical physics of the symmetric group, the key quantity in building our model (i.e., in going from Eq.(2.7) to Eq.(2.11)) was the number of "derangements" of a list, that is the number of ways to completely rearrange the components of a list so that no component coincides with its original placement. For a list in which each component appears once, we found that the number of derangements could be written as

$$d_N = \int_0^\infty dx \, e^{-x} (x-1)^N. \tag{5.11}$$

What about for a list in which components ω_k occurs n_k times? In 1976 Gillis and Even (Even and Gillis, 1976), worked out the mathematical expression for this problem and found that the number of derangements was given by

$$P_{\mathbf{n}} = \int_0^\infty dx \, e^{-x} L_{n_1}(x) L_{n_2}(x) \cdots L_{n_N}(x), \tag{5.12}$$

where L_j is the jth Laguerre polynomial and $\mathbf{n} = (n_1, \ldots, n_N)$. Eq.(5.12) is often termed the "Generalized Derangement formula" because it contains Eq.(5.11) as a special case; if we set $n_k = 1$ for all k, then Eq.(5.12) reduces to Eq.(5.11). Now, using Eq.(5.12) to construct a statistical physics of generalized derangements in a way analogous to the construction presented in Chapter 2, we first pre-define a zero-energy arrangement of the components and require that the system incur an energy cost of $+\lambda_k$ whenever a component ω_k is not in this zeroth-energy arrangement. With this definition, one can show (see Appendix E.1) that the partition function for the system is given by

$$Z_{\mathbf{n}}(\{\beta\lambda_k\}) = \int_0^\infty dx \, e^{-x} \prod_{k=1}^N \left(1 - e^{-\beta\lambda_k}\right)^{n_k} L_{n_k}\left(\frac{x}{1 - e^{\beta\lambda_k}}\right). \tag{5.13}$$
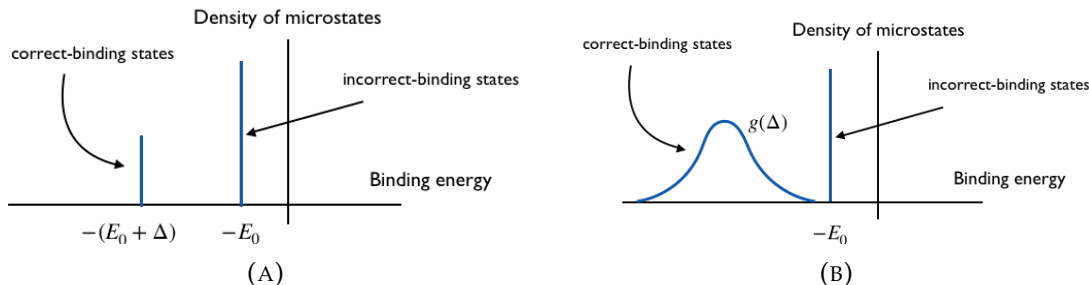
FIGURE 5.1: (a) For the dimer system considered in Chapter 4, all incorrect dimers have one binding energy and all correct dimers have another binding energy. (b) For the dimer system defined by Eq.(5.14), the incorrect dimers have the binding energy $-E_0$, but the correct dimers have a spectrum of binding energies. Because of the spectrum of binding energies for correct dimers, the system depicted by Fig. 5.1b is more general, but also more analytically difficult to study.

Like the permutation glass partition function Eq.(3.3) in Chapter 3, Eq.(5.13) defines a system of quenched-disorder where the disorder is encoded in the distribution of energy costs $\{\lambda_k\}$. In analogy to the analysis in Chapter 3, we could define order parameters for this system and attempt to understand under what parameter conditions the system settles into its lowest energy configuration. Complicating the picture in this case is the multiplicity of each component, a property which itself represents a sort of quenched disorder in the system and which would have to be incorporated into the standard analysis presented in Chapter 3.

5.3 Quenched Distribution for Dimer Self-Assembly

In Chapter 4, our goal was to analyze correct and incorrect interactions in a systems of dimer-forming biomolecules. As a simplifying assumption, we took all correct interactions to be defined by the same binding energy and all incorrect interactions to be defined by a different binding energy. Clearly, however, the most general interaction scenario would be defined by a $2N \times 2N$ binding matrix where each of the $2N$ monomers has a binding energy unique to every other monomer. Working in the direction of the most general problem, we consider the simpler case in which all incorrect interactions have the same binding energy and each correct interaction has binding energies dependent on the particular interacting monomers. Specifically, say we have $2N$ monomers $\alpha_1, \ldots, \alpha_{2N}$ where

each monomer can bind to any other monomer. If two α monomers come into contact (say α_i and α_j where $i < j$) the two form a dimer with binding energy

$$
\mathcal{E}(\alpha_i, \alpha_j) = \begin{cases} -(E_0 + \Delta_i) & \text{if } j = i + N, \\ -E_0 & \text{otherwise.} \end{cases} \tag{5.14}
$$

We note that $\mathcal{E}(\alpha_i, \alpha_j) = \mathcal{E}(\alpha_j, \alpha_i)$. Eq.(5.14) differs from the binding energy profile Eq.(4.3) in Chapter 4 in that the correct binding energies are parameterized by Δ_i and thus there is a distribution of correct binding energies instead of a single binding energy defining all correct contacts (Fig. 5.1). From Eq.(5.14), we can work through a derivation similar to that used to obtain Eq.(4.15) and find (see Appendix E.2) that the partition function for the system is given by

$$
Z_N(V, T, E_0, \{\Delta_k\}) = c_{0,N} \int_0^\infty dx\, dy\, \frac{e^{-x-y}}{\sqrt{xy}} \oint_C \frac{dz}{z} B_N(z) \prod_{\ell=1}^N \left[z\, x + \delta\, y(\eta_\ell + 2x - 1) \right], \tag{5.15}
$$

where C is a closed contour around the origin in the complex plane,

$$
c_{0,N} = \frac{(V/\lambda_0^3)^{2N}}{2\pi i \sqrt{\pi} \Gamma(N + 1/2)}, \qquad \delta \equiv \frac{2\sqrt{2}\lambda_0^3}{V} e^{\beta E_0}, \quad \text{and} \quad \eta_\ell = e^{\beta \Delta_\ell}. \tag{5.16}
$$

and

$$
B_N(z) = \frac{N+1}{2} \int_0^1 dt\, \left[\left(\sqrt{1-t} + \sqrt{t/z} \right)^{2N} + \left(\sqrt{1-t} - \sqrt{t/z} \right)^{2N} \right]. \tag{5.17}
$$

Although the partition function Eq.(5.15) is more general than Eq.(4.15), it is not clear whether the additional insight gained into self-assembling dimer systems is worth the additional analytical effort needed to study the more general case. Phrased differently, does considering a distribution of correct energies rather than a single one bring us so much closer to the properties of the motivating systems (of TF-DNA, ssDNA-ssDNA, and

protein-protein interactions) that it is worth pursuing? In any case, regardless of the answer to this question, since Eq.(5.14) represents a quenched-energy distribution, the properties of Eq.(5.15) might be of interests to at least mathematical physicists if not to biophysicists.

5.4 Particle Aggregation

Finally, if the ethos presented in this thesis (i.e., that molecular biology can contribute to statistical physics) has any wider validity, we should be able to find biomolecular systems distinct from those discussed in the previous chapters which can also be framed in terms of combinatorial problems and which lead to exactly-solved statistical physics models. We present one such system here.

In (Kindt, 2012), Kindt computationally studied the problem of aggregating monomers by relating it to the number theoretic concept of partitions. In molecular biology, aggregation refers to the process in which individual monomers bind together to form larger structures, which are either functional or non-functional depending on the interaction and monomer properties. In number theory, a partition of a number is a way of expressing that number as a sum of smaller numbers. The relationship between aggregation and partitions is evident upon example. If a system has N particles, the number of different ways these particles can aggregate together is given by the number of different partitions for the number N (Fig. 5.2). Kindt used this relationship to computationally study aggregation. However, since partitions have played such an important role in number theory for much of the 20th century, it should be possible to use the methods developed in number theory to study aggregation analytically.

We can build analytical models of aggregation based on the number-theoretic concept of partitions as follows. The number of partitions $p(N)$ of a number N can be expressed as

$$p(N) = \sum_{n_1=0}^{\infty} \cdots \sum_{n_N=0}^{\infty} \delta\left(N, \sum_{k=1}^{N} kn_k\right), \tag{5.18}$$

What are the different ways to partition the number 5 (i.e., to write 5 as a sum of integers)?

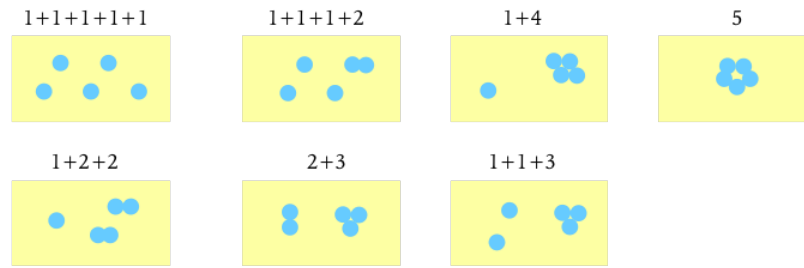What different aggregates are possible with 5 monomers?

FIGURE 5.2: Two questions and one answer. Asking "what are the number of partitions of the number 5?" and "what are the number of possible aggregate configurations (ignoring translational entropy) of 5 particles?" yields the same answer.

where δ is the Kronecker delta. There is a large literature of analytical results in which $p(N)$ is approximated for $N \gg 1$. The first and most famous of these approximations is the Hardy-Ramanujan result (Hardy and Ramanujan, 1918), in which $p(N)$ is written as a contour integral and then evaluated with the method of steepest descent for $N \gg 1$:

$$p(N) = \frac{1}{2\pi i} \oint_\Gamma \frac{dz}{z^{N+1}} \prod_{k=1}^{N} \frac{1}{1 - z^k} \simeq \frac{1}{4N\sqrt{3}} \exp\left(\pi\sqrt{\frac{2N}{3}}\right), \qquad (5.19)$$

where Γ is a closed-contour around the origin in the complex plane. Now, to connect these results to physics we can envision a simple aggregation scenario. Say we have N identical monomers which can form aggregates of any size from 2-particle aggregates to N-particle aggregates. We say that a k-particle aggregate is formed with a binding energy $-E_k$, and that each monomer in the aggregate has mass m_0. Taking the system to comprise a volume V and exist at a temperature T (see Fig. 5.3), we can write the partition function for this system as

$$Z_N(\{E_i\}, V, T) = \sum_{n_1=0}^{\infty} \cdots \sum_{n_N=0}^{\infty} \delta\left(N, \sum_{k=1}^{N} k n_k\right) \exp\left(-\beta \sum_{i=1}^{N} E_i n_i\right) \prod_{j=1}^{N} \frac{1}{n_j!} \left(\frac{V}{\lambda_j^3}\right)^{n_j}, \quad (5.20)$$

where $\beta = 1/k_B T$ and $\lambda_j = h/\sqrt{2\pi j m_0 k_B T}$ is the de Broglie wavelength of a j-particle aggregate. In Eq.(5.20), the first factor within the summation is the combinatorial factor that leads to a count of the number of aggregates for an N particle system; the second
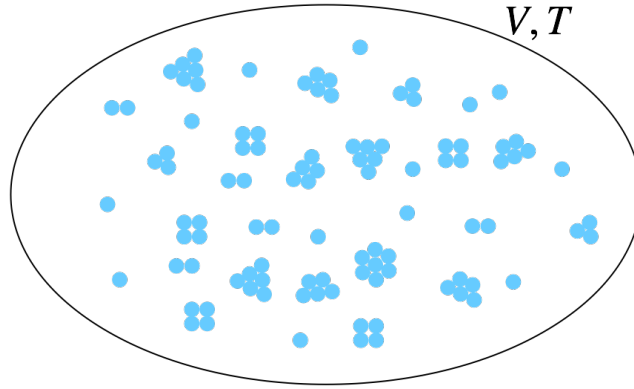
FIGURE 5.3: Example microstate with aggregates of various size and in various copy number.

factor is the Boltzmann factor for a particular aggregate configuration; the third factor is the net translational partition function for a particular aggregate configuration. Representing Eq.(5.20) as a contour integral akin to the representation of $p(N)$ in Eq.(5.19), we find (see Appendix E.3) that the partition function becomes

$$Z_N(\{E_i\}, V, T) = \frac{1}{(2\pi i)^{N+1}} \oint_\Gamma \frac{dw}{w^{N+1}} \prod_{k=1}^{N} \oint_{\Gamma_k} dz_k \frac{e^{z_k}}{z_k} \left(1 - w^k \frac{V e^{-\beta E_k}}{\lambda_k^3 z_k} \right)^{-1}. \tag{5.21}$$

Eq.(5.21) is a complicated results but preliminary calculations suggest it is possible to find corresponding equilibrium configurations using the same steepest descent methods used to establish the approximation Eq.(5.19). Being able to find and solve such equilibrium conditions would yield a statistical physics perspective on aggregation which might prove more fruitful than the phenomenological perspective provided by law of mass action analyses (e.g., such as those given in (Israelachvili, Mitchell, and Ninham, 1976)).

5.5 Final Remarks

The aforementioned models generalize the main results in the thesis and present a new context in which the discussed techniques can be applied. The intention in this presentation was to add further evidence to one of the motivating claims for this work: that
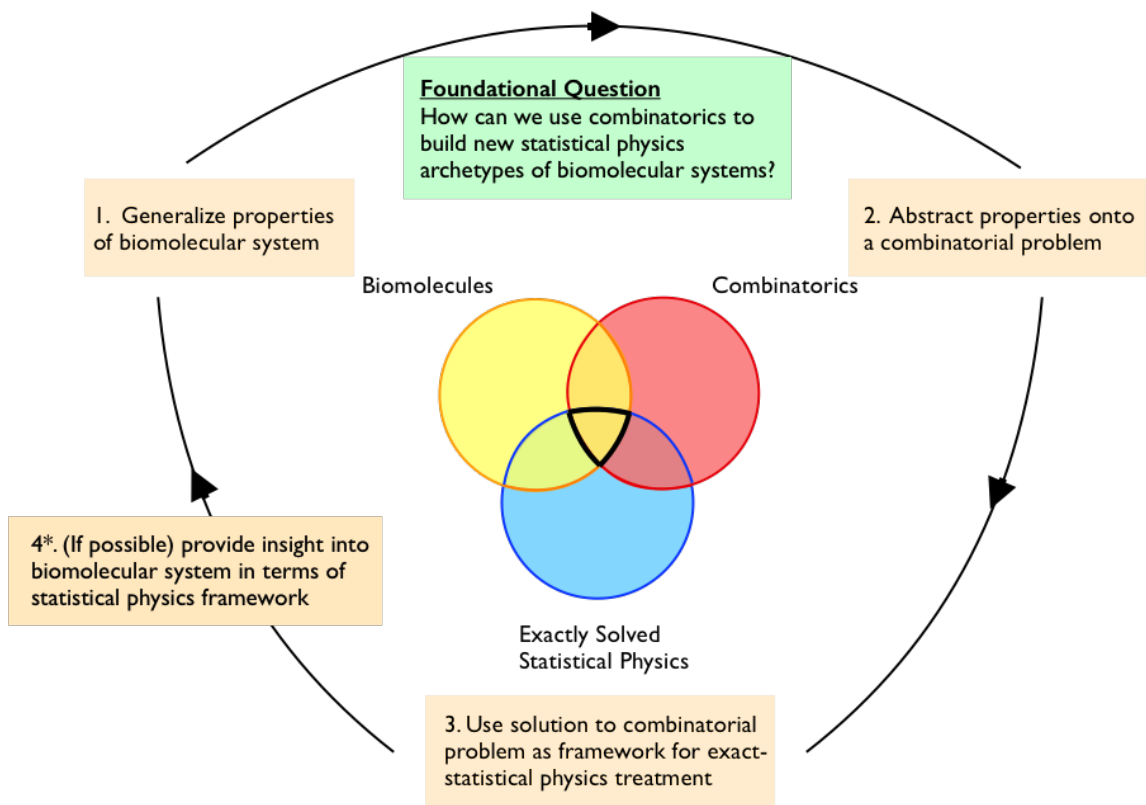
FIGURE 5.4: General strategy for building combinatorial models of biomolecular systems.

there are interesting problems in the intersection between exactly-solved models and combinatorics that have been unexplored by physicists because the motivation for these problems existed in a place that physicists ordinarily do not look; namely in the study of biomolecules.

A second motivation for this work stemmed from the desire to find a new archetype for studying biomolecules. From considering the process that went into creating the presented models, we can abstract away a general strategy for building combinatorial models of biomolecular systems. First, beginning with the biomolecular system of interest, we generalize its properties of interest by listing the features shared by all systems of a similar type. From these properties, we abstract a combinatorial problem whose solution forms the basis for counting the number of microstates in the generalized system. We then use the solution to this combinatorial problem to build a statistical physics model of the system. If possible, we use this new model to gain a deeper understanding of the underlying system of interest or at least a better understanding of some of its properties (See Fig. 5.4).

We applied this strategy in our study of protein design, biomolecular dimers, and the discussion of particle aggregation in this conclusion, and we can see it as a combinatorial archetype in the physical modeling of biomolecular system in much the same way the Ising model is used as an archetype in such systems. One main difference between the two archetypes is in the microstate spaces they most conveniently model. While the Ising model is useful in modeling systems with many independent and discretely valued state spaces, the combinatorial archetype is useful in modeling systems in which the space of states is drawn from the number of ways to reorder the elements in a set.

The hope is that the work in this thesis can serve as a collection of proof-of-concept examples of studies according to this combinatorial strategy and will encourage further study in these directions.

Appendix A

From Protein Design to the Symmetric Group, Derivations

A.1 Alternative Derivations of Eq.(2.36)

A.1.1 Hubbard-Stratonovich Approach

We re-derive Eq.(2.36) using the Hubbard-Stratonovich method. We start this derivation assuming $\lambda_2 = -|\lambda_2|$; we will later see our resulting free energy can be analytically continued to the $\lambda_2 > 0$ case.

For $\lambda_2 = -|\lambda_2|$, the partition function is

$$Z_N(\beta; \lambda_1, \lambda_2) = \sum_{j=0}^{N} g_N(j) e^{-\beta\lambda_1 j + \beta|\lambda_2|j^2/2N}. \tag{A.1}$$

Then, applying the identity

$$e^{\beta|\lambda_2|j^2/2N} = \sqrt{\frac{N}{2\pi\beta|\lambda_2|}} \int_{-\infty}^{\infty} dx \, e^{-Nx^2/2\beta|\lambda_2|-jx}, \tag{A.2}$$

we have

$$Z_N(\beta; \lambda_1, \lambda_2) = \sqrt{\frac{N}{2\pi\beta|\lambda_2|}} \int_{-\infty}^{\infty} dx \, e^{-Nx^2/2\beta|\lambda_2|} \sum_{j=0}^{N} g_N(j) e^{-j(\beta\lambda_1 + x)}$$

$$= \sqrt{\frac{N}{2\pi\beta|\lambda_2|}} \int_{-\infty}^{\infty} dx \, e^{-Nx^2/2\beta|\lambda_2|} Z_N(\beta\lambda_1 + x), \tag{A.3}$$

where $z_N(x) \equiv \sum_{j=0}^{N} g_N(j)e^{-jx}$. From Eq.(2.14) we found

$$z_N(x) = \int_0^\infty ds\, e^{-s} \left(1 + (s-1)e^{-x}\right)^N . \tag{A.4}$$

So Eq.(A.3) becomes

$$Z_N(\beta; \lambda_1, \lambda_2) = \sqrt{\frac{N}{2\pi\beta|\lambda_2|}} \int_0^\infty ds \int_{-\infty}^\infty dx \left(1 + (s-1)e^{-\beta\lambda_1 - x}\right)^N e^{-s - Nx^2/2\beta|\lambda_2|} . \tag{A.5}$$

The function to which we apply steepest descent is then

$$h(s,x) = s + \frac{Nx^2}{2\beta|\lambda_2|} - N\ln\left(1 + (s-1)e^{-\beta\lambda_1 - x}\right) . \tag{A.6}$$

Computing the conditions for $\partial_s h(s = \bar{s}, x = \bar{x}) = 0$ and $\partial_x h(s = \bar{s}, x = \bar{x}) = 0$ we obtain, respectively,

$$1 - N \frac{e^{-\beta\lambda_1 - \bar{x}}}{1 + (\bar{s} - 1)e^{-\beta\lambda_1 - \bar{x}}} = 0 \tag{A.7}$$

$$\frac{\bar{x}}{\beta|\lambda_2|} + \frac{(\bar{s} - 1)e^{-\beta\lambda_1 - \bar{x}}}{1 + (\bar{s} - 1)e^{-\beta\lambda_1 - \bar{x}}} = 0. \tag{A.8}$$

Solving for $\bar{s}$ in the first equation we have

$$\bar{s} = N + 1 - e^{\beta\lambda_1 + \bar{x}} \tag{A.9}$$

and with the second equation we have the condition

$$\frac{\bar{x}}{\beta|\lambda_2|} = -\frac{1}{N}(\bar{s} - 1). \tag{A.10}$$

Substituting the second condition into the first yields

$$\bar{s} - 1 = N - e^{\beta\lambda_1 - \beta|\lambda_2|(\bar{s}-1)/N} , \tag{A.11}$$

or

$$e^{-\beta|\lambda_2|(\bar{s}-1)/N} = e^{\beta\lambda_1}\left(N - (\bar{s} - 1)\right). \tag{A.12}$$

Thus, the solution for $\bar{s}$ can be expressed in terms of the Lambert W function as

$$\frac{\bar{s}-1}{N} = 1 + \frac{1}{\beta|\lambda_2|} W\left(-\frac{\beta|\lambda_2|}{N} e^{\beta\lambda_1 - \beta|\lambda_2|}\right). \tag{A.13}$$

For $\lambda_2 > 0$, we can employ the complex version of the Hubbard-Stratonovich identity:

$$e^{-\beta\lambda_2 j^2/2N} = \sqrt{\frac{N}{2\pi\beta\lambda_2}} \int_{-\infty}^{\infty} dx\, e^{-Nx^2/2\beta\lambda_2 - ijx}. \tag{A.14}$$

Working through an analogous steepest descent procedure, we find that the equilibrium value for $\bar{s}$ is

$$\frac{\bar{s}-1}{N} = 1 - \frac{1}{\beta\lambda_2} W\left(\frac{\beta\lambda_2}{N} e^{\beta\lambda_1 + \beta\lambda_2}\right) \equiv \frac{\bar{j}}{N}, \tag{A.15}$$

which could have been extrapolated from Eq.(A.13) by taking $|\lambda_2| \to -\lambda_2$. From this expression for the equilibrium condition, and as an analogy with the non-interacting case, it turns out the order parameter in this case is not $\bar{s}$ but rather $\bar{s} - 1$.

A.1.2 Gibbs-Bogoliubov Inequality Derivation of Eq.(2.36)

We re-derive Eq.(2.36) using the Gibbs-Bogoliubov Inequality(Yeomans, 1992). The inequality is

$$F[\mathcal{H}] \leq F[\mathcal{H}_0] + \langle \mathcal{H} - \mathcal{H}_0 \rangle_0. \tag{A.16}$$

The Hamiltonian which defines our system is

$$\mathcal{H} = \lambda_1 \sum_{i=1}^{N} I_{\theta_i \neq \omega_i} + \frac{\lambda_2}{2N} \sum_{i,j} I_{\theta_i \neq \omega_i} I_{\theta_j \neq \omega_j} \equiv \lambda_1 j + \frac{\lambda_2}{2N} j^2, \tag{A.17}$$

and our variational Hamiltonian is instead

$$\mathcal{H}_0 = \lambda_0 \sum_{i=1}^{N} I_{\theta_i \neq \omega_i} = \lambda_0 j. \tag{A.18}$$

From Eq.(2.14) we know

$$F[\mathcal{H}_0] = -\frac{1}{\beta} \ln Z_N(\beta\lambda_0) = -\frac{1}{\beta} \ln\left\{\int_0^{\infty} ds\, e^{-s} \left(1 + (s-1)e^{-\beta\lambda_0}\right)^N\right\}. \tag{A.19}$$

We can also define

$$\langle \mathcal{O}(j) \rangle_{0,N} = \sum_{j=0}^{N} \mathcal{O}(j) \, e^{-\beta \lambda_0 j}, \tag{A.20}$$

as the average with respect to our variational Hamiltonian Eq.(A.18). Thus, Eq.(A.16) becomes

$$F[\mathcal{H}] \le -\frac{1}{\beta} \ln Z_N(\beta \lambda_0) + (\lambda_1 - \lambda_0) \langle j \rangle_{0,N} + \frac{\lambda_2}{2N} \langle j^2 \rangle_{0,N} \equiv f(\lambda_0) \tag{A.21}$$

Differentiating f with respect to λ_0 allows us to compute the maximum of this quantity. Given $\langle j \rangle_{0,N} = -\partial \ln Z_N(\beta \lambda_0) / \partial(\beta \lambda_0)$, we then find

$$f'(\lambda_0) = (\lambda_1 - \lambda_0) \frac{\partial}{\partial \lambda_0} \langle j \rangle_{0,N} + \frac{\lambda_2}{2N} \frac{\partial}{\partial \lambda_0} \langle j^2 \rangle_{0,N}, \tag{A.22}$$

which if we take to be zero at some $\lambda_0 = \overline{\lambda}_0$ gives us

$$0 = (\lambda_1 - \overline{\lambda}_0) \frac{\partial}{\partial \lambda_0} \langle j \rangle_{0,N} \bigg|_{\lambda_0 = \overline{\lambda}_0} + \frac{\lambda_2}{2N} \frac{\partial}{\partial \lambda_0} \langle j^2 \rangle_{0,N} \bigg|_{\lambda_0 = \overline{\lambda}_0}. \tag{A.23}$$

To compute these derivatives we make use of various identities. First we note

$$\langle j^2 \rangle_{0,N} = \frac{1}{Z_N(\beta \lambda_0)} \frac{\partial^2}{\partial(\beta \lambda_0)^2} Z_N(\beta \lambda_0), \tag{A.24}$$

so

$$\frac{\partial}{\partial(\beta \lambda_0)} \langle j \rangle_{0,N} = -\frac{\partial^2}{\partial(\beta \lambda_0)^2} \ln Z_N(\beta \lambda_0)$$

$$= -\frac{1}{Z_N(\beta \lambda_0)} \frac{\partial^2}{\partial(\beta \lambda_0)^2} Z_N(\beta \lambda_0) + \frac{1}{Z_N(\beta \lambda_0)^2} \left(\frac{\partial}{\partial(\beta \lambda_0)} Z_N(\beta \lambda_0) \right)^2$$

$$= -\langle j^2 \rangle_{0,N} + \langle j \rangle_{0,N}^2. \tag{A.25}$$

This last equality implies

$$\frac{\partial}{\partial(\beta \lambda_0)} \langle j^2 \rangle_{0,N} = -\frac{\partial^2 \langle j \rangle_{0,N}}{\partial(\beta \lambda_0)^2} + 2 \langle j \rangle_{0,N} \frac{\partial \langle j \rangle_{0,N}}{\partial(\beta \lambda_0)}, \tag{A.26}$$

and so Eq.(A.23) becomes

$$0 = \left[\lambda_1 - \bar{\lambda}_0 + \frac{\lambda_2}{N}\langle j\rangle_{0,N}\right] \frac{\partial}{\partial \lambda_0} \langle j\rangle_{0,N}\bigg|_{\lambda_0=\bar{\lambda}_0} - \frac{\lambda_2}{2N\beta} \frac{\partial^2 \langle j\rangle_{0,N}}{\partial \lambda_0^2}\bigg|_{\lambda_0=\bar{\lambda}_0} \tag{A.27}$$

To compute these quantities we need to approximate the partition function for our variational system. Using the method of steepest descent

$$\begin{aligned}
Z_N(\beta\lambda_0) &= \int_0^\infty ds\, e^{-s} \left(1 + (s-1)e^{-\beta\lambda_0}\right)^N \\
&= \sqrt{2\pi N} \left(\frac{N}{e^{\beta\lambda_0}}\right)^N \exp\left(e^{\beta\lambda_0} - N - 1\right)\left(1 + \mathcal{O}\left(N^{-1}\right)\right),
\end{aligned} \tag{A.28}$$

and so we have

$$\begin{aligned}
\langle j\rangle_{0,N} &= -\frac{\partial}{\partial(\beta\lambda_0)} \ln Z_N(\beta\lambda_0) \\
&= N - e^{\beta\lambda_0} + \mathcal{O}\left(N^{-1}\right).
\end{aligned} \tag{A.29}$$

Computing the relevant derivatives in Eq.(A.27) we find

$$\begin{aligned}
0 &= \left[\lambda_1 - \bar{\lambda}_0 + \frac{\lambda_2}{N}\langle j\rangle_{0,N}\right]\left(-e^{\beta\lambda_0} + \mathcal{O}\left(N^{-1}\right)\right) - \frac{\lambda_2}{2N}\left(-e^{\beta\lambda_0} + \mathcal{O}\left(N^{-1}\right)\right) = 0 \\
&= \left[\lambda_1 - \bar{\lambda}_0 + \frac{\lambda_2}{N}\langle j\rangle_{0,N} - \frac{\lambda_2}{2N}\right]e^{\beta\lambda_0} + \mathcal{O}\left(N^{-1}\right)
\end{aligned} \tag{A.30}$$

Neglecting subleading terms of $\mathcal{O}(1/N)$ (a choice only valid for $\langle j\rangle_{0,N} \gg 1$), solving for $\bar{\lambda}_0$, and using Eq.(A.29) we then obtain the equilibrium constraint

$$e^{\beta\lambda_1 - \beta\lambda_2/2N + \beta\lambda_2\langle j\rangle_{0,N}/2N} = N - \langle j\rangle_{0,N}, \tag{A.31}$$

which when solved for $\langle j\rangle_{0,N}/N$ gives us

$$\langle j\rangle_{0,N}/N = 1 - \frac{1}{\beta\lambda_2}W\left(\frac{\beta\lambda_2}{N}e^{\beta\lambda_1 + \beta\lambda_2\left(1 - \frac{1}{2N}\right)}\right), \tag{A.32}$$

or, given our approximations and limiting expressions, the result

$$\langle j \rangle_{0,N}/N = 1 - \frac{1}{\beta\lambda_2}W\left(\frac{\beta\lambda_2}{N}e^{\beta\lambda_1+\beta\lambda_2}\right) + \mathcal{O}\left(N^{-1}\right). \tag{A.33}$$

A.2   Monte-Carlo Procedure for Parameter Space

To generate Fig. 2.4, we implemented the following MC algorithm:

1. Uniformly sample two points for λ_1 and λ_2 separately from within a certain bounded domain.

2. Draw the free energy curve Eq.(2.33) corresponding to the sampled values (λ_1, λ_2).

3. Label the curve according to which schematic curve in Fig. 2.3 it corresponds (i.e., according to its $\bar{j}_0$, $\bar{j}_-$ and $f_N(N,\beta)$ properties).

4. Color the point to signify the label.

We repeated this procedure for $10,000$ points with $\beta = 1$. The regime separation lines were included after the MC procedure from the analytic forms cited in the text.

A.3   Analytic Functions of Regime Boundaries

Order to Partial-Order Transition

The regime boundary which separates the ordered and the partially ordered regime is defined by the condition $\bar{j}_0 \geq 0$. For this regime boundary we have the condition

$$1 - \frac{1}{\beta\lambda_2}W_0\left(\frac{\beta\lambda_2}{N}e^{\beta\lambda_1+\beta\lambda_2}\right) \geq 0, \tag{A.34}$$

or

$$W_0\left(\frac{e^{\beta\lambda_1}}{N}\beta\lambda_2 e^{\beta\lambda_2}\right) \geq \beta\lambda_2. \tag{A.35}$$

From a plot of $W_0(a\,xe^x)/x$ for real a, we see that $W(axe^x)/x > 1$ if $a > 1$ and $W(axe^x)/x < 1$ if $a < 1$. Thus this order to partial-order transition is defined by the condition $e^{\beta\lambda_1}/N =$

1, or

$$\lambda_1 = \frac{\ln N}{\beta}. \tag{A.36}$$

Order to Order-Partial-Order Metastability Transition

The regime boundary which separates the ordered regime from the order and partial-order metastability regime is defined by the condition $-1 \leq W < 0$. This condition is where the $\bar{j}_0$ and $\bar{j}_-$ begin coexisting (Weisstein, 2002d), thus creating the mutual existence of a local maxima and local minima in Fig. 2.3. Thus for this regime boundary we have the condition

$$-1 \leq W\left(\frac{\beta\lambda_2}{N}e^{\beta\lambda_1 + \beta\lambda_2}\right) < 0, \tag{A.37}$$

This condition is valid so long as the argument of W satisfies

$$-e^{-1} \leq \frac{\beta\lambda_2}{N}e^{\beta\lambda_1 + \beta\lambda_2} < 0. \tag{A.38}$$

This inequality can only possibly be satisfied for $\lambda_2 < 0$ and if $\lambda_2 < 0$ the right inequality is automatically true. So, our transition condition is given by

$$-\frac{N}{e}e^{-\beta\lambda_1} = \beta\lambda_2 e^{\beta\lambda_2}. \tag{A.39}$$

In the Order phase we automatically have $\beta\lambda_1 > \ln N$, so the LHS of Eq.(A.39) is greater than or equal to $-e^{-1}$. Moreover, since λ_2 is exclusively negative, at $\beta\lambda_2 = \ln N$, $\beta\lambda_1$ is at a maximum value of $\beta\lambda_2 = -1$. For $\beta\lambda_2 \leq -1$, the solution to Eq.(A.39) is then

$$\lambda_2 = \frac{1}{\beta}W_{-1}\left(-\frac{N}{e}e^{-\beta\lambda_1}\right). \tag{A.40}$$

Order to Disorder Transition

The regime boundary which separates the partially ordered regime from the disordered regime is defined by the condition $\bar{j}_0 \leq N - 1$. We set the maximum value of $\bar{j}_0$ to $N - 1$ rather than N because Eq.(2.41) is associated with a free energy which diverges at $\bar{j}_0 = N$

and this approximate result is thus only physical up to $N - 1$. Alternatively we could see the maximum condition $\bar{j}_0 = N - 1$ as respecting the fact that Eq.(2.41) is only valid up to $\mathcal{O}(N^{-1})$. For this regime boundary we have the condition

$$1 - 1/N \geq 1 - \frac{1}{\beta \lambda_2} W_0 \left(\frac{\beta \lambda_2}{N} e^{\beta \lambda_1 + \beta \lambda_2} \right) \tag{A.41}$$

or

$$\frac{\beta \lambda_2}{N} \leq W_0 \left(\frac{\beta \lambda_2}{N} e^{\beta \lambda_2 / N} e^{\beta \lambda_1 - \beta \lambda_2 - \beta \lambda_2 / N} \right). \tag{A.42}$$

Again, using the condition that $W_0(a\, x e^x)/x > 1$ if $a > 1$, we find that the critical condition for this transition is $\beta \lambda_1 + \beta \lambda_2 - \beta \lambda_2 / N = 0$ or

$$\lambda_2 = -\frac{\lambda_1}{1 - 1/N}. \tag{A.43}$$

Appendix B

Permutation Glass, Derivations

B.1 Derivation of Correlation

For our permutation system with the partition function

$$Z_N(\beta\lambda_0) = \sum_{\{\vec{\theta}\}} \exp\left(-\beta\lambda_0 \sum_{i=1}^{N} I_{\theta_i \neq \omega_i}\right), \tag{B.1}$$

the sum of all the site-site correlations is given by

$$\sum_{i,j}^{N} \sigma_{ij}^2 = \sum_{i,j}^{N} \left(\langle I_{\theta_i \neq \omega_i} I_{\theta_j \neq \omega_j}\rangle - \langle I_{\theta_i \neq \omega_i}\rangle \langle I_{\theta_j \neq \omega_j}\rangle\right). \tag{B.2}$$

Given that no site is special we can expect the the site-site correlations for different sites to be the same regardless of which two sites we choose. Thus, we have

$$\sum_{i,j}^{N} \sigma_{ij}^2 = N(N-1)\sigma_{i\neq j}^2 + \sum_{i=1}^{N} \left(\langle I_{\theta_i \neq \omega_i}\rangle - \langle I_{\theta_i \neq \omega_i}\rangle^2\right), \tag{B.3}$$

where we used $I_{\theta_i \neq \omega_i}^2 = I_{\theta_i \neq \omega_i}$ in the last line. Thus we find that the site-site correlation for different sites is

$$\sigma_{i\neq j}^2 = \frac{1}{N(N-1)} \left[\frac{\partial^2}{\partial(\beta\lambda_0)^2} \ln Z_N(\beta\lambda_0) - \sum_{i=1}^{N} \langle I_{\theta_i \neq \omega_i}\rangle \left(1 - \langle I_{\theta_i \neq \omega_i}\rangle\right)\right]. \tag{B.4}$$

From Williams, 2017, we have

$$\ln Z_N(\beta\lambda_0) \simeq -N\beta\lambda_0 + e^{\beta\lambda_0} - N - 1 + G_0(N), \tag{B.5}$$

where $G_0(N)$ is independent of $\beta\lambda_0$. We also have that average incorrectness of a single site is

$$\langle I_{\theta_i \neq \omega_i} \rangle \simeq 1 - e^{\beta\lambda_0}/N. \tag{B.6}$$

Using Eq.(B.6) and Eq.(B.5) in Eq.(B.4) we obtain

$$\sigma_{i\neq j}^2 \simeq \frac{1}{N-1}\left(\frac{e^{\beta\lambda_0}}{N}\right)^2, \tag{B.7}$$

which, given the limits of the Laplace's method result Eq.(B.6), is only valid for $\beta\lambda_0 < \ln N$.

B.2 Replica Symmetric Solution

In this appendix, we will show Eq.(3.11) is consistent with the replica symmetric solution to the permutation model with quenched disorder. To study quenched disorder in our permutation system, we must evaluate the quantity

$$\langle \ln Z_N(\{\beta\lambda_i\}) \rangle = \int_{-\infty}^{\infty} \prod_{k=1}^{N} d\lambda_k \, \rho(\{\lambda_j\}) \ln \int_0^{\infty} dt \, e^{-s} \prod_{\ell=1}^{N} \left(1 + (s-1)e^{-\beta\lambda_\ell}\right). \tag{B.8}$$

For generality we will not specify a particular form for $\rho(\{\lambda_k\})$ other than to assume each λ_k has the same distribution:

$$\rho(\{\lambda_k\}) = \prod_{j=1}^{N} \rho_0(\lambda_j). \tag{B.9}$$

To implement the replica procedure, we apply the identity

$$\ln Z = \lim_{n\to 0} \frac{Z^n - 1}{n}, \tag{B.10}$$

and then compute $\langle Z^n \rangle$. Doing so, given the definition of Z and our distribution of λ_k values, we have

$$\langle Z_N(\{\beta\lambda_i\})^n \rangle = \int_{-\infty}^{\infty} \prod_{k=1}^{N} d\lambda_k \, \rho_0(\lambda_k) \int_0^{\infty} \prod_{\beta=1}^{n} ds_\beta \, e^{-\sum_{\alpha=1}^{n} s_\alpha} \prod_{i=1}^{N} \prod_{\alpha=1}^{n} \left(1 + (s_\alpha - 1)e^{-\beta\lambda_i}\right),$$

(B.11)

where Greek indices denote our replicas while Roman indices denote lattice places.

Now, to make progress, we posit a replica symmetric ansatz in place of Eq.(B.11). The motivation for this replacement is that we introduced our replicas as an analytic trick, and they are thus unphysical aspects of our analysis. Therefore, any distinguishing elements between two replicas are unphysical. In the absence of any other supporting evidence, this motivation is in general an insufficient reason to accept the replica symmetric solution as valid, but we will find that this solution reproduces the thermodynamically stable result Eq.(3.9), which was derived through alternative means.

For the replica symmetric ansatz, we replace our distinct n replica variables $s_1, \ldots, s_n$ with the single variable s. Doing so, we obtain

$$\langle Z_N(\{\beta\lambda_i\})^n \rangle \rightarrow \int_{-\infty}^{\infty} \prod_{k=1}^{N} d\lambda_k \, \rho_0(\lambda_k) \int_0^{\infty} ds \, e^{-ns} \prod_{i=1}^{N} \left(1 + (s_\alpha - 1)e^{-\beta\lambda_i}\right)^n$$

$$= \int_0^{\infty} ds \, \exp\left[-ns + \ln \mathrm{Tr} \, \exp L_n(s, \{\lambda_k\})\right], \quad (B.12)$$

where we defined

$$\mathrm{Tr}[\cdots] \equiv \int_{-\infty}^{\infty} \prod_{k=1}^{N} d\lambda_k \, [\cdots] \quad (B.13)$$

$$L_n(s, \{\lambda_k\}) \equiv \sum_{k=1}^{N} \ln \rho_0(\lambda_k) + n \sum_{k=1}^{N} \ln\left(1 + (s-1)e^{-\beta\lambda_k}\right). \quad (B.14)$$

Computing Eq.(B.12) via Laplace's method, and using the identity Eq.(B.10) we find the quenched average free energy to be

$$\langle \ln Z \rangle = \lim_{n \to 0} \frac{1}{n} \left\{ \exp\left[-ns_0 + \ln \mathrm{Tr} \, \exp L_n(s_0, \{\lambda_k\})\right] - 1\right\}$$

$$= -s_0 + \lim_{n \to 0} \frac{1}{n} \ln \mathrm{Tr} \exp L_n(s_0, \{\lambda_k\}), \tag{B.15}$$

where s_0 is defined by the condition

$$-1 + \lim_{n \to 0} \frac{1}{n} \frac{\partial}{\partial s} \ln \mathrm{Tr} \exp L_n(s, \{\lambda_k\}) \Big|_{s=s_0} = 0. \tag{B.16}$$

Computing the argument of the limit in Eq.(B.16), we find

$$\frac{\partial}{\partial s} \mathrm{Tr} \exp L_n(s, \{\lambda_k\}) = \frac{\partial}{\partial s} \int_{-\infty}^{\infty} \prod_{k=1}^{N} d\lambda_k \, \exp \left[\sum_{k=1}^{N} \ln \rho_0(\lambda_k) + n \sum_{k=1}^{N} \ln \left(1 + (s-1)e^{-\beta \lambda_k} \right) \right]$$

$$= \int_{-\infty}^{\infty} \prod_{k=1}^{N} d\lambda_k \, \exp \left[L_n(s, \{\lambda_k\}) \right] \sum_{k=1}^{N} \frac{n e^{-\beta \lambda_k}}{1 + (s-1)e^{-\beta \lambda_k}}. \tag{B.17}$$

Thus given Eq.(B.16), we have that s_0 must satisfy

$$1 = \lim_{n \to 0} \int_{-\infty}^{\infty} \prod_{k=1}^{N} d\lambda_k \, \exp \left[L_n(s_0, \{\lambda_k\}) \right] \sum_{k=1}^{N} \frac{e^{-\beta \lambda_k}}{1 + (s_0-1)e^{-\beta \lambda_k}}$$

$$= \int_{-\infty}^{\infty} \prod_{k=1}^{N} d\lambda_k \, \rho_0(\lambda_k) \sum_{k=1}^{N} \frac{1}{e^{\beta \lambda_k} + s_0 - 1}$$

$$= N \int_{-\infty}^{\infty} d\lambda \, \frac{\rho_0(\lambda)}{e^{\beta \lambda} + s_0 - 1}, \tag{B.18}$$

where we used the independent normalization of each $\rho_0(\lambda)$ in the final line. Given the definition $s_0 - 1 = \langle j \rangle$, Eq.(B.18) is identical to Eq.(3.11). The consistency between the replica symmetric ansatz and Eq.(3.11) suggests that this system of quenched disorder does not bear the more interesting features (e.g., multiple equilibria andergodicity breaking) of replica symmetry breaking solutions to statistical mechanics systems.

B.3 Heuristic Derivation of Eq.(3.16)

In this appendix, we derive Eq.(3.16) heuristically and thus lend quantitative justification to the qualitative argument outlined in Sec. 3.3. We begin with the simple permutation model with no disorder. The energy of a microstate in such a system is $E = \lambda_0 j$ where λ_0 is the energy cost of an incorrect component and j is the number of incorrect components.

Also, the number of such microstates for a given j is $\binom{N}{j}d_j$ where N is the number of components in the system, and d_j is the number of derangements of a list with j elements. Thus, the microcanonical ensemble entropy for a given E, λ_0, and N is

$$S_N(E, \lambda_0) = k_B \ln \left[\binom{N}{E/\lambda_0} d_{E/\lambda_0} \right]$$

$$\simeq -k_B \ln \Gamma(N - E/\lambda_0 + 1) + k_B \ln \Gamma(N + 1). \tag{B.19}$$

If we were to introduce a small amount of disorder σ_0 into our system, such that λ_0 (instead of being fixed at a single value) had a non-negligible probability to be found within the domain $[\lambda_0 - \sigma_0, \lambda_0 + \sigma_0]$, then we could approximate this new entropy as a two-point average over the ends of this domain. Defining this entropy as $\langle S(E) \rangle_{\lambda_0, \sigma_0}$ we have

$$\langle S_N(E, \lambda_0) \rangle_{\sigma_0}$$

$$\equiv \frac{1}{2} S_N(E, \lambda_0 - \sigma_0) + \frac{1}{2} S_N(E, \lambda_0 + \sigma_0)$$

$$= S_N(E, \lambda_0) + \frac{\sigma_0^2}{2} \frac{\partial^2}{\partial \lambda^2} S_N(E, \lambda) \Big|_{\lambda = \lambda_0} + \mathcal{O}(\sigma_0^4). \tag{B.20}$$

We note that Eq.(B.20), given the convexity of $S(N, \lambda)$ with respect to λ, is consistent with the intuition that introducing disorder into our system effectively increases the entropy. By the thermodynamic definition, the temperature of this disordered system is

$$\frac{1}{T(\sigma_0)} = \frac{\partial}{\partial E} \langle S_N(E, \lambda_0) \rangle_{\sigma_0}. \tag{B.21}$$

Our goal is to compute the transition temperature for the $\langle j \rangle = 0$ transition. By $E = \lambda_0 j$, we take this transition temperature to be the same as that associated with a microstate energy $E = 0$ in Eq.(B.21). Using Eq.(B.19), we thus find

$$\frac{1}{T_c(\sigma_0)} = \frac{\partial}{\partial E} \langle S_N(E, \lambda_0) \rangle_{\sigma_0} \Big|_{E=0}$$

$$= \frac{\partial}{\partial E} S_N(E, \lambda_0) \Big|_{E=0} + \frac{\sigma_0^2}{2} \frac{\partial}{\partial E} \left[\frac{\partial^2}{\partial \lambda^2} S_N(E, \lambda) \Big|_{\lambda = \lambda_0} \right]_{E=0} + \mathcal{O}(\sigma_0^4 / \lambda_0^4)$$

$$= \frac{k_B \ln N}{\lambda_0} + \frac{2k_B}{\lambda_0^3} \cdot \frac{\sigma_0^2}{2} \ln N + \mathcal{O}(\sigma_0^4 / \lambda_0^4), \tag{B.22}$$

where we used $\psi_0(N) \simeq \ln(N)$ (with ψ_0 being the digamma function) for $N \gg 1$. Eq.(B.22) then implies

$$k_B T_c(\sigma_0) = \frac{\lambda_0}{\ln N} \left[1 - \frac{\sigma_0^2}{\lambda_0^2} + \mathcal{O}(\sigma_0^4/\lambda_0^4) \right], \tag{B.23}$$

which reproduces, up to an order of magnitude, the $\mathcal{O}(\sigma_0^2)$ correction in Eq.(3.16).

B.4 Order Parameter for The Symmetric Bernoulli distribution

In this appendix, we will use Eq.(3.11) to derive an exact expression for the order parameter of the permutation glass with a symmetric Bernoulli distribution of energy costs; there seem to be no clean analytic expressions for the order parameters associated with the Gaussian or uniform distributions of energy costs.

Integrating the distribution Eq.(3.10) according to Eq.(3.11), we find

$$\frac{1}{N} = \frac{q}{e^{\beta\bar{\lambda}} + \langle j \rangle} + \frac{1-q}{e^{-\beta\bar{\lambda}} + \langle j \rangle}. \tag{B.24}$$

Solving Eq.(B.24) and dropping the solution which does not reduce to $N - e^{\beta\lambda}$ in the $q \to 0$ limit, we find the order parameter

$$\langle j \rangle / N = \frac{1}{2} \left[1 - \frac{2}{N} \cosh(\beta\bar{\lambda}) + \sqrt{1 + \frac{4}{N}(1 - 2q)\sinh(\beta\bar{\lambda}) + \frac{4}{N^2}\sinh^2(\beta\bar{\lambda})} \right], \tag{B.25}$$

where $\langle j \rangle$ could be written in terms of λ_0 and σ_0 by inverting the system Eq.(3.29).

B.5 Deriving Probability limits

In this appendix, we derive the probabilities Eq.(3.38), Eq.(3.39), and Eq.(3.40) which establish the constraints the respective distributions must satisfy in order for β_c to exist and $\langle j \rangle = 0$ to be an equilibrium. We begin with the mean-variance inequalities Eq.(3.20),

Eq.(3.24), and Eq.(3.30) expressed as limits on the maximum value of the standard deviation:

$$\sigma_0 \leq \sigma_0^{\max} = \begin{cases} \dfrac{\lambda_0}{\sqrt{3}}\left(1 - \dfrac{2}{Ne}\right)^{-1} & \text{[Uniform]} \\[3mm] \dfrac{\lambda_0}{\sqrt{2\ln N}} & \text{[Gaussian]} \\[3mm] \dfrac{\lambda_0}{\sqrt{N^2 - 1}} & \text{[Symm. Bernoulli]} \end{cases} \tag{B.26}$$

In order for β_c to exist, the mean λ_0 of each distribution must be greater than zero. Consequently the maximum values of σ_0 must be associated with maximum probabilities of obtaining a $\lambda < 0$ from the distribution. Computing these probability inequalities for each distribution, we find

$$P_{\lambda<0}^{\text{uniform}} \leq \frac{1}{2\sigma_0^{\max}\sqrt{3}}\left(\sigma_0^{\max}\sqrt{3} - \lambda_0\right) = \frac{1}{Ne} \tag{B.27}$$

$$P_{\lambda<0}^{\text{gauss}} \leq \int_{-\infty}^{0} \frac{d\lambda}{2\pi(\sigma^{\max})_0^2} e^{-(\lambda-\lambda_0)^2/2(\sigma_0^{\max})^2}$$

$$= \frac{1}{2}\left[1 - \text{erf}\left(-\sqrt{\ln N}\right)\right] \simeq \frac{1}{2N\sqrt{\pi \ln N}} \tag{B.28}$$

$$P_{\lambda<0}^{\text{bernoulli}} \leq \frac{1}{2}\left(1 - \sqrt{1 - \frac{1}{N^2}}\right) \simeq \frac{1}{4N^2}, \tag{B.29}$$

Where each quantity is expanded in the large N limit where relevant, and Eq.(B.29) follows from Eq.(3.28) and the identification of $1 - q = P_{\lambda<0}^{\text{bernoulli}}$.

Appendix C

Self-Assembly of a Dimer System, Derivations

C.1   Link to Supplementary Code

IPython code for creating Fig. 4.5, Fig. 4.6, and for the biophysics calculations in Sec. 4.6 in the main text can be found at

https://github.com/mowillia/dimer_self_assembly_code.

C.2   Deriving $a_{n,\ell}$ as a Series and an Integral

We are seeking a formula that answers the following question:

> Given $2n$ distinguishable objects that are all initially paired in some way, what is the number of ways to form ℓ pairs such that none of these new pairs coincide with any original pairings?

We call this number $a_{n,\ell}$, and it is easy to see what its value should be for $\ell = n$ and $\ell = 1$. If we were to take $\ell = n$, we would have the case of the "bridge couples problem" and we should obtain the formula derived in Margolius, 2001. If were were to take $\ell = 1$, we could infer that $a_{n,1} = 2n(2n-2)/2$ since there are $2n$ ways to select the first element, $2n - 2$ ways to select an element that was not initially paired with this first element, and a factor of $1/2$ for double counting.

To find the general formula for $a_{n,\ell}$, we employ the inclusion-exclusion principle Chuan-Chong and Khee-Meng, 1992.

First, we establish some definitions. We define $|A_i|_{n,\ell}$ as the number of way to reform ℓ pairs, out of $2n$ initially paired elements, such that in the new set of pairs, we include the ith pair of the initial pairings. We in turn say that the quantity

$$|A_{i_1} \cap \cdots \cap A_{i_k}|_{n,\ell}, \tag{C.1}$$

equals the size of the set where, out of $2n$ initially paired elements, we have formed $\ell \leq n$ new pairs which include the pairs $i_1, \ldots, i_k$ (for $k \leq \ell$) of the original pairings. By this definition, our desired quantity $a_{n,\ell}$ can be written as

$$\sum_{1 \leq i_1 < \cdots < i_\ell \leq n}^{n} |A_{i_1}^c \cap \cdots \cap A_{i_\ell}^c|_{n,\ell}, \tag{C.2}$$

where A_k^c is the complement of A_k. Eq.(C.2) is the total number of ways to reform ℓ pairs out of $2n$ initially paired elements such that none of the ℓ pairs is found in the initial pairings. Given that the intersection of complements is equal to the complement of the union, we have.

$$\sum_{1 \leq i_1 < \cdots < i_\ell \leq n}^{n} |A_{i_1}^c \cap \cdots \cap A_{i_\ell}^c|_{n,\ell} = \sum_{1 \leq i_1 < \cdots < i_\ell \leq n}^{n} |(A_{i_1} \cup \cdots \cup A_{i_\ell})^c|_{n,\ell}$$

$$= |\mathcal{S}|_{n,\ell} - \sum_{1 \leq i_1 < \cdots < i_\ell \leq n}^{n} |A_{i_1} \cup \cdots \cup A_{i_\ell}|_n, \tag{C.3}$$

where we we defined $|\mathcal{S}|_{n,\ell}$ as the number of ways to create $\ell \leq n$ pairs out of a set of $2n$ elements. Combinatorics tells us that $|\mathcal{S}|_{n,\ell}$ is

$$|\mathcal{S}|_{n,\ell} = \binom{2n}{2\ell} \frac{(2\ell)!}{2^\ell \ell!} = \binom{2n}{2\ell}(2\ell - 1)!!, \tag{C.4}$$

Now, to compute Eq.(C.2), we must calculate the last quantitys in Eq.(C.3), and we do so by the inclusion-exclusion principle. By the principle, we have

$$
\sum_{1 \leq i_1 < \cdots < i_\ell \leq n}^{n} |A_{i_1} \cup \cdots \cup A_{i_\ell}|_{n,\ell}
$$
$$
= \sum_{i=1}^{n} |A_i|_{n,\ell} - \sum_{1 \leq i < j \leq n}^{n} |A_i \cap A_j|_{n,\ell} + \cdots + \sum_{1 \leq i_1 < \cdots < i_\ell \leq n}^{n} (-1)^{\ell-1} |A_{i_1} \cap \cdots \cap A_{i_\ell}|_{n,\ell}.
$$
(C.5)

We recall that $|A_i|_{n,\ell}$ equals the number of way to reform ℓ pairs, out of $2n$ initially paired elements, such that in the new set of pairs, we include the ith pair of the initial pairings. Since the ith pair is fixed in this pairing, the number of ways to achieve this new pairing is simply the number of ways to form $\ell - 1$ pairs out of a set of $2n - 2$ elements. Thus we have

$$
|A_i|_{n,\ell} = \binom{2n-2}{2\ell-2}(2\ell-2-1)!!.
$$
(C.6)

This quantity is independent of which i we choose, so, in Eq.(C.5), the summation can be replaced with the factor $\binom{n}{1}$. Similarly, the quantity $|A_i \cap A_j|_{n,\ell}$ is the number of ways to choose ℓ pairs, out of $2n$ initially paired elements, such that we include the ith and jth pairs of the original pairing. Thus, we have

$$
|A_i \cap A_j|_{n,\ell} = \binom{2n-4}{2\ell-4}(2\ell-4-1)!!,
$$
(C.7)

and the summation is replaced with the factor $\binom{n}{2}$. Following this pattern, we find that Eq.(C.5) becomes

$$
\sum_{1 \leq i_1 < \cdots < i_\ell \leq n}^{n} |A_{i_1} \cup \cdots \cup A_{i_\ell}|_{n,\ell} = \sum_{j=1}^{\ell} (-1)^{j-1} \binom{n}{j} \binom{2n-2j}{2\ell-2j}(2\ell-2j-1)!!.
$$
(C.8)

Finally, using Eq.(C.4) in Eq.(C.3), and noting that final result is our desired $a_{n,\ell}$, we have

$$
a_{n,\ell} = \sum_{j=0}^{\ell} (-1)^{j} \binom{n}{j} \binom{2n-2j}{2\ell-2j}(2\ell-2j-1)!!.
$$
(C.9)

We can also write Eq.(C.9) as an integral which will later allow us to write the partition function as a double integral. The first step is to rewrite the second combinatorial factor as

$$\binom{2n-2j}{2\ell-2j} = \frac{2^{n-j}(n-j)!}{(2n-2\ell)!(2\ell-2j)!}(2n-2j-1)!!. \tag{C.10}$$

We then find

$$
\begin{aligned}
a_{n,\ell} &= \sum_{j=0}^{\ell}(-1)^j\binom{n}{j}\frac{2^{n-j}(n-j)!}{(2n-2\ell)!(2\ell-2j)!}(2n-2j-1)!!\,(2\ell-2j-1)!! \\
&= \frac{2^{n-\ell}}{(2n-2\ell)!}\frac{n!}{\ell!}\sum_{j=0}^{\ell}(-1)^j\frac{\ell!}{j!(\ell-j)!}(2n-2j-1)!! \\
&= \frac{2^{n-\ell}(n-\ell)!}{(2n-2\ell)!}\frac{n!}{\ell!(n-\ell)!}\sum_{j=0}^{\ell}(-1)^j\binom{\ell}{j}\frac{2^{n-j}}{\sqrt{\pi}}\Gamma(n-j+1/2),
\end{aligned} \tag{C.11}
$$

Using the integral definition of the Gamma function, we obtain.

$$a_{n,\ell} = \frac{1}{(2n-2\ell-1)!!}\binom{n}{\ell}\frac{1}{\sqrt{\pi}}\int_0^{\infty}dt\,e^{-t}t^{-1/2}(2t)^n(1-1/2t)^{\ell}. \tag{C.12}$$

C.3 Derivation of Non-Gendered Partition Function

In deriving the final form of the partition function for the non-gendered system, we begin with the partition function expressed as a summation over the total number of dimers and the total number of correct dimers:

$$Z_N(V,T,E_0,\Delta) = \sum_{k=0}^{N}\sum_{m=0}^{k}\binom{N}{m}a_{N-m,k-m}\,e^{\beta(kE_0+m\Delta)}\left(\frac{V}{\lambda_0^3}\right)^{2N-2k}\left(\frac{V}{(\lambda_0/\sqrt{2})^3}\right)^k \tag{C.13}$$

Using the integral expression Eq.(C.12), we find Eq.(C.13) becomes

$$Z_N(V,T,E_0,\Delta)$$
$$= \frac{(V/\lambda_0^3)^N}{\sqrt{\pi}}\int_0^{\infty}dx\,\frac{e^{-x}}{\sqrt{x}}\sum_{k=0}^{N}\sum_{m=0}^{k}\delta^k\eta^m\frac{1}{(2N-2k-1)!!}\binom{N}{m}\binom{N-m}{k-m}(2x)^{N-k}(2x-1)^{k-m}$$

$$= \frac{(V/\lambda_0^3)^N}{\sqrt{\pi}} \int_0^\infty dx \frac{e^{-x}}{\sqrt{x}}(2x)^N \sum_{k=0}^{N} \sum_{m=0}^{k} \frac{[\delta(1-1/2x)]^k}{(2N-2k-1)!!} \binom{N}{N-m}\binom{N-m}{k-m}\left(\frac{\eta}{2x-1}\right)^m$$

$$\text{(C.14)}$$

where we denoted

$$\delta \equiv \frac{2\sqrt{2}\lambda_0^3}{V}e^{\beta E_0}, \qquad \eta \equiv e^{\beta\Delta}. \tag{C.15}$$

Next, we isolate the sum over m to find

$$\sum_{m=0}^{k} \binom{N}{N-m}\binom{N-m}{k-m}\left(\frac{\eta}{2x-1}\right)^m = \binom{N}{k}\left(\frac{\eta}{2x-1}+1\right)^k, \tag{C.16}$$

where we used the fact that $\binom{n}{k} = 0$ if $k < 0$, and the identity $\sum_{k=0}^{n}\binom{n}{k}\binom{k}{r}x^k = x^r(1+x)^{n-r}\binom{n}{r}$. Returning to Eq.(C.14), we find

$$Z_N(V,T,E_0,\Delta)$$

$$= \frac{(V/\lambda_0^3)^N}{\sqrt{\pi}}\int_0^\infty dx \frac{e^{-x}}{\sqrt{x}}(2x)^N \sum_{k=0}^{N}\binom{N}{k}\frac{1}{(2N-2k-1)!!}\left[\frac{\delta}{2x}(\eta+2x-1)\right]^k$$

$$= \frac{(V/\lambda_0^3)^N 2^N}{\sqrt{\pi}(2N-1)!!}\int_0^\infty dx \frac{e^{-x}}{\sqrt{x}}x^N \sum_{k=0}^{N}\binom{2N}{2k}(2k-1)!!\left[\frac{\delta}{2x}(\eta+2x-1)\right]^k. \quad \text{(C.17)}$$

Then, using the integral identity

$$\sum_{k=0}^{N}\binom{2N}{2k}(2k-1)!!\,\Lambda^k = \frac{1}{2\sqrt{\pi}}\int_0^\infty dy \frac{e^{-y}}{\sqrt{y}}\left[\left(1+\sqrt{2\Lambda y}\right)^{2N} + \left(1-\sqrt{2\Lambda y}\right)^{2N}\right], \quad \text{(C.18)}$$

derived from the integral definition of $(2k-1)!!$ and the binomial theorem, Eq.(C.17) becomes

$$Z_N(V,T,E_0,\Delta)$$

$$= \frac{(V/\lambda_0^3)^N 2^N}{2\pi(2N-1)!!}\int_0^\infty \int_0^\infty dx\,dy \frac{e^{-x-y}}{\sqrt{xy}}x^N\left[\left(1+\sqrt{y\delta(\eta+2x-1)/x}\right)^{2N} + (\sqrt{y}\to-\sqrt{y})\right]$$

$$= \frac{(V/\lambda_0^3)^N 2^N}{2\pi(2N-1)!!}\int_0^\infty \int_0^\infty dx\,dy \frac{e^{-x-y}}{\sqrt{xy}}\left[\left(\sqrt{x}+\sqrt{y\delta(\eta+2x-1)}\right)^{2N} + (\sqrt{y}\to-\sqrt{y})\right],$$

$$\text{(C.19)}$$

where $(\sqrt{\bar{y}} \to -\sqrt{\bar{y}})$ stands in for the preceding term with $\sqrt{\bar{y}}$ replaced with $-\sqrt{\bar{y}}$. Next, using the identity

$$(2N-1)!! = \frac{2^N}{\sqrt{\pi}} \Gamma(N+1/2), \tag{C.20}$$

gives the final form of the partition function.

C.4 Equilibrium Conditions for Non-Gendered System

In this section, we justify the conditions defining the Laplace's method approximation of the partition function and show that they result in a system of equations for $\langle k \rangle$ and $\langle m \rangle$, the average number of dimers and the average number of correct dimers, respectively.

In the main text, we made the approximation

$$Z_N(V,T;E_0,\Delta) = \int_0^\infty \int_0^\infty dx\, dy\, \exp\left[-\beta F_N(x,y;V,T,E_0,\Delta) \right]$$

$$\simeq 2\pi \left(\det H \right)^{-1/2} \exp\left[-\beta F_N(\bar{x},\bar{y};V,T,E_0,\Delta) \right], \tag{C.21}$$

where we defined

$$\beta F_N(x,y;V,T,E_0,\Delta) \equiv x + y + \frac{1}{2}\ln(xy) - \ln\left(\mathcal{M}_+^{2N} + \mathcal{M}_-^{2N} \right) + \beta F_0(N,V,T), \tag{C.22}$$

with $\beta F_0(N,V,T)$ composed of terms that are independent of the variables x and y and of the parameters E_0 and Δ. In Eq.(C.21), $\bar{x}$ and $\bar{y}$ are the critical points of $F_N(x,y;V,T,E_0,\Delta)$, defined by

$$\left. \partial_i(\beta F_N) \right|_{x=\bar{x},y=\bar{y}} = 0, \tag{C.23}$$

for $i = x,y$, and H is the Hessian matrix with the elements

$$H_{ij} = \left. \partial_i\partial_j(\beta F_N) \right|_{x=\bar{x},y=\bar{y}}. \tag{C.24}$$

For the validity of Eq.(C.21), H must satisfy

$$\det H > 0, \quad \operatorname{Tr} H > 0. \tag{C.25}$$

Eq.(C.25) also ensures that the critical points defined by Eq.(4.24) are stable. We can compute the average number of dimers and the average number of correct dimers from the partition function via

$$\langle k \rangle = \frac{\partial}{\partial(\beta E_0)} \ln Z_N(V, T; E_0, \Delta), \qquad \langle m \rangle = \frac{\partial}{\partial(\beta \Delta)} \ln Z_N(V, T; E_0, \Delta). \qquad \text{(C.26)}$$

In Sec. C.4.1, we will use the conditions Eq.(C.23) along with the definitions in Eq.(C.26) to calculate equilibrium constraints on $\langle k \rangle$ and $\langle m \rangle$. In Sec. C.4.2, we will show the equilibria derived from these conditions satisfy Eq.(C.25) and are indeed stable. Also, by computing the Hessian, we will show that the $\ln \det H$ contribution the Hessian could make to the free energy in Eq.(C.22) is sub-leading in the large N limit because it is of the same order as the terms we drop in our derivation of the equilibrium conditions.

C.4.1   Computing Critical Points

Here we will derive the equilibrium conditions on $\langle k \rangle$ and $\langle m \rangle$ resulting from a $N \gg 1$ approximation of the partition function. We write the free energy Eq.(C.22) slightly differently as

$$\beta F_N(x, y; V, T, E_0, \Delta) = x + y + (1/2 - N) \ln x + \frac{1}{2} \ln y - \ln \left(\mathcal{N}_+^{2N} + \mathcal{N}_-^{2N} \right) + \beta F_0(N, V, T),$$

$$\text{(C.27)}$$

where

$$\mathcal{N}_\pm \equiv 1 \pm \delta^{1/2} \sqrt{y \, \Lambda(x; \beta \Delta)}, \qquad \text{(C.28)}$$

and

$$\Lambda(x; \beta \Delta) \equiv \frac{e^{\beta \Delta} - 1}{x} + 2, \qquad \delta \equiv \frac{2\sqrt{2} \lambda_0^3}{V} e^{\beta E_0}. \qquad \text{(C.29)}$$

We can simplify Eq.(C.27) by considering our presumed $N \gg 1$ limit. First we note that $(1 + Q)^N + (1 - Q)^N = (1 + Q)^N + \phi_N$ where, if $Q > 0$, then $\phi_N \to 0$ as an inverse power of N for $N \to \infty$. Thus, Eq.(C.27) can be written as

$$\beta F_N(x, y; V, T, E_0, \Delta) = x + y - N \ln x + \frac{1}{2} \ln y - 2N \ln \mathcal{N}_+ + \beta F_0(N, V, T) + \epsilon_N, \quad \text{(C.30)}$$

where ϵ_N is the error term which includes all terms that are subleading in the $N \gg 1$ limit to the shown quantities. Now, using Eq.(C.28) and Eq.(C.30), we see that Eq.(C.23) yield the equations

$$0 = \partial_x(\beta F_N)\Big|_{x=\bar{x}, y=\bar{y}} = 1 - \frac{N}{\bar{x}} - \frac{N\delta^{1/2}\sqrt{\bar{y}/\Lambda(\bar{x};\beta\Delta)}}{1 + \delta^{1/2}\sqrt{\bar{y}\Lambda(\bar{x};\beta\Delta)}} \cdot \left(-\frac{e^{\beta\Delta} - 1}{\bar{x}^2}\right), \qquad \text{(C.31)}$$

$$0 = \partial_y(\beta F_N)\Big|_{x=\bar{x}, y=\bar{y}} = 1 + \frac{1}{2\bar{y}} - \frac{N\delta^{1/2}\sqrt{\Lambda(\bar{x};\beta\Delta)/\bar{y}}}{1 + \delta^{1/2}\sqrt{\bar{y}\Lambda(\bar{x};\beta\Delta)}}. \qquad \text{(C.32)}$$

From the definitions in Eq.(C.26), we can express $\langle k \rangle$ and $\langle m \rangle$ in terms of $\bar{x}$ and $\bar{y}$:

$$\langle k \rangle = \partial_{\beta E_0} \ln Z_N = -\partial_{\beta E_0}(\beta F_N)\Big|_{x=\bar{x}, y=\bar{y}}$$

$$= \frac{N\delta^{1/2}\sqrt{\bar{y}\Lambda(\bar{x};\beta\Delta)}}{1 + \delta^{1/2}\sqrt{\bar{y}\Lambda(\bar{x};\beta\Delta)}} \qquad \text{(C.33)}$$

$$\langle m \rangle = \partial_{\beta\Delta} \ln Z_N = -\partial_{\beta\Delta}(\beta F_N)\Big|_{x=\bar{x}, y=\bar{y}}$$

$$= \frac{N\delta^{1/2}\sqrt{\bar{y}/\Lambda(\bar{x};\beta\Delta)}}{1 + \delta^{1/2}\sqrt{\bar{y}\Lambda(\bar{x};\beta\Delta)}} \cdot \frac{e^{\beta\Delta}}{\bar{x}}, \qquad \text{(C.34)}$$

where we used Eq.(C.31) and Eq.(C.32) to set the coefficients of $\partial\bar{x}/\partial(\beta E_0)$ and $\partial\bar{y}/\partial(\beta E_0)$ (and similarly for the $\bar{x}$ and $\bar{y}$ derivatives with respect to $\beta\Delta$) to zero. To be explicit, we note that the second equalities in both Eq.(C.33) and Eq.(C.34) would be better expressed as approximations derived from Eq.(C.21). However, for the analytical calculations of this system we will always be working in the $N \gg 1$ regime and we will take the free energy Eq.(C.30) as the true free energy of the system.

From Eq.(C.32), we find the condition

$$\bar{y} + 1/2 = \frac{N\delta^{1/2}\sqrt{\bar{y}\Lambda(\bar{x};\beta\Delta)}}{1 + \delta^{1/2}\sqrt{\bar{y}\Lambda(\bar{x};\beta\Delta)}}, \qquad \text{(C.35)}$$

and with Eq.(C.33), we obtain

$$\bar{y} + 1/2 = \langle k \rangle. \qquad \text{(C.36)}$$

Inverting Eq.(C.35), we find

$$\delta \, \bar{y} \, \Lambda(\bar{x}; \beta\Delta) = \frac{(\bar{y} + 1/2)^2}{(N - (\bar{y} + 1/2))^2},$$ (C.37)

or, with Eq.(C.36),

$$\delta \left(\langle k \rangle - 1/2 \right) \Lambda(\bar{x}; \beta\Delta) = \frac{\langle k \rangle^2}{\left(N - \langle k \rangle \right)^2}.$$ (C.38)

We can further reduce this result by solving for $\Lambda(\bar{x}; \beta\Delta)$ in terms of $\langle k \rangle$ and $\langle m \rangle$. Dividing Eq.(C.33) by Eq.(C.34), yields

$$\frac{\langle k \rangle}{\langle m \rangle} = \bar{x} \, \Lambda(\bar{x}; \beta\Delta) e^{-\beta\Delta},$$ (C.39)

which when solved for $\bar{x}$, gives us

$$\bar{x} = \frac{1}{2} \left[1 + \frac{\langle k \rangle - \langle m \rangle}{\langle m \rangle} e^{\beta\Delta} \right].$$ (C.40)

Substituting Eq.(C.40) into Eq.(C.39), then gives us

$$\Lambda(\bar{x}; \beta\Delta) = \frac{2\langle k \rangle}{\langle k \rangle - \langle m \rangle (1 - e^{-\beta\Delta})}.$$ (C.41)

Returning to Eq.(C.38), we obtain

$$2\delta \left(1 - \frac{1}{2\langle k \rangle} \right) = \frac{\langle k \rangle - \langle m \rangle (1 - e^{-\beta\Delta})}{\left(N - \langle k \rangle \right)^2}.$$ (C.42)

which is the first equilibrium condition constraining $\langle k \rangle$ and $\langle m \rangle$. We will primarily be interested in temperature ranges at which $\langle k \rangle$ assumes a non-trivial value much larger than of $\mathcal{O}(1)$. Thus we can take $\langle k \rangle \gg 1$ leading to the result

$$\frac{4\sqrt{2}\lambda_0^3}{V} e^{\beta E_0} = \frac{\langle k \rangle - \langle m \rangle (1 - e^{-\beta\Delta})}{\left(N - \langle k \rangle \right)^2} + \mathcal{O}(\langle k \rangle^{-1})$$ (C.43)

To find the second equilibrium condition, we note that Eq.(C.31) can be written as

$$(N - \bar{x})\Lambda(\bar{x}; \beta\Delta)\bar{x} = \langle k \rangle (e^{\beta\Delta} - 1). \tag{C.44}$$

Using Eq.(C.39) and Eq.(C.40), this result becomes

$$N - \frac{1}{2}\left[1 + \frac{\langle k \rangle - \langle m \rangle}{\langle m \rangle}e^{\beta\Delta}\right] = \langle m \rangle (1 - e^{-\beta\Delta}), \tag{C.45}$$

or, with some rearranging,

$$\frac{e^{\beta\Delta}}{2} = \langle m \rangle \frac{N - \langle m \rangle(1 - e^{-\beta\Delta})}{\langle k \rangle - \langle m \rangle(1 - e^{-\beta\Delta})}, \tag{C.46}$$

which is our second equilibrium condition. With the equilibrium conditions Eq.(C.43) and Eq.(C.46) established, we can now turn to showing that these equilibria define stable minima of the free energy.

C.4.2   Demonstrating Stability

To check whether the equilibrium conditions Eq.(C.43) and Eq.(C.46) define stable equilibria for this system, we need to compute the various elements of the Hessian matrix

$$H_{ij} = \partial_i \partial_j (\beta F_N)\Big|_{x=\bar{x}, y=\bar{y}}, \tag{C.47}$$

and ensure that the matrix is positive definite. By definition, a positive definite matrix is one with positive eigenvalues. For the 2×2 matrix considered here, this amounts to having a positive determinant and positive trace:

$$\text{Tr}\, H > 0, \qquad \det H > 0. \tag{C.48}$$

We will first compute the diagonal elements composing $\text{Tr}\, H$. To compute

$\partial_y^2(\beta F_N)|_{x=\bar{x},y=\bar{y}}$, we must compute the first and second-order y derivatives of the free energy as general functions. Given Eq.(C.30), we obtain

$$\partial_y(\beta F_N) = 1 + \frac{1}{2y} - \frac{2N}{\mathcal{N}_+}\partial_y \mathcal{N}_+ \tag{C.49}$$

$$\partial_y^2(\beta F_N) = -\frac{1}{2y^2} + 2N\left[\frac{(\partial_y \mathcal{N})_+^2}{\mathcal{N}_+^2} - \frac{\partial_y^2 \mathcal{N}_+}{\mathcal{N}_+}\right]. \tag{C.50}$$

From Eq.(C.28), we have

$$\partial_y \mathcal{N}_+ = \frac{\delta^{1/2}}{2}\sqrt{\frac{\Lambda(x;\beta\Delta)}{y}}, \qquad \partial_y^2 \mathcal{N}_+ = -\frac{\delta^{1/2}}{4}\sqrt{\frac{\Lambda(x;\beta\Delta)}{y^3}} = -\frac{1}{2y}\partial_y \mathcal{N}_+. \tag{C.51}$$

Thus, Eq.(C.50) becomes

$$\partial_y^2(\beta F_N) = -\frac{1}{2y^2} + 2N\left[\frac{(\partial_y \mathcal{N})_+^2}{\mathcal{N}_+^2} + \frac{1}{2y}\frac{\partial_y \mathcal{N}_+}{\mathcal{N}_+}\right]. \tag{C.52}$$

Setting $x = \bar{x}$ and $y = \bar{y}$ in Eq.(C.52) and noting that $\partial_y(\beta F_N) = 0$ at these values, we find

$$\partial_y^2(\beta F_N)\Big|_{x=\bar{x},y=\bar{y}} = \frac{1}{2N\bar{y}^2}\big[-N + (\bar{y}+1/2)^2 + N(\bar{y}+1/2)\big], \tag{C.53}$$

where we used Eq.(C.49) evaluated at $x = \bar{x}$ and $y = \bar{y}$. Considering the argument of the above expression, we find that it is positive for $\bar{y} > 1/2 + \mathcal{O}(N^{-1})$. In terms of our order parameter, this result translates into $\partial_y^2(\beta F_N)|_{x=\bar{x},y=\bar{y}}$ being positive for $\langle k \rangle > 1$ which is only violated when we are well-outside the range for non-trivial values of $\langle k \rangle$.

Next, computing $\partial_x^2(\beta F_N)$ given Eq.(C.30), we obtain

$$\partial_x(\beta F_N) = 1 - \frac{N}{x} - \frac{2N}{\mathcal{N}_+}\partial_x \mathcal{N}_+ \tag{C.54}$$

$$\partial_x^2(\beta F_N) = \frac{N}{x^2} + 2N\left[\frac{(\partial_x \mathcal{N})_+^2}{\mathcal{N}_+^2} - \frac{\partial_x^2 \mathcal{N}_+}{\mathcal{N}_+}\right], \tag{C.55}$$

where

$$\partial_x \mathcal{N}_+ = \frac{\delta^{1/2}}{2}\sqrt{\frac{y}{\Lambda(x;\beta\Delta)}} \cdot \partial_x \Lambda(x;\beta\Delta), \tag{C.56}$$

and

$$\partial_x^2 \mathcal{N}_+ = \frac{\partial_x \mathcal{N}_+}{\partial_x \Lambda(x;\beta\Delta)} \cdot \frac{1}{\Lambda(x;\beta\Delta)} \cdot \left[\Lambda(x;\beta\Delta)\partial_x^2 \Lambda(x;\beta\Delta) - \frac{1}{2}\left(\partial_x \Lambda(x;\beta\Delta)\right)^2 \right]. \tag{C.57}$$

Using the definition of $\Lambda(x;\beta\Delta)$ (given in Eq.(C.29)) in the quantity in the brackets above yields

$$\left[\Lambda(x;\beta\Delta)\partial_x^2 \Lambda(x;\beta\Delta) - \frac{1}{2}\left(\partial_x \Lambda(x;\beta\Delta)\right)^2 \right] = -\frac{\partial_x \Lambda(x;\beta\Delta)}{x}\left[\frac{3}{2}\Lambda(x;\beta\Delta) + 1 \right]. \tag{C.58}$$

Thus Eq.(C.57) becomes

$$\partial_x^2 \mathcal{N}_+ = -\frac{\partial_x \mathcal{N}_+}{x}\left[\frac{3}{2} + \frac{1}{\Lambda(x;\beta\Delta)} \right]. \tag{C.59}$$

Now, returning to Eq.(C.55) we have

$$\partial_x^2(\beta F_N) = \frac{N}{x^2} + 2N\left(\frac{\partial_x \mathcal{N}_+}{\mathcal{N}_+}\right)^2 + 2N\frac{\partial_x \mathcal{N}_+}{\mathcal{N}_+}\left[\frac{3}{2x} + \frac{1}{x\Lambda(x;\beta\Delta)} \right]. \tag{C.60}$$

Setting $x = \bar{x}$ and $y = \bar{y}$ in Eq.(C.60) and noting that $\partial_x(\beta F_N) = 0$ at these values, we obtain

$$\partial_x^2(\beta F_N)\Big|_{x=\bar{x},y=\bar{y}} = \frac{1}{2N\bar{x}^2}\left[\bar{x}(\bar{x}+N) + \frac{2N(\bar{x}-N)}{\Lambda(\bar{x};\beta\Delta)} \right]. \tag{C.61}$$

We can make further progress by expressing $\Lambda(\bar{x};\beta\Delta)$ in terms of $\bar{x}$ and $\bar{y}$. First, we note that Eq.(C.40) and Eq.(C.46) together yield

$$\bar{x} = N - \langle m \rangle(1 - e^{-\beta\Delta}), \tag{C.62}$$

and inverting Eq.(C.41) gives us

$$\frac{1}{\Lambda(\bar{x};\beta\Delta)} = \frac{1}{2}\left(1 - \frac{\langle m \rangle(1 - e^{-\beta\Delta})}{\langle k \rangle}\right) = \frac{1}{2}\left(1 - \frac{N - \bar{x}}{\bar{y} + 1/2}\right), \tag{C.63}$$

where we used Eq.(C.62) and Eq.(C.36) in the final equality. Returning to Eq.(C.61), we find

$$\partial_x^2(\beta F_N)\Big|_{x=\bar{x},y=\bar{y}} = \frac{1}{2N\bar{x}^2}\left[\bar{x}^2(\lambda+1) - 2N\bar{x}(\lambda-1) + N^2(\lambda-1)\right], \tag{C.64}$$

where we defined

$$\lambda \equiv \frac{N}{\bar{y}+1/2}. \tag{C.65}$$

Since $\bar{y}+1/2 = \langle k \rangle$ and $\langle k \rangle < N$, we have $\lambda > 1$ for non-zero temperature. For the function

$$f(z) = z^2(\lambda+1) - 2z(\lambda-1) + \lambda - 1 \tag{C.66}$$

where $z \in \mathbb{R}^+$, it can be shown that the minimum satisfies

$$[f(z)]_{\min} = \frac{\lambda-1}{\lambda+1}. \tag{C.67}$$

Thus, for $\lambda > 1$, we find that $f(z) > 0$. Therefore, Eq.(C.64) is greater than zero for equilibrium values $\bar{x}$ and $\bar{y}$. With Eq.(C.53) and Eq.(C.64), we can thus conclude

$$\operatorname{Tr} H = \left[\partial_y^2(\beta F_N) + \partial_x^2(\beta F_N)\right]\Big|_{x=\bar{x},y=\bar{y}} > 0, \tag{C.68}$$

for $\langle m \rangle$ and $\langle k \rangle$ constrained by Eq.(C.43) and Eq.(C.46).

Now, we compute the off-diagonal elements that make up, together with the diagonal elements, $\det H$. Taking the y-partial derivative of Eq.(C.54), we have

$$\partial_y\partial_x(\beta F_N) = -2N\left[\frac{1}{\mathcal{N}_+}\partial_y\partial_x\mathcal{N}_+ - \frac{1}{\mathcal{N}_+^2}\partial_x\mathcal{N}_+\partial_y\mathcal{N}_+\right]. \tag{C.69}$$

From Eq.(C.28), we have that the mixed partial of $\mathcal{N}_+$ is

$$\begin{aligned}
\partial_y\partial_x\mathcal{N}_+ &= \partial_y\left[\frac{\delta^{1/2}}{2}\sqrt{\frac{y}{\Lambda(x;\beta\Delta)}}\cdot\partial_x\Lambda(x;\beta\Delta)\right]\\
&= \frac{\delta^{1/2}}{4}\sqrt{\frac{1}{y\Lambda(x;\beta\Delta)}}\cdot\partial_x\Lambda(x;\beta\Delta) = \frac{1}{2y}\partial_x\mathcal{N}_+,
\end{aligned} \tag{C.70}$$

where we used Eq.(C.56), in the final equality. Evaluating Eq.(C.69) at $x = \bar{x}$ and $y = \bar{y}$ and using

$$\frac{1}{\mathcal{N}_+}\partial_y\mathcal{N}_+\Big|_{x=\bar{x},y=\bar{y}} = \frac{1}{2N}\left(1 + \frac{1}{2\bar{y}}\right), \qquad \frac{1}{\mathcal{N}_+}\partial_x\mathcal{N}_+\Big|_{x=\bar{x},y=\bar{y}} = \frac{1}{2N}\left(1 - \frac{N}{\bar{x}}\right), \qquad (C.71)$$

found from Eq.(C.49), Eq.(C.54), and the critical point condition, we obtain

$$\partial_y\partial_x(\beta F_N)\Big|_{x=\bar{x},y=\bar{y}} = \frac{(N - \bar{x})(N - \bar{y} - 1/2)}{2N\bar{x}\bar{y}}. \qquad (C.72)$$

Before we compute the determinant, it will prove useful to express the $\bar{y}$ in Eq.(C.53) and Eq.(C.72) in terms of λ given in Eq.(C.65). From Eq.(C.65), we find

$$\partial_y^2(\beta F_N)\Big|_{x=\bar{x},y=\bar{y}} = \frac{(\bar{y} + 1/2)^2}{2N\bar{y}^2}\left(-\frac{N}{(\bar{y} + 1/2)^2} + 1 + \frac{N}{\bar{y} + 1/2}\right)$$

$$= \frac{N}{2\lambda^2\bar{y}^2}\left(-\frac{\lambda^2}{N} + 1 + \lambda\right) \qquad (C.73)$$

$$\partial_y\partial_x(\beta F_N)\Big|_{x=\bar{x},y=\bar{y}} = \frac{1}{2N\bar{x}\bar{y}}(\bar{y} + 1/2)(N - \bar{x})\left(\frac{N}{\bar{y} + 1/2} - 1\right)$$

$$= \frac{1}{2\lambda\bar{x}\bar{y}}(N - \bar{x})(\lambda - 1) \qquad (C.74)$$

Finally, computing the determinant of the Hessian from Eq.(C.64), Eq.(C.73), and Eq.(C.74), we thus find

$$\det H = \left[\partial_y^2(\beta F_N)\partial_x^2(\beta F_N) - (\partial_y\partial_x(\beta F_N))^2\right]\Big|_{x=\bar{x},y=\bar{y}}$$

$$= \frac{1}{4\lambda^2\bar{x}^2\bar{y}^2}\left[A_\lambda\bar{x}^2 - 2NB_\lambda\bar{x} + B_\lambda\right], \qquad (C.75)$$

where

$$A_\lambda = \lambda\left(4 - \frac{\lambda(\lambda + 1)}{N}\right) \qquad (C.76)$$

$$B_\lambda = (\lambda - 1)\left(2 - \frac{\lambda^2}{N}\right). \qquad (C.77)$$

We want to show that Eq.(C.75) is always positive. We will employ a method similar to that used in showing that $\partial_x^2(\beta F_N)|_{x=\bar{x},y=\bar{y}}$ is positive. For the function

$$g(z) = A_\lambda z^2 - 2B_\lambda z + B_\lambda, \tag{C.78}$$

where $z \in \mathbb{R}^+$, it can be shown that the minimum is given by

$$[g(z)]_{\min} = B_\lambda \left(1 - \frac{B_\lambda}{A_\lambda}\right). \tag{C.79}$$

From Eq.(C.76), Eq.(C.77), and the condition $1 < \langle \lambda \rangle < N$, we find that $B_\lambda < A_\lambda$ for all valid λ. From this inequality, we find

$$\frac{B_\lambda}{A_\lambda} < 1, \quad \text{if } B_\lambda > 0, \quad \text{and} \quad \frac{B_\lambda}{A_\lambda} > 1, \quad \text{if } B_\lambda < 0. \tag{C.80}$$

Thus, we can conclude that Eq.(C.79) is always positive for the entire domain of z and for valid values of λ. Considering Eq.(C.75) we then have

$$\det H = \left[\partial_y^2(\beta F_N)\partial_x^2(\beta F_N) - \left(\partial_y\partial_x(\beta F_N)\right)^2\right]\Big|_{x=\bar{x},y=\bar{y}} > 0. \tag{C.81}$$

With Eq.(C.68) and Eq.(C.81), we can conclude that the Hessian matrix is positive definite and thus that the derived equilibrium conditions Eq.(C.43) and Eq.(C.46) define stable equilibria of the free energy Eq.(4.21), and, moreover, that our Laplace's method approximation of the partition function Eq.(4.23) is valid.

Finally, in Eq.(C.75), we see that $\ln \det H$ is on the order of a linear combination of $\ln \bar{x}$ and $\ln \bar{y}$. Given that we ultimately dropped such terms from our calculation of the equilibrium conditions Eq.(C.43) and Eq.(C.46), we now see that we were also justified in ignoring the $\ln \det H$ contributions to our free energy.

C.5 Simulation of Dimer System

The simulation results in Fig. 4.5 were obtained using the Metropolis-Hastings Monte Carlo algorithm. We defined the microstate of our system by two lists: One defining the particles that are monomers and the other defining the monomer-monomer pairs making up the dimers. For example, a $2N = 10$ particle system, could have a microstate defined by the monomer list $[1, 4, 6, 9]$ and the dimer list $[(3, 5), (2, 8), (7, 10)]$. The free energy of a microstate was given by

$$f(k, m) = -kE_0 - m\Delta - k\, k_B T \ln(V/\lambda_0^3) - (2N - 2k)k_B T \ln(2\sqrt{2}\, V/\lambda_0^3), \qquad \text{(C.82)}$$

for a system with k dimers of which m consisted of correct dimers.

To efficiently explore the state space of the system, we used three different types of transitions with unique probability weights for each one. In the following, N_m and N_d represent the lengths of the monomer and dimer lists, respectively, before the transition.

1. **Monomer Association:** Two randomly chosen monomers are removed from the monomer list, joined as a pair, and the pair is appended to the dimer list. Weight $= \binom{N_m}{2}/(N_d + 1)$

   Example: mon $= [1, 3, 4, 5, 6, 9]$ and dim $= [(2, 8), (7, 10)] \rightarrow$ mon $= [1, 4, 6, 9]$ and dim $= [(3, 5), (2, 8), (7, 10)]$; Weight $= 15/3$.

2. **Dimer Dissociation:** One randomly chosen dimer is removed from the dimer list, and both of its elements are appended to the monomer lists. Weight $= N_d/\binom{N_m+2}{2}$

   Example: mon $= [6, 9]$ and dim $= [(1, 4), (3, 5), (2, 8), (7, 10)] \rightarrow$ mon $= [2, 6, 8, 9]$ and dim $= [(1, 4), (3, 5), (7, 10)]$; Weight $= 4/6$.

3. **Dimer Cross-Over:** Two dimers are chosen randomly. One randomly chosen element from one dimer is switched with a randomly chosen element of the other dimer. Weight $=1$.

   Example: dim $= [(1, 4), (3, 5)(7, 10)] \rightarrow$ dim $= [(1, 10), (3, 5), (4, 10)]$]; Weight $= 1$.

The third type of transition is unphysical but is necessary to ensure that the system can quickly escape kinetic traps that lead to inefficient sampling of the state space.

For each simulation step, there was a $1/3$ probability of selecting each transition type and the suggested step was accepted with log-probability

$$\ln p_{\text{accept}} = -(f_{\text{fin.}} - f_{\text{init.}})/k_B T + \ln(\text{Weight}), \tag{C.83}$$

where f_{fin} and f_{init} are the final and initial free energies of the microstate defined according to Eq.(C.82), and "(Weight)" is the ratio between the number of ways to make the forward transition and the number of ways to make the reverse transition. This weight was chosen for each transition type to ensure that detailed balance was maintained. For impossible transitions (e.g., monomer association for a microstate with no monomers), p_{accept} was set to zero.

At each temperature, the simulation was run for $30,000$ time steps, of which the last 600 were used to compute ensemble averages of $\langle k \rangle$ and $\langle m \rangle$. These simulations were repeated 50 times and each point in Fig. 4.5 represents the average $\langle k \rangle$ and $\langle m \rangle$ over these runs. IPython code for procedure is found in the *Supplementary Code*.

C.6   Temperature Changes in Parameter Space

In Fig. C.1 we depict how the plots in Fig. 5 change as we change the value of $k_B T$. We note that since the regions are defined by temperature dependent boundaries, changing the temperature of a system represented by a point also changes the arrangement of the boundaries that surround the point.
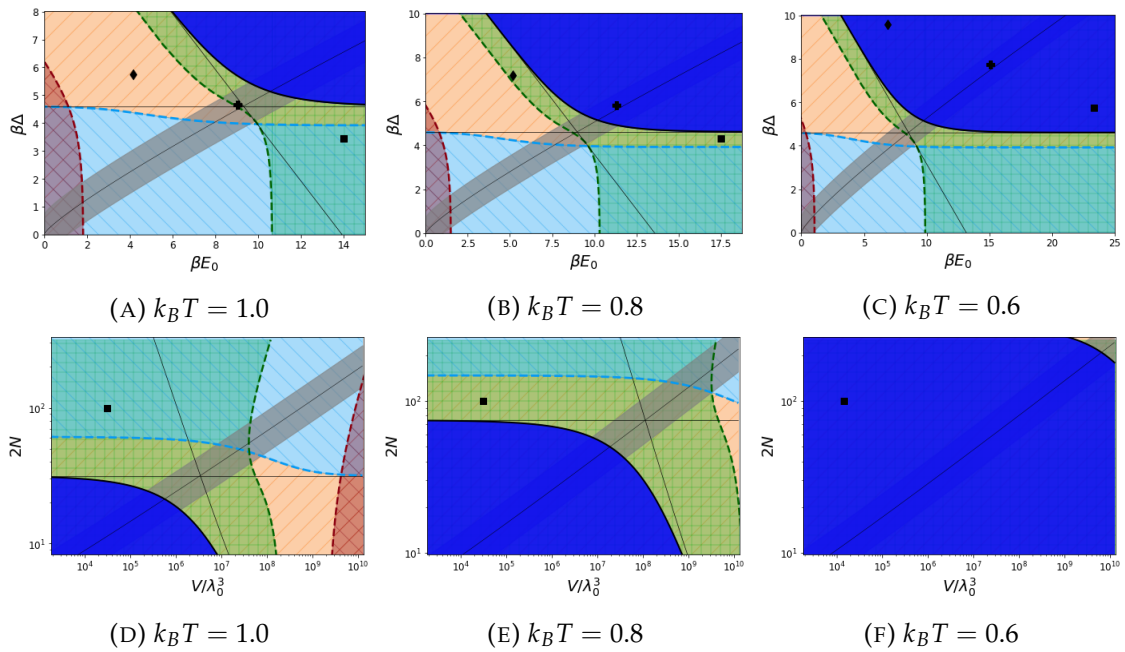
FIGURE C.1: (a), (b), and (c): Plots of the points in Fig. 5a in the main text as we lower the system temperature. Consistent with the simulation plots in Fig. 4, at $k_B T = 0.6$ all the systems are in the "fully correct assembly" regime. (d), (e), and (f): Plots of the point in Fig. 5b as we lower the system temperature. Consistent with the simulation plots in Fig. 4(c), at $k_B T = 0.6$ the systems is in the "fully correct assembly" regime.

Appendix D

Gendered Dimer System

In Sec. 4.2, we introduced our study of the self-assembly of a dimer system by considering a collection of monomers where each monomer could form a dimer with any other monomer. In this sense, we labeled this system as "non-gendered" to differentiate it from systems in which monomers have constraints on the type of monomers to which they can bind. In this section, we introduce a model with such constraints, namely one in which there are two types of monomers and each monomer can only form a dimer with the monomer of the opposite type. The statistical physics analysis of this gendered dimer system is very similar to that of the non-gendered system, so we focus on the major results rather than derivations.

D.1   Gendered partition function

Say that our system contains $2N$ distinguishable monomers of two kinds. There are N distinguishable monomers labeled $\beta_1, \beta_2, \ldots, \beta_N$ each of which has mass m_β, and there are N distinguishable monomers labeled $\alpha_1, \alpha_2, \ldots, \alpha_N$ each of which has mass m_α. The $2N$ total monomers exist in thermal equilibrium at temperature T and in a volume V. Each α monomer can bind to any β monomer (and vice versa), but α monomers cannot bind to each other, and β monomers cannot bind to each other. When monomer α_k binds to monomer β_ℓ, the two form the dimer (α_k, β_ℓ), where the ordering within the pair is not important. We define correct dimers as those consisting of α_k binding to β_k for $k = 1, \ldots, N$; all other dimers are considered incorrect. Thus there are N possible correct dimers in this
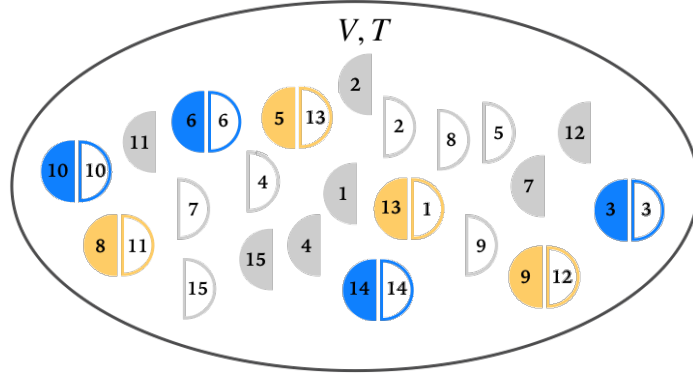
FIGURE D.1: Example microstate of the gendered system with $2N = 30$ subunits. We represent the monomers of either gender as filled or unfilled half circles. Filled half-circles can only bind to unfilled half-circles. Correct dimers consist of binding k to k and have binding energy $-(E_0 + \Delta)$. All other dimers are incorrect and have binding energy $-E_0$. This microstate has four correct dimers (in blue), four incorrect dimers (in yellow), and fourteen monomers (in grey). The total binding energy for this microstate is $-(8E_0 + 4\Delta)$. For pictorial clarity, the figure represents monomers as half-circles, but monomers are taken to be point particles in the model.

system and $N(N-1)$ possible incorrect dimers. The binding energy for the dimers is given by

$$\mathcal{E}'(\alpha_m, \beta_n) = \begin{cases} -(E_0 + \Delta) & \text{if } m = n \\ -E_0 & \text{if } m \neq n, \end{cases} \tag{D.1}$$

indicating that correct dimers have a binding energy of $-(E_0 + \Delta)$ and incorrect dimers have a binding energy of $-E_0$, where $E_0, \Delta > 0$.

We assume that the monomers and dimers are point particles with no rotational or vibrational properties and that apart from the binding energy, the monomers and the dimers are free particles that do not interact with one another. An example microstate for this system is shown in Fig. D.1.

We want to compute the partition function for this system. By an argument similar to that used to establish Eq.(4.9) and Eq.(4.10), we find that the partition function can be written as

$$Z'_N(V, T, E_0, \Delta) = \sum_{j=0}^{N} \sum_{\ell=0}^{j} \binom{N}{\ell} b_{N-\ell, j-\ell} \, e^{\beta(jE_0 + \ell\Delta)} \left(\frac{V}{\lambda_\alpha^3}\right)^{N-j} \left(\frac{V}{\lambda_\beta^3}\right)^{N-j} \left(\frac{V}{\lambda_{\alpha\beta}^3}\right)^{j}, \tag{D.2}$$

where λ_α, λ_β, and $\lambda_{\alpha\beta}$ are the thermal de Broglie wavelengths of an α monomer, a β

monomer, and an (α, β) dimer respectively. In the summations in Eq.(D.2), j counts the number of dimers in the system, and ℓ counts the number of correct dimers. The factor

$$\binom{N}{\ell} b_{N-\ell, j-\ell} \tag{D.3}$$

is the answer to the following question:

> N man-woman pairs enter a dance hall. All the pairs separate, and people mingle with one another such that at some later time, there are some man-woman pairs and there are some men and women who are alone. At this later time, there are j man-woman pairs on the dance floor, and of this set, there are ℓ pairs from the set of original pairs. How many ways can this happen?

Interpreting Eq.(D.3) more physically, the factor $\binom{N}{\ell}$ corresponds to the number of ways to choose ℓ dimers from the set of N possible correct dimers. Under the constraint that each dimer consists of opposite gender monomers, the factor $b_{N-\ell, j-\ell}$ is the number of ways of forming $j - \ell$ dimers from a set of $2(N - \ell)$ monomers such that none of the chosen dimers is amongst the set of $N - \ell$ correct dimers.

In computing Eq.(D.2), the pivotal quantity is $b_{N-\ell, j-\ell}$. We can determine this quantity by considering another question:

> Given n original man-woman pairs, what is the number of ways to form $k \leq n$ man-woman pairs such that none of these new pairs coincide with any of the original pairs?

We call this number $b_{n,k}$. Applying the principle of inclusion/exclusion in a way similar to the application in *SM Sec. 2*, we find

$$b_{n,k} = \sum_{m=0}^{k} (-1)^m \binom{n}{m} \binom{n-m}{k-m}^2 (k-m)! \tag{D.4}$$

Using the definition of the Gamma function to express $(n - m)!$ as an integral, we then obtain

$$b_{n,k} = \frac{1}{(n-k)!} \binom{n}{k} \int_0^\infty dx \, e^{-x} x^{n-k} (x-1)^k. \tag{D.5}$$

151

As a consistency check, we can use Eq.(D.5) to prove the identity

$$\binom{N}{j}^2 j! = \sum_{\ell=0}^{j} \binom{N}{\ell} b_{N-\ell, j-\ell}, \tag{D.6}$$

which asserts that the total number of unique ways to form $j \leq N$ man-woman pairs (regardless of coincidence with some original pairing), is the sum of the number of ways to choose ℓ original pairs multiplied by the number of ways to choose $j - \ell$ non-original pairs.

We are now ready to return to Eq.(D.2). First, we rewrite the ideal gas contributions to the partition function as

$$\left(\frac{V}{\lambda_\alpha^3}\right)^{N-j} \left(\frac{V}{\lambda_\beta^3}\right)^{N-j} \left(\frac{V}{\lambda_{\alpha\beta}^3}\right)^{j} = \left(\frac{V}{\bar{\lambda}^3}\right)^{2N} \left(\frac{\lambda_\mu^3}{V}\right)^{j}, \tag{D.7}$$

where we defined

$$\bar{\lambda} \equiv \frac{h}{\sqrt{2\pi (m_\alpha m_\beta)^{1/2} k_B T}}, \quad \lambda_\mu \equiv \frac{h}{\sqrt{2\pi k_B T}} \sqrt{\frac{1}{m_\alpha} + \frac{1}{m_\beta}}, \tag{D.8}$$

Now, with the Laplace's integral form of the Legendre Polynomial $P_n(x)$ (Gould, 2010)

$$P_n(x) = \frac{1}{2\pi} \int_0^{2\pi} d\phi \left(x + \sqrt{x^2 - 1} \cos \phi \right)^n. \tag{D.9}$$

and the series representation of the Legendre Polynomial (Gould, 2010)

$$P_n = \left(\frac{x-1}{2}\right)^n \sum_{k=0}^{n} \binom{n}{k}^2 \left(\frac{x+1}{x-1}\right)^k. \tag{D.10}$$

we can establish the integration identity

$$\sum_{k=0}^{n} \binom{n}{k}^2 u^k = \frac{1}{2\pi} \int_0^{2\pi} d\phi \left(1 + u + 2\sqrt{u} \cos \phi \right)^n. \tag{D.11}$$

Incorporating Eq.(D.5) into Eq.(D.2), following a derivation analogous to that in *SM Sec. 3*, and using Eq.(D.11), we ultimately find that the partition function for this system is

$$Z'_N(V, T, E_0, \Delta) = \frac{1}{2\pi N!} \left(\frac{V}{\bar{\lambda}^3}\right)^{2N} \int_0^{2\pi} d\phi \int_0^\infty \int_0^\infty dx\, dy\, e^{-(x+y)} \mathcal{I}^N, \tag{D.12}$$

where

$$\mathcal{I} \equiv x + \frac{\lambda_\mu^3}{V} e^{\beta E_0} y\, \Omega(x; \beta\Delta) - 2\left(\frac{\lambda_\mu^3}{V}\right)^{1/2} e^{\beta E_0/2} \sqrt{y\, x\, \Omega(x; \beta\Delta)} \cos\phi, \tag{D.13}$$

and

$$\Omega(x; \beta\Delta) \equiv e^{\beta\Delta} + x - 1. \tag{D.14}$$

The thermal de Broglie wavelength in these expressions is defined as $\lambda_\mu = h/\sqrt{2\pi\mu k_B T}$ with $\mu = m_\beta m_\alpha/(m_\beta + m_\alpha)$, the reduced mass of an (α, β) dimer.

D.2 Equilibrium Conditions

With Eq.(D.12), the next step in studying the equilibrium properties of the gendered dimer system is to derive the equilibrium conditions. Given Eq.(D.2), we see that we can compute the average number of total dimers and the average number of correct dimers, respectively, with

$$\langle j \rangle = \frac{\partial}{\partial(\beta E_0)} \ln Z'_N, \tag{D.15}$$

$$\langle \ell \rangle = \frac{\partial}{\partial(\beta\Delta)} \ln Z'_N. \tag{D.16}$$

We can also compute the variances and covariances between these quantities through

$$\begin{pmatrix} \sigma_j^2 & \sigma_{j\ell}^2 \\ \sigma_{\ell j}^2 & \sigma_\ell^2 \end{pmatrix} = \begin{pmatrix} \partial_{\beta E_0}^2 & \partial_{\beta E_0}\partial_{\beta\Delta} \\ \partial_{\beta\Delta}\partial_{\beta E_0} & \partial_{\beta\Delta}^2 \end{pmatrix} \ln Z'_N, \tag{D.17}$$

where σ_j^2 is the variance in the total number of dimers, σ_ℓ^2 is the variance in the number of correct dimers, and $\sigma_{\ell j}^2 = \sigma_{j\ell}^2$ is the covariance between the total number of dimers and the number of correct dimers.

Using Eq.(D.12) directly in Eq.(D.15) and Eq.(D.16) would result in cumbersome integral expressions for $\langle \ell \rangle$ and $\langle j \rangle$, so we will use Laplace's method to approximate the partition function. We can expect the exact calculation of this approximation to mirror that in *SM Sec. 4*, but first we need to reduce Eq.(D.12) from a three-dimensional to a two-dimensional integral. Implementing Laplace's method on the ϕ variable alone, we find that the integrand of Eq.(D.12) is maximized for $\phi = \pi$. Therefore, we can make the approximation

$$\ln Z_N'(V, T, E_0, \Delta) = \ln \int_0^\infty \int_0^\infty dx\, dy\, e^{-(x+y)} \mathcal{I}_{\phi=\pi}^N + \cdots, \tag{D.18}$$

where $\mathcal{I}_{\phi=\pi}$ is Eq.(D.13) evaluated at $\phi = \pi$ and where "$\cdots$" stands in for terms that are independent of E_0 and Δ or are sub-leading to order N. Now, from the definitions Eq.(D.15) and Eq.(D.16) and implementing the standard Laplace's method algorithm in a way akin to its application in *SM Sec. 4*, we find the system of equations

$$\frac{\lambda_\mu^3}{V} e^{\beta E_0} = \frac{\langle j \rangle - \langle \ell \rangle (1 - e^{-\beta\Delta})}{(N - \langle j \rangle)^2}, \tag{D.19}$$

$$e^{\beta\Delta} = \langle \ell \rangle \frac{N - \langle \ell \rangle (1 - e^{-\beta\Delta})}{\langle j \rangle - \langle \ell \rangle (1 - e^{-\beta\Delta})}. \tag{D.20}$$

We similarly find the variances and covariances between the number of dimers and the number of correct dimers is

$$\sigma_j^2 = \frac{1}{2N} \langle j \rangle (N - \langle j \rangle), \quad \sigma_{j\ell}^2 = \frac{1}{2N} \langle \ell \rangle (N - \langle j \rangle), \tag{D.21}$$

$$\sigma_\ell^2 = \langle \ell \rangle - \frac{\langle \ell \rangle^2}{2} \left(\frac{1}{\langle j \rangle} + \frac{1}{N} \right), \tag{D.22}$$

Comparing Eq.(D.19) and Eq.(D.20) with Eq.(4.27) and Eq.(4.28), we see that the sets of equilibrium conditions for the non-gendered and gendered systems are identical except for numerical factors. Therefore, the discussion in the main text also applies to this gendered

154

system with only slight changes to the arguments of important expressions. In particular, considering the fully-correct assembly condition for the gendered system (i.e., $\langle j \rangle = \langle \ell \rangle$), we find that the critical temperature $k_B T_c = \beta_c^{-1}$ at which this condition is satisfied is

$$\frac{\lambda_{\mu,c}^3}{V} e^{\beta_c(E_0+\Delta)} \frac{\left(1 - Ne^{-\beta_c\Delta}\right)^2}{1 - e^{-\beta_c\Delta}} = N - 1, \tag{D.23}$$

where $\lambda_{\mu,c} = h/\sqrt{2\pi\mu k_B T_c}$. Similarly to Eq.(4.44), we can categorize the system as Type I or II according to the limiting behavior of the solution to Eq.(D.23). We define T_I' as

$$k_B T_\text{I}' \equiv \frac{2}{3}(E_0 + \Delta) \left[W_0 \left(\frac{2(E_0 + \Delta)}{3E_{\mu,V}} N^{2/3} \right) \right]^{-1} + \mathcal{O}\left(N^{-1}\right) \tag{D.24}$$

where $E_{\mu,V} \equiv h^2/2\pi\mu V^{2/3}$, and T_II' as

$$k_B T_\text{II}' \equiv \frac{\Delta}{\ln(N)}, \tag{D.25}$$

Then a gendered system is Type I or Type II according to

$$\text{System Type} = \begin{cases} \text{Type I} & \text{for } T_c \simeq T_\text{I}', \\ \text{Type II} & \text{for } T_c \simeq T_\text{II}'. \end{cases} \tag{D.26}$$

The parameter space behavior of this system is identical to that in Fig. 4.6, with T_I' and T_II' replacing T_I and T_II, respectively.

D.3 Inequalities for Assembly and Type

With Eq.(D.24) and Eq.(D.25), we can derive inequalities analogous to Eq.(4.45), Eq.(4.46), and Eq.(4.48).

For the gendered dimer system, the "search-limiting" condition, derived from $T < T_\text{I}'$, is

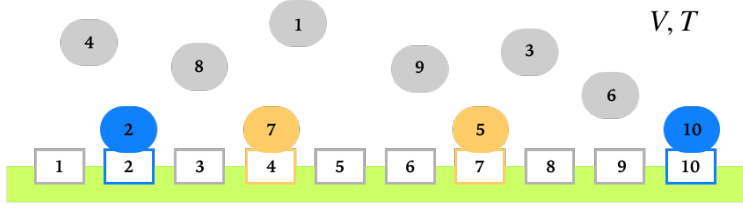$$NV < \lambda_\mu^3 e^{\beta(E_0+\Delta)}, \tag{D.27}$$

FIGURE D.2: Example microstate of the gendered system with $2N = 20$ subunits where one type of monomer is fixed in space. We represent the two genders as shaded or unshaded shapes. This microstate has two correct contacts (in blue), two incorrect contacts (in yellow), and six monomers and unpaired binding sites (in grey). The total binding energy for this microstate is $-(4E_0 + 2\Delta)$.

where, consistent with the $N \gg 1$ limit, we dropped the $\mathcal{O}(N^{-1})$ term in Eq.(D.24). The "combinatorics-limiting" condition, derived from $T < T'_{\text{II}}$, is

$$N < e^{\beta \Delta}. \tag{D.28}$$

Eq.(D.27) and Eq.(D.28) are the two necessary, but not sufficient, conditions a gendered dimer system must satisfy to be in the fully-correct assembly regime of its parameter space.

For a Type I dimer system, we require $T'_{\text{I}} < T'_{\text{II}}$. Using Eq.(D.24) and Eq.(D.25) in the inequality $T'_{\text{I}} < T'_{\text{II}}$, and noting that if $W_0(X) > k$, then $X > ke^k$, we obtain an inequality that when solved for N yields

$$N < \exp\left[\frac{3\Delta}{2E_0} W_0\left(\frac{2E_0}{3E_{\mu,V}}\right)\right] \tag{D.29}$$

Eq.(D.29) is a necessary, but not sufficient, condition for a gendered dimer system to be of Type I.

D.4   One type of monomer fixed; $m_\alpha \to \infty$ limit

A special case of the gendered dimer system occurs when one of the two types of monomers is fixed in space. We can envision such a system as having N distinguishable monomers interacting with N binding sites where each monomer has a preferred binding site to which it binds with energy $-(E_0 + \Delta)$; for all other binding sites, the monomer binds with energy $-E_0$.

An example microstate of such a system is shown in Fig. D.2. The general partition function for this system can be directly obtained from Eq.(D.12) by removing the V^N/λ_α^{3N} factor from the coefficient and taking $\lambda_\mu \to \lambda_\beta$. That is, if we are taking the particles of type α to be fixed, then we ignore their dynamics by taking $m_\alpha \to \infty$, thus taking the reduced mass μ to m_β.

The equilibrium conditions for this system are similarly given by Eq.(D.19) and Eq.(D.20) with λ_μ replaced with λ_β in the former.

Appendix E

Additional Models

In this appendix, we derive the partition functions presented in Chapter 5.

E.1   Generalized Thermal Derangements

In this section we derive Eq.(5.13). We first define our state space as all the unique permutations of an ordered list of N elements where there are $r \leq N$ unique types of elements. The original ordered list is defined as the "zeroth-energy arrangement" and it consists of n_1 copies of an element ω_1, n_2 copies of an element ω_3, ..., and n_r copies of an element ω_r in a specific ordering. The exact ordering of this list is not important; it only matters that an exact ordering exists.

The problem of counting the various ways one can completely derange (i.e., reorder such that no element is in its original place) a list of elements with repeated elements was solved in (Even and Gillis, 1976). For a list with n_k copies of an element ω_k for $k = 1, \ldots, r$, it was found that the number of derangements is given by

$$P_{\mathbf{n}} = \int_0^\infty dx \, e^{-x} \prod_{k=1}^r (-1)^{n_k} L_{n_k}(x), \tag{E.1}$$

where $\mathbf{n} = (n_1, \ldots, n_r)$ and where L_n is the nth Laguerre Polynomial.

We say that our permutation system incurs an energy cost of $+\lambda_k$ whenever a component ω_k is not in this zeroth-energy arrangement. Therefore, if j_1 elements ω_1, j_2 elements ω_2, ..., and j_r elements ω_r, for a particular microstate, do not match their positions in the

zeroth-energy arrangement, then the energy of the microstate is

$$\mathcal{E}_j = \sum_{i=1}^{r} \lambda_k j_k. \tag{E.2}$$

We are almost at the stage where we can write down the partition function for this system. We need only find the degeneracy factor associated with the energy Eq.(E.2). The number of ways to reorder the elements in our key-sequence such that j_1 elements ω_1, ..., and j_r elements ω_r are not in their original positions can be found combinatorially. Given that there are $\binom{n}{k}$ ways to choose k elements from a set of n, (and that all j_k chosen elements from a set of n_k are identical), the desired quantity is given by

$$\Omega_j^{\mathbf{n}} = \binom{n_1}{j_1} \cdots \binom{n_r}{j_r} P_j, \tag{E.3}$$

where P_j is defined in Eq.(E.1). The partition function is then

$$Z_{\mathbf{n}}(\{\beta\lambda_k\}) = \sum_{j_1=0}^{n_1} \cdots \sum_{j_r=0}^{n_r} e^{-\beta(\lambda_1 j_1 + \cdots + \lambda_r j_r)} \binom{n_1}{j_1} \cdots \binom{n_r}{j_r} P_{j_1,\dots,j_r}, \tag{E.4}$$

where $\beta = 1/k_B T$. Given Eq.(E.1), Eq.(E.4) can then be written as

$$Z_{\mathbf{n}}(\{\beta\lambda_k\}) = \sum_{j_1=0}^{n_1} \cdots \sum_{j_r=0}^{n_r} e^{-\beta(\lambda_1 j_1 + \cdots + \lambda_r j_r)} \binom{n_1}{j_1} \cdots \binom{n_r}{j_r} \int_0^\infty dx\, e^{-x} \prod_{k=1}^{r} (-1)^{j_k} L_{j_k}(x)$$

$$= \int_0^\infty dx\, e^{-x} \prod_{k=1}^{r} \sum_{j_k=0}^{n_k} \binom{n_k}{j_k} (-e^{-\beta\lambda_k})^{j_k} L_{j_k}(x). \tag{E.5}$$

Now, given the definition of the Laguerre polynomial,

$$L_n(x) = \sum_{k=0}^{n} \binom{n}{k} \frac{(-1)^k}{k!} x^k, \tag{E.6}$$

we find

$$\sum_{j=0}^{n} \binom{n}{j} u^j L_j(x) = \sum_{j=0}^{n} \sum_{k=0}^{j} \binom{n}{j}\binom{j}{k} u^j (-1)^k \frac{x^k}{k!}$$

$$= \sum_{k=0}^{n} (-1)^k \frac{x^k}{k!} \sum_{j=k}^{n} \binom{n}{j}\binom{j}{k} u^j$$

$$= \sum_{k=0}^{n} (-1)^k \frac{x^k}{k!} \binom{n}{k} u^k (1+u)^{n-k}$$

$$= (1+u)^n L_n \left(\frac{ux}{1+u} \right). \tag{E.7}$$

Thus Eq.(E.5) becomes

$$Z_{\mathbf{n}}(\{\beta\lambda_k\}) = \int_0^{\infty} dx \, e^{-x} \prod_{k=1}^{r} \left(1 - e^{-\beta\lambda_k} \right)^{n_k} L_{n_k} \left(\frac{x}{1 - e^{\beta\lambda_k}} \right). \tag{E.8}$$

E.2 Quenched Distribution for Dimer Self-Assembly

In this section we derive the partition function Eq.(5.15). We have monomers α_k for $k = 1, \ldots, N, N+1, \ldots, 2N$ which are distinct, have mass m_0, and exist as single copies. If two α monomers come into contact (say α_i and α_j) the two can form a dimer with binding energy

$$\mathcal{E}(\alpha_i, \alpha_j) = \begin{cases} -(E_0 + \Delta_i) & \text{if } |j - i| = N, \\ -E_0 & \text{otherwise.} \end{cases} \tag{E.9}$$

A preliminary partition function for the non-quenched case is

$$Z_N(V, T, E_0, \Delta) = \sum_{k=0}^{N} \sum_{m=0}^{k} a_{N-m,k-m} \binom{N}{m} e^{\beta\Delta m} \left(\frac{V}{\lambda_0^3} \right)^{2N-2k} \left(\frac{V}{(\lambda_0/\sqrt{2})^3} \right)^k e^{\beta E_0 k}, \tag{E.10}$$

and from this form we can extrapolate to the quenched case:

$$Z_N(V, T, E_0, \{\Delta_i\})$$

$$= \sum_{k=0}^{N} \sum_{m=0}^{k} a_{N-m,k-m} \Pi_m \left(e^{\beta\Delta_1}, \ldots, e^{\beta\Delta_N} \right) \left(\frac{V}{\lambda_0^3} \right)^{2N-2k} \left(\frac{V}{(\lambda_0/\sqrt{2})^3} \right)^k e^{\beta E_0 k}$$

$$= \left(\frac{V}{\lambda_0^3} \right)^{2N} \sum_{k=0}^{N} \sum_{m=0}^{k} a_{N-m,k-m} \Pi_m \left(e^{\beta\Delta_1}, \ldots, e^{\beta\Delta_N} \right) \left(\frac{2\sqrt{2}\lambda_0^3 e^{\beta E_0}}{V} \right)^k, \tag{E.11}$$

where $\Pi_m(x_1, \ldots, x_N)$ is the mth elementary symmetric polynomial in the variables $(x_1, \ldots, x_N)$ and $a_{N-m,k-m}$ is the number of ways to form, from a set of $2N$ initially paired elements, k pairs of which exactly m are found in the set of initial pairs. In Appendix B.5, we found

that an integral expression for $a_{n,\ell}$ is

$$a_{n,\ell} = \frac{1}{(2n - 2\ell - 1)!!} \binom{n}{\ell} \frac{1}{\sqrt{\pi}} \int_0^\infty dt\, e^{-t} t^{-1/2} (2t)^n (1 - 1/2t)^\ell. \tag{E.12}$$

Therefore, the partition function Eq.(E.11) becomes

$$
\begin{aligned}
Z_N&(V, T, E_0, \{\Delta_i\}) \\
&= \frac{(V/\lambda_0^3)^{2N}}{\sqrt{\pi}} \int_0^\infty dx\, \frac{e^{-x}}{\sqrt{x}} \sum_{k=0}^N \sum_{m=0}^k \delta^k \frac{1}{(2N - 2k - 1)!!} \Pi_m(\eta_1, \ldots, \eta_N) \\
&\quad \times \binom{N-m}{k-m} (2x)^{N-m} (1 - 1/2x)^{k-m} \\
&= \frac{(V/\lambda_0^3)^{2N}}{\sqrt{\pi}} \int_0^\infty dx\, \frac{e^{-x}}{\sqrt{x}} (2x)^N \sum_{k=0}^N \frac{[\delta(1 - 1/2x)]^k}{(2N - 2k - 1)!!} \\
&\quad \times \sum_{m=0}^k \binom{N-m}{k-m} \Pi_m(\eta_1, \ldots, \eta_N) (2x - 1)^{-m},
\end{aligned}
\tag{E.13}
$$

where we defined

$$\Delta \equiv \frac{2\sqrt{2}\lambda_0^3 e^{\beta E_0}}{V}, \quad \eta_\ell \equiv e^{\beta \Delta_\ell}. \tag{E.14}$$

From the properties of the elementary symmetric polynomial, we can show

$$\sum_{m=0}^k \binom{N-m}{N-k} \Pi_m(x_1, \ldots, x_N) \alpha^m = \Pi_k(1 + \alpha x_1, \ldots, 1 + \alpha x_N). \tag{E.15}$$

Therefore, Eq.(E.13) becomes

$$
\begin{aligned}
Z_N&(V, T, E_0, \{\Delta_i\}) \\
&= \frac{(V/\lambda_0^3)^{2N}}{\sqrt{\pi}} \int_0^\infty dx\, \frac{e^{-x}}{\sqrt{x}} (2x)^N \sum_{k=0}^N \frac{[\delta(1 - 1/2x)]^k}{(2N - 2k - 1)!!} \\
&\quad \times (2x - 1)^{-k} \Pi_k(2x - 1 + \eta_1, \ldots, 2x - 1 + \eta_N) \\
&= \frac{(V/\lambda_0^3)^{2N}}{\sqrt{\pi}} \int_0^\infty dx\, \frac{e^{-x}}{\sqrt{x}} (2x)^N \sum_{k=0}^N \frac{(\delta/2x)^k}{(2N - 2k - 1)!!} \\
&\quad \times \Pi_k(2x - 1 + \eta_1, \ldots, 2x - 1 + \eta_N).
\end{aligned}
\tag{E.16}
$$

Using the identity

$$\frac{1}{(2N - 2k - 1)!!} = \frac{(2k-1)!!}{(2N-1)!!}\frac{\binom{2N}{2k}}{\binom{N}{k}} = \frac{1}{\sqrt{\pi}(2N-1)!!}\int_0^\infty dy\, \frac{e^{-y}}{\sqrt{y}}\frac{\binom{2N}{2k}}{\binom{N}{k}}(2y)^k, \tag{E.17}$$

Eq.(E.16) becomes

$$
\begin{aligned}
Z_N&(V,T,E_0,\{\Delta_i\})\\
&= \frac{(V/\lambda_0^3)^{2N}}{\pi(2N-1)!!}\int_0^\infty dx\,dy\, \frac{e^{-x-y}}{\sqrt{xy}}(2x)^N \sum_{k=0}^N (\delta y/x)^k \frac{\binom{2N}{2k}}{\binom{N}{k}}\\
&\qquad\times \Pi_k\,(2x - 1 + \eta_1,\dots,2x - 1 + \eta_N)\\
&= \frac{(V/\lambda_0^3)^{2N}}{\sqrt{\pi}\Gamma(N+1/2)}\int_0^\infty dx\,dy\, \frac{e^{-x-y}}{\sqrt{xy}}x^N \sum_{k=0}^N (\delta y/x)^k \frac{\binom{2N}{2k}}{\binom{N}{k}}\\
&\qquad\times \Pi_k\,(2x - 1 + \eta_1,\dots,2x - 1 + \eta_N)\,.
\end{aligned}
\tag{E.18}
$$

To move forward we need to derive one more identity. First, by the definition of the Beta function,

$$B(x,y) = \frac{(x-1)!(y-1)!}{(x+y-1)!} = \int_0^1 dt\, t^{x-1}(1-t)^{y-1}, \tag{E.19}$$

we can show

$$\frac{1}{\binom{N}{k}} = (N+1)\int_0^t dt\, t^{N-k}(1-t)^k. \tag{E.20}$$

And from the Cauchy integral formula (Zill and Shanahan, 2009), we can derive the identity

$$\binom{2N}{2k} = \frac{1}{4\pi i}\oint \frac{dz}{z}\frac{1}{z^{2k}}\left[(z+1)^{2N} + (z-1)^{2N}\right], \tag{E.21}$$

where the integral is over a closed contour about the origin in the complex plane. Using Eq.(E.21) and Eq.(E.20) in Eq.(E.18), leads to

$$
\begin{aligned}
\sum_{k=0}^N &\frac{\binom{2N}{2k}}{\binom{N}{k}}\Pi_k(x_1,\dots,x_N)\alpha^k\\
&= \frac{N+1}{4\pi i}\int_0^1 dt\oint \frac{dz}{z}\sum_{k=0}^N t^N\left(\frac{1}{t}-1\right)^k \frac{(z+1)^{2N}}{z^{2k}}\alpha^k \Pi_k(x_1,\dots,x_N)\\
&\quad + (z\to -z)
\end{aligned}
$$

$$= \frac{N+1}{4\pi i} \int_0^1 dt \oint \frac{dz}{z} (z+1)^{2N} t^N \prod_{\ell=1}^N \left[1 + \frac{\alpha}{z^2} \left(\frac{1}{t} - 1 \right) x_\ell \right]$$

$$+ (z \to -z)$$

$$= \frac{N+1}{4\pi i} \int_0^1 dt \oint \frac{dz}{z} \left(1 + \frac{1}{z} \right)^{2N} \prod_{\ell=1}^N \left[z^2 t + \alpha (1-t) x_\ell \right]$$

$$+ (z \to -z). \tag{E.22}$$

Now, within the contour integral, we make the transformation

$$z^2 \to z \frac{1-t}{t}, \tag{E.23}$$

From which we can show that the differentials transform as

$$\frac{dz}{z} \to \frac{dz}{2z}. \tag{E.24}$$

Thus, Eq.(E.22) becomes

$$\sum_{k=0}^N \alpha^k \frac{\binom{2N}{2k}}{\binom{N}{k}} \Pi_k(x_1, \dots, x_N)$$

$$= \frac{N+1}{4\pi i} \oint \frac{dz}{z} \int_0^1 dt \left(1 + \sqrt{t/z(1-t)} \right)^{2N} \prod_{\ell=1}^N \left[z(1-t) + \alpha (1-t) x_\ell \right]$$

$$+ (\sqrt{z} \to -\sqrt{z})$$

$$= \frac{N+1}{4\pi i} \oint \frac{dz}{z} \int_0^1 dt \left(\sqrt{1-t} + \sqrt{t/z} \right)^{2N} \prod_{\ell=1}^N (z + \alpha x_\ell)$$

$$+ (\sqrt{z} \to -\sqrt{z}). \tag{E.25}$$

Using this identity to evaluate Eq.(E.18), we find

$$Z_N(V, T, E_0, \{\Delta_i\}) = c_{0,N} \int_0^\infty dx \, dy \, \frac{e^{-x-y}}{\sqrt{xy}} x^N \oint \frac{dz}{z} B_N(z) \prod_{\ell=1}^N \left[z + \delta y / x (\eta_\ell + 2x - 1) \right],$$

$$\tag{E.26}$$

where we defined

$$c_{0,N} \equiv \frac{(V/\lambda_0^3)^{2N}}{2\pi i \sqrt{\pi}\Gamma(N+1/2)}, \tag{E.27}$$

and

$$B_N(z) \equiv \frac{N+1}{2}\int_0^1 dt \left[\left(\sqrt{1-t}+\sqrt{t/z}\right)^{2N} + \left(\sqrt{1-t}-\sqrt{t/z}\right)^{2N}\right]. \tag{E.28}$$

E.3 Particle Aggregation

In this section we derive Eq.(5.21). We begin from Eq.(5.20), rewritten here for convenience:

$$Z_N(\{E_i\}, V, T) = \sum_{n_1=0}^{\infty} \cdots \sum_{n_N=0}^{\infty} \delta\left(N, \sum_{k=1}^{N} kn_k\right)\exp\left(\beta\sum_{i=1}^{N} E_i n_i\right)\prod_{j=1}^{N}\frac{1}{n_j!}\left(\frac{V}{\lambda_j^3}\right)^{n_j} \tag{E.29}$$

In Eq.(E.29), $\delta(\ell, k)$ is the Kronecker delta, n_k is the number of k-particle clusters, and λ_k is the thermal de Broglie wavelength of a single k-particle cluster of mass $m_k = km_0$. Given that each particle has mass m_0 the thermal de Broglie wavelength of a k-particle cluster has a simple relationship with the wavelength of a single particle:

$$\lambda_k = \frac{h}{\sqrt{2\pi(km_0)k_B T}} = \frac{1}{\sqrt{k}}\lambda_0, \tag{E.30}$$

where $\lambda_0 \equiv \lambda_1 = h/\sqrt{2\pi m_0 k_B T}$. Finally, using the contour integral identities

$$\delta(\ell, k) = \frac{1}{2\pi i}\oint \frac{dw}{w}w^{k-\ell}, \qquad \frac{1}{N!} = \frac{1}{2\pi i}\oint dz\, \frac{e^z}{z^{N+1}}, \tag{E.31}$$

we find Eq.(E.29) becomes

$$Z_N(\{E_i\}, V, T) = \frac{1}{2\pi i}\oint\frac{dw}{w^{N+1}}\prod_{j=1}^{N}\sum_{n_j=0}^{\infty}\frac{1}{2\pi i}\oint dz_j\,\frac{e^{z_j}}{(z_j)^{n_j+1}}\left(\frac{V}{\lambda_j^3}\right)^{n_j}e^{\beta E_j n_j}w^{jn_j}$$

$$= \frac{1}{(2\pi i)^{N+1}}\oint\frac{dw}{w^{N+1}}\prod_{j=1}^{N}\oint dz_j\,\frac{e^{z_j}}{z_j}\sum_{n_j=0}^{\infty}\left(w^j\frac{Ve^{\beta E_j}}{\lambda_j^3}\right)^{n_j}. \tag{E.32}$$

And using the geometric series formula to evaluate the quantity in the summation, we find

$$Z_N(\{E_i\}, V, T) = \frac{1}{(2\pi i)^{N+1}} \oint \frac{dw}{w^{N+1}} \prod_{j=1}^{N} \oint dz_j \frac{e^{z_j}}{z_j} \left(1 - w^j \frac{V e^{\beta E_j}}{\lambda_j^3 z_j}\right)^{-1}, \tag{E.33}$$

which affirms Eq.(5.21).

Bibliography

Alberts, Bruce (1998). "The cell as a collection of protein machines: preparing the next generation of molecular biologists". In: *Cell* 92.3, pp. 291–294.

Alberts, Bruce et al. (2013). *Essential cell biology*. 4th. Garland Science.

Baxter, Rodney J (2016). *Exactly solved models in statistical mechanics*. Elsevier.

Berg, Howard C and Edward M Purcell (1977). "Physics of chemoreception". In: *Biophysical journal* 20.2, pp. 193–219.

Binder, Kurt and A Peter Young (1986). "Spin glasses: Experimental facts, theoretical concepts, and open questions". In: *Reviews of Modern physics* 58.4, p. 801.

Blitzstein, Joseph K and Jessica Hwang (2014). *Introduction to probability*. CRC Press.

Borwein, Peter and Tamás Erdélyi (2012). *Polynomials and polynomial inequalities*. Vol. 161. Springer Science & Business Media.

Breitung, Karl W (2006). *Asymptotic approximations for probability integrals*. Springer.

Brush, Stephen G (1967). "History of the Lenz-Ising model". In: *Reviews of modern physics* 39.4, p. 883.

Bryngelson, Joseph D and Peter G Wolynes (1987). "Spin glasses and the statistical mechanics of protein folding". In: *Proceedings of the National Academy of Sciences* 84.21, pp. 7524–7528.

Chandler, David (1987). *Introduction to modern statistical mechanics*. Oxford University Press, p. 288.

Chuan-Chong, Chen and Koh Khee-Meng (1992). *Principles and techniques in combinatorics*. Vol. 2. World Scientific.

Collins, Jesse Wronka (2014). *Self-assembly of colloidal spheres with specific interactions*. Harvard University.

Corbin, Rebecca W et al. (2003). "Toward a protein profile of Escherichia coli: comparison to its transcription profile". In: *Proceedings of the National Academy of Sciences* 100.16, pp. 9232–9237.

Deeds, Eric J et al. (2007). "Robust protein–protein interactions in crowded cellular environments". In: *Proceedings of the National Academy of Sciences* 104.38, pp. 14952–14957.

Derrida, Bernard (1980). "Random-energy model: Limit of a family of disordered models". In: *Physical Review Letters* 45.2, p. 79.

Dixon, John D and Brian Mortimer (1996). *Permutation groups*. Vol. 163. Springer Science & Business Media.

Derangements and Laguerre polynomials (1976). Vol. 79. 1. Cambridge University Press, pp. 135–143.

Fei, Jingyi and Taekjip Ha (2013). "Watching DNA breath one molecule at a time". In: *Proceedings of the National Academy of Sciences* 110.43, pp. 17173–17174.

Finkelstein, Alexei V and Joël Janin (1989). "The price of lost freedom: entropy of bimolecular complex formation". In: *Protein Engineering, Design and Selection* 3.1, pp. 1–3.

Fulton, Alice B (1982). "How crowded is the cytoplasm?" In: *Cell* 30.2, pp. 345–347.

Go, Nobuhiro (1983). "Theoretical studies of protein folding". In: *Annual review of biophysics and bioengineering* 12.1, pp. 183–210.

Gould, Henry W (2010). "Combinatorial Identities: Table II: Advanced Techniques for Summing Finite Series". document at https://www.math.wvu.edu/~gould/Vol.5.PDF.

Hagan, Michael F, Oren M Elrad, and Robert L Jack (2011). "Mechanisms of kinetic trapping in self-assembly and phase transformation". In: *The Journal of chemical physics* 135.10, p. 104115.

Hardy, Godfrey H and Srinivasa Ramanujan (1918). "Asymptotic formulaæ in combinatory analysis". In: *Proceedings of the London Mathematical Society* 2.1, pp. 75–115.

Hippel, Peter H von and Otto G Berg (1989). "Facilitated target location in biological systems." In: *Journal of Biological Chemistry* 264.2, pp. 675–678.

Hopfield, John J (1982). "Neural networks and physical systems with emergent collective computational abilities". In: *Proceedings of the national academy of sciences* 79.8, pp. 2554–2558.

— (1984). "Neurons with graded response have collective computational properties like those of two-state neurons". In: *Proceedings of the national academy of sciences* 81.10, pp. 3088–3092.

Hubbard, John H and Barbara Burke Hubbard (2015). *Vector calculus, linear algebra, and differential forms: a unified approach*. Matrix Editions.

Innis, Michael and David Gelfand (1999). "Optimization of PCR: conversations between Michael and David". In: *PCR Applications*. Elsevier, pp. 3–22.

Irving, Ron (2013). *Beyond the quadratic formula*. Vol. 43. MAA.

Ising, Ernst (1925). "Beitrag zur theorie des ferromagnetismus". In: *Zeitschrift für Physik* 31.1, pp. 253–258.

Israelachvili, Jacob N, D John Mitchell, and Barry W Ninham (1976). "Theory of self-assembly of hydrocarbon amphiphiles into micelles and bilayers". In: *Journal of the Chemical Society, Faraday Transactions 2: Molecular and Chemical Physics* 72, pp. 1525–1568.

Jen-Jacobson, Linda (1997). "Protein—DNA recognition complexes: Conservation of structure and binding energy in the transition state". In: *Biopolymers: Original Research on Biomolecules* 44.2, pp. 153–180.

Johnson, Margaret E and Gerhard Hummer (2010). "Nonspecific binding limits the number of proteins in a cell and shapes their interaction networks". In: *Proceedings of the National Academy of Sciences*.

Johnston, Iain G, Ard A Louis, and Jonathan PK Doye (2010). "Modelling the self-assembly of virus capsids". In: *Journal of Physics: Condensed Matter* 22.10, p. 104101.

Kardar, Mehran (2007a). "Statistical physics of particles". In: Cambridge University Press. Chap. 2, pp. 48–50.

— (2007b). *Statistical physics of particles*. Cambridge University Press.

Kardar, Mehran (2007c). "Statistical physics of particles". In: Cambridge University Press. Chap. 5, pp. 48–50.

Kastritis, Panagiotis L et al. (2011). "A structure-based benchmark for protein–protein binding affinity". In: *Protein Science* 20.3, pp. 482–491.

Kay, Lily E (1985). "Conceptual models and analytical tools: The biology of physicist Max Delbrück". In: *Journal of the History of Biology* 18.2, pp. 207–246.

Kindt, James T (2012). "Accounting for finite-number effects on cluster size distributions in simulations of equilibrium aggregation". In: *Journal of chemical theory and computation* 9.1, pp. 147–152.

Kuhn, Werner (1934). "Über die gestalt fadenförmiger moleküle in lösungen". In: *Kolloid-Zeitschrift* 68.1, pp. 2–15.

Landau, Lev D, EM Lifshitz, and LP Pitaevskii (1980). *Statistical Physics (Course of Theoretical Physics, Volume 5)*. Pergamon Oxford.

Lukatsky, DB, KB Zeldovich, and EI Shakhnovich (2006). "Statistically enhanced self-attraction of random patterns". In: *Physical review letters* 97.17, p. 178101.

Luria, Salvador E (1984). *A slot machine, a broken test tube: An autobiography*. Harpercollins.

Luria, Salvador E and Max Delbrück (1943). "Mutations of bacteria from virus sensitivity to virus resistance". In: *Genetics* 28.6, p. 491.

Margolius, Barbara H (2001). "Avoiding your spouse at a bridge party". In: *Mathematics Magazine* 74.1, pp. 33–41.

Marko, John F and Eric D Siggia (1995). "Stretching dna". In: *Macromolecules* 28.26, pp. 8759–8770.

Marsh, Derek (2012). "Thermodynamics of phospholipid self-assembly". In: *Biophysical journal* 102.5, pp. 1079–1087.

Mehra, Jagdish (2001). "Erwin Schrödinger and the Rise of Wave Mechanics II. The Creation of Wave Mechanics". In: *The Golden Age of Theoretical Physics*. 1st ed. Vol. 2. World Scientific Publishing Co Inc. Chap. 22, pp. 762–763.

Metzler, David E (2001). "Biochemistry: The Chemical Reactions of Living Cells". In: vol. 1. Academic Press. Chap. 1, p. 4.

Milo, Ron and Rob Phillips (2015). *Cell biology by the numbers*. Garland Science.

Morrissey, Michael P and Eugene I Shakhnovich (1996). "Design of proteins with selected thermal properties". In: *Folding and Design* 1.5, pp. 391–405.

Nelson, Philip (2004). "Biological physics: Energy, information life". In: *Physics Today* 57.11, pp. 63–64.

Nemilov, Sergei V (2009). "Zero-point entropy of glasses as physical reality". In: *Journal of Non-Crystalline Solids* 355.10-12, pp. 607–616.

Nguyen, Hung D, Vijay S Reddy, and Charles L Brooks (2007). "Deciphering the kinetic mechanism of spontaneous self-assembly of icosahedral capsids". In: *Nano letters* 7.2, pp. 338–344.

Nguyen, Michael and Suriyanarayanan Vaikuntanathan (2016). "Design principles for nonequilibrium self-assembly". In: *Proceedings of the National Academy of Sciences* 113.50, pp. 14231–14236.

Nooren, Irene MA and Janet M Thornton (2003). "Diversity of protein–protein interactions". In: *The EMBO journal* 22.14, pp. 3486–3492.

Norn, Christoffer H and Ingemar André (2016). "Computational design of protein self-assembly". In: *Current opinion in structural biology* 39, pp. 39–45.

Onsager, Lars (1944). "Crystal statistics. I. A two-dimensional model with an order-disorder transition". In: *Physical Review* 65.3-4, p. 117.

Paine, Gregory H and Harold A Scheraga (1985). "Prediction of the native conformation of a polypeptide by a statistical-mechanical procedure. I. Backbone structure of enkephalin". In: *Biopolymers: Original Research on Biomolecules* 24.8, pp. 1391–1436.

Pérez-Rueda, Ernesto and Julio Collado-Vides (2000). "The repertoire of DNA-binding transcriptional regulators in Escherichia coli K-12". In: *Nucleic acids research* 28.8, pp. 1838–1847.

Perlmutter, Jason D and Michael F Hagan (2015). "Mechanisms of virus assembly". In: *Annual review of physical chemistry* 66, pp. 217–239.

Poland, Douglas and Harold A Scheraga (1970). "Theory of helix-coil transitions in biopolymers". In:

Saitô, Nobuhiko, Kunihiko Takahashi, and Yasuo Yunoki (1967). "The statistical mechanical theory of stiff chains". In: *Journal of the Physical Society of Japan* 22.1, pp. 219–226.

SantaLucia, John (1998). "A unified view of polymer, dumbbell, and oligonucleotide DNA nearest-neighbor thermodynamics". In: *Proceedings of the National Academy of Sciences* 95.4, pp. 1460–1465.

Sayre, Anne (2000). *Rosalind Franklin and DNA*. WW Norton & Company.

Schellman, John A (1974). "Flexibility of DNA". In: *Biopolymers: Original Research on Biomolecules* 13.1, pp. 217–226.

Sethna, James P (2006). *Statistical mechanics: entropy, order parameters, and complexity*. Vol. 14. Oxford University Press Oxford. Chap. 6.

Shakhnovich, EI and AM Gutin (1993a). "A new approach to the design of stable proteins". In: *Protein Engineering* 6.8, pp. 793–800.

Shakhnovich, Eugene I (1998). "Protein design: a perspective from simple tractable models". In: *Folding and Design* 3.3, R45–R58.

Shakhnovich, Eugene I and Alexander M Gutin (1993b). "Engineering of stable and fast-folding sequences of model proteins". In: *Proceedings of the National Academy of Sciences* 90.15, pp. 7195–7199.

Sherrington, David and Scott Kirkpatrick (1975). "Solvable model of a spin-glass". In: *Physical review letters* 35.26, p. 1792.

Soufi, Boumediene et al. (2015). "Characterization of the E. coli proteome and its modifications during growth and ethanol stress". In: *Frontiers in microbiology* 6, p. 103.

Stein, Daniel L (1992). *Spin glasses and biology*. Vol. 6. World scientific.

Storm, Cornelis and Philip C Nelson (2003). "Theory of high-force DNA stretching and overstretching". In: *Physical Review E* 67.5, p. 051906.

Wales, David J (2005). "The energy landscape as a unifying theme in molecular science". In: *Philosophical Transactions of the Royal Society of London A: Mathematical, Physical and Engineering Sciences* 363.1827, pp. 357–377.

Watson, James D and Francis HC Crick (1953). "Genetical implications of the structure of deoxyribonucleic acid". In: *Nature* 171.4361, pp. 964–967.

Weisstein, Eric W (2002a). "Closed-Form Solution". In:

— (2002b). "Digamma function". In: *Wolfram Mathworld*.

— (2002c). "Incomplete Gamma function". In: *Wolfram Mathworld*.

— (2002d). "Lambert W-function". In: *Wolfram Mathworld*.

Williams, Mobolaji (2017). "Statistical physics of the symmetric group". In: *Physical Review E* 95.4, p. 042126.

Yeomans, Julia M (1992). *Statistical mechanics of phase transitions*. Oxford University Press.

Zhang, Jingshan, Sergei Maslov, and Eugene I Shakhnovich (2008). "Constraints imposed by non-functional protein–protein interactions on gene expression and proteome size". In: *Molecular systems biology* 4.1, p. 210.

Zill, Dennis and Patrick Shanahan (2009). *A first course in complex analysis with applications*. Jones & Bartlett Learning.

Zimm, BH, Paul Doty, and K Iso (1959). "Determination of the parameters for helix formation in poly-γ-benzyl-L-glutamate". In: *Proceedings of the National Academy of Sciences* 45.11, pp. 1601–1607.

Zimm, Bruno H (1960). "Theory of"melting"of the helical form in double chains of the DNA type". In: *The Journal of Chemical Physics* 33.5, pp. 1349–1356.

Zimm, Bruno H and JK Bragg (1959). "Theory of the phase transition between helix and random coil in polypeptide chains". In: *The journal of chemical physics* 31.2, pp. 526–535.